1982

Assessment of the stability of a multimachine power system by the transient energy margin

Stewart Elliott Stanton
Iowa State University

Stanton, Stewart Elliott

ASSESSMENT OF THE STABILITY OF A MULTIMACHINE POWER SYSTEM BY THE TRANSIENT ENERGY MARGIN

Iowa State University PH.D. 1982

PLEASE NOTE:

In all cases this material has been filmed in the best possible way from the available copy. Problems encountered with this document have been identified here with a check mark __√__.

1. Glossy photographs or pages _____
2. Colored illustrations, paper or print _____
3. Photographs with dark background _____
4. Illustrations are poor copy _____
5. Pages with black marks, not original copy _____
6. Print shows through as there is text on both sides of page _____
7. Indistinct, broken or small print on several pages ✓
8. Print exceeds margin requirements _____
9. Tightly bound copy with print lost in spine _____
10. Computer printout pages with indistinct print _____
11. Page(s) _____ lacking when material received, and not available from school or author.
12. Page(s) _____ seem to be missing in numbering only as text follows.
13. Two pages numbered _____. Text follows.
14. Curling and wrinkled pages _____
15. Other _____

University
Microfilms
International

Assessment of the stability of a multimachine power system by the transient energy margin

by

Stewart Elliott Stanton

A Dissertation Submitted to the
Graduate Faculty in Partial Fulfillment of the
Requirements for the Degree of
DOCTOR OF PHILOSOPHY

Major: Electrical Engineering

Approved:

Signature was redacted for privacy.

In Charge of Major Work

Signature was redacted for privacy.

For the Major Department

Signature was redacted for privacy.

For the Graduate College

Iowa State University
Ames, Iowa

1982

TABLE OF CONTENTS

CHAPTER 1. INTRODUCTION

Survey of On-line Security Practices

Computer automated power system security practices in the United States are reviewed in a recent IEEE paper (1) written by the Current Operations Problems Working Group of IEEE's Systems Operations Subcommittee. Security monitoring is limited to steady state performance considerations only. The system is monitored, and a static state estimation process describes the entire system state. An interactive dispatcher's load-flow program is used with a list of selected contingencies to assess the suitability of the system operating states under these contingencies. Reports are made to the operator when it is ascertained that the operating conditions, in the event of specific contingencies, would exceed prescribed limits for bus voltages or line flows.

A similar survey by the System Planning and Operations Committee No. 32-12 of CIGRE (1972) (2) reports on the various security monitoring schemes of the member systems throughout the world. The most common basis for analysis is calculation of power flows and short circuit levels. Some of the systems use transient stability analysis data, but these attempts at assessing transient stability use precalculated limits and attempt to infer the suitability of the transient response by inspecting the steady state power flow parameters.

In Japan, a security monitoring scheme (3,4) of the Tokyo Electric Power Company uses a procedure that runs a series of operating limit checks. The operating limits are computed using a contingency evaluation procedure that selects contingencies from a prepared list and applies a variety of on-line computer methods for analysis. An important aspect of this scheme is that it assesses the transient behavior of the power system as well as the suitability of the post-disturbance performance. Another scheme proposed by the Mitsubishi Electric Corporation (5) is designed to evaluate the so called "dynamic reliability" with a procedure which takes into account the probability of cascading failure introduced by a primary disturbance.

In Canada, the Ontario Hydro System uses precalculated stability studies to determine stability limits for certain network configurations. Computer monitoring schemes are used to ascertain which limits apply to the current configuration, and to assess whether these limits are being approached (6).

In summary, it is clear that computer-automated security assessment is in its infancy. Schemes currently in use depend primarily on tools developed as power systems planning procedure, and the schemes attempt assessment by inspecting steady state aspects of the power system. When transient behavior of a power system is considered, only precalculated limits are used.

The Operating States of a Power System

In introductory work by Dyliacco in 1968 (7), power system operation was divided into four operating modes: Normal, Alert, Emergency, and Restorative. In 1978, Fink and Carlsen (8) expanded this concept by identifying a fifth operating mode (In extremis), and proposing, for each mode, identification of equality and inequality constraints satisfied or violated. The operating states they gave are:

1. Normal: All constraints are satisfied; reserve margins are adequate to withstand stresses.

2. Alert: All constraints are still satisfied; reserve margins are such that some disturbance could result in a violation of some inequality constraint.

3. Emergency: Inequality constraints are violated; system is still intact and control action could be initiated to restore system to at least the alert state.

4. In extremis: Equality constraints and inequality constraints are violated; the system will no longer be intact and a portion of the load will be lost.

5. Restorative: Control action is being taken to pick up the lost load and to reconnect the system.

Current Issues to be Resolved

To be truly responsive to the needs of the system operator, automated (or dynamic) security assessment must monitor the states of the system, compute limits, and assess security, according to the system configuration that exists at that time. The methodology for this dynamic security

assessment must deal specifically with a transition from normal to alert and emergency states. The emphasis must be on alerting the system operator to potential situations in which breaches of security may occur. This should be done continually, with computations performed in near-real time to give the operator the opportunity to take any preventive measures he should deem necessary. Development of such a methodology, however, requires that three fundamental issues be resolved. These questions (9-11) reflect serious obstacles that need to be overcome:

1. System security is not well-defined. It deals with the transition of the power system, under the influence of a disturbance, from one operating state to another. Assessment of this transition requires:
   -- An assessment of the final state (or steady state response) of the system, which requires a definition of acceptable and unacceptable post-disturbance operating conditions.

   -- An assessment of the system transient response, which requires a definition of what constitutes an acceptable transient performance.
2. Procedures for executing both types of assessments

must be developed. Suitable analysis procedures and reporting criteria must be developed into an integrated assessment package.

3. Analysis of power system behavior has traditionally been conducted in a systems planning environment. Repetitive techniques are used to carefully isolate individual problem conditions before considering remedial action; the technique is used to assure the validity of the resulting design decisions. On-line system analysis, however, must detect weaknesses and suggest remedial action without repetitive search to isolate individual problems; a valid basis for decision-making must be developed directly. This requires development of a new methodology specifically designed to yield information that is valid for decision-making during system operation.

A successful methodology, therefore, must be capable of:

- Offering a clear definition of what constitutes acceptable system performance, thus establishing a criterion for failure
- Recognizing the states of the system in near-real time
- Detecting situations that may lead to emergencies
- Assessing the security of the system in terms

meaningful to the system operator

- Identifying the weaknesses of the system and suggesting preventive measures

Steady State and Transient Responses

The key to computer-automated security assessment appears to be emerging as the process of evaluating the suitability of the current operating conditions in terms of the many possible contingencies which that system might have to face. The quality of the response to these contingencies is evaluated in terms of:

1. Whether in the post-disturbance operating state (steady-state response) all constraints (equality and inequality) are satisfied, and
2. Whether the transient response threatens the system's integrity. These threats are primarily in terms of:
   - Loss of lines due to relaying
   - Shedding of loads by underfrequency relays
   - Loss of synchronism of one or more generators
   - In extreme situations, system islanding and cascading outages.

An unsuitable transient response might be possible even though the post-disturbance operating states are suitable; likewise, a suitable transient response might be possible even though

the post-disturbance state does not satisfy its limiting constraints.

The Margin Concept

The quality of the system response can be dealt with in terms of a margin of acceptable operation. The margin reports the degree to which the equality and inequality constraints are approached. Performance margins are the parameters an operator is likely to watch in monitoring the status of the system. Margins are in common use in the analysis of power system security in terms of equality and inequality constraints; additionally, the concept is implied in most approaches. The literature in this area is vast and only a small representative sample will be cited. A number of authors (12-15) deal with analysis of power dispatch in terms of meeting the network constraints. Garver et al. (16) calculated the load-supplying capability of the generator-transmission network. Optimization techniques using linear programming are given by some authors to develop optimal scheduling from the security standpoint (17). Rescheduling of generators and loads in an emergency is dealt with by Chan and Schweppe (18) and Blaschak et al. (19); while Jarjis and Galiana (20) calculated the steady-state stability limit for a given set of network constraints. Venikov et al. (21) used load flow analysis to identify operating regions

permissible under steady state stability constraints. Ohkubo, Takeda, and Umeura (22) proposed a steady state stability "test index" to evaluate load conditions and interconnection strength.

In contrast to steady state conditions, the transient response cannot be quantified in terms of simple equality and inequality constraints. Most techniques attempt to identify the quality of the transient response in terms of transient stability limits or critical clearing times, while a few authors have introduced transient stability indices. In 1970, Tiechgaeber et al. (23) proposed a parameter which measures the relative transient stability of a power system by direct methods. Rahimi et al. (24) defined transient stability indices based on the concept of potential and kinetic energies. Kuruganty and Billington (25) used a probabilistic technique to develop a single index of transient stability of the overall system, while Ribbens-Pavella et al. (26) introduced a transient stability index using a Lyapunov-like criteria.

Though the margin concept is easily defined, it is seldom used in assessing the transient response of the power system. Recently, a few authors have suggested using a margin for assessing the transient behavior. Di Caprio (27) and Di Capprio and Ribbens-Pavella (28) used a classical model of a multi-area power system in using direct methods to determine

maximum values of perturbation allowable in each area before loss of synchronism; the allowable perturbations were then used to identify a stability margin. Fouad (29) proposed the use of the stability margin concept to deal with multiple disturbances and suggested that the allowable perturbations can be related to either load (generation) changes or network changes. The concept of a transient stability margin also appeared in the Soviet literature as a means of assessing transient system behavior (30).

Review of Direct Methods of Transient Stability Analysis

Assessing transient stability by accounting for transient energy is currently the central focus of direct methods of transient stability analysis. For many years there has been a great interest in using these direct methods of analysis (see (31) for a comprehensive review). These methods all attempt to develop a special function by which the stability of the post-disturbance system can be examined; this function is used to identify a region of stability. A system is stable if, at the end of the disturbance (e.g., the instant of fault clearing), the system trajectory is within this region of stability. Usually, the region of stability is conservative; instability is not assured when the trajectory, at the end of the disturbed period, is outside the region of stability.

Direct methods of transient stability analysis have received a great deal of attention by investigators. Early investigators used functions that described system energy (31,32,33). Later, Lyapunov-type functions were suggested; more recently, energy-type functions are again being used (34,35).

The assessment of transient stability using direct methods has generally produced predictions that are too conservative for practical use. The determination of the region of stability has generally been recognized as the major cause of the conservative results. In general, determination of this region is inferred by using the unstable equilibrium point (UEP). In early work, the region of stability was determined by considering the UEP nearest to the stable equilibrium point (SEP). Later efforts have focused on determining a more appropriate UEP, based upon the particular disturbance under consideration (36,37,34).

One such method, developed by System Control, Inc. (SCI), inspects the motion of a disturbed system and uses the accelerations and the first derivatives of accelerations to determine which UEP is approached by the fault-on trajectory. The technique uses an energy function that is derived from the dynamic equation that describes the motion of the machine rotors relative to the system's inertial center. This energy function is used to calculate the system's critical energy and

the system's fault transient energy; stability is assessed by the comparison of the two (34). This method, called the energy function method, provides the energy function used in this project.

Improvements to the Energy Function Method

As with the other methods of direct stability analysis, SCI's energy function method has not yet proven sufficiently reliable for practical application. The method often fails to predict the mode of instability that is actually encountered by the critical disturbance. Though the concepts behind the energy function method seem sound, predictions based on a UEP of the fault-on trajectory often produce excessively conservative energies. Furthermore, when there are more than one infinitely large inertias (e.g., lumped equivalents of machines outside the study area), the method often fails to converge to and identify a UEP. On the other hand, the energy function method occasionally produces excellent results, well within the accuracy necessary for practical use. The method, itself, and in particular the function used, seems particularly suitable for potential use as a practical direct method of stability analysis.

Scope of This Project

This project deals with developing a tool for assessing the quality of the transient response; this is done in terms of the loss of synchronism of one or more generators. The project also illustrates the potential of this tool in assessing the degree of robustness (or vulnerability) of a power system.

The approach is to develop a tool that assesses the quality of the system transient response to a disturbance in terms of an energy margin for acceptable behavior. This margin will characterize the quality of the transient response as the system moves from its pre-disturbance operating condition to its post-disturbance operating condition.

In exploring the energy function method, and in developing the concept of the transient energy margin, this research found it necessary to develop a fundamental understanding of the issues associated with the use of direct methods of stability analysis. Careful analysis of system trajectories following a large disturbance has contributed valuable information on: the concept of a controlling UEP, the manner in which some machines tend to lose synchronism, and the various components of system transient energy. A significant contribution to the state-of-the-art in this subject has been made by clearly identifying the components of

transient energy directly responsible for system separation.

In assessing the quality of the transient response, a distinction is made between assessing system stability and assessing system security. The first part of this dissertation (Chapters 4-6) focuses on assessing transient stability; Chapter 7 focuses on assessing security. A transient energy margin profile is developed for a given operating condition. This profile is used for assessment. The procedure used is to compute a transient energy margin for various fault contingencies. Faults are placed at various pre-chosen locations within the study system and various breaker operations (or failures) are assumed in clearing the fault. The process is repeated for other hypothetical disturbances from the same initial operating condition. The transient energy margin is then normalized, ranked, and examined for potentially unacceptable situations. The result is a transient energy margin profile of the system at its current operating condition.

Throughout, the project simulation and validation studies were conducted on two power networks: a 4-generator, 11-bus, system, and on a 17-generator, 163-bus, system. The latter is a reduced version of the actual power network of the State of Iowa.

CHAPTER 2. TRANSIENT STABILITY ANALYSIS USING THE ENERGY FUNCTION

Discussion of Transient Stability

In a small power system subjected to a large disturbance, the motion of the synchronous machines is simple to understand. A disturbance, such as a fault or an abrupt switching of significant loads, creates a power imbalance at each machine. The electrical power transmitted out to the system does not equal the net mechanical power that drives the generator. The mismatch between "power-out" and "power-in" accelerates (or decelerates) the generators. At the beginning of the disturbance, the generator rotors are at their pre-fault steady state operating state, i.e., at their stable equilibrium point (SEP). Following the disturbance, the rotors will seek new equilibrium positions. Usually the pre-fault and post-fault equilibrium positions are different. They are referred as the stable equilibrium points (SEPs). The transient response of the system is the motion (or trajectories) of the rotors as they move from the pre-fault SEP and attempt to settle at the post-fault SEP.

A fault condition introduces an initial fault-on period during which a portion of the transmission system is disabled, substantially reducing the power output of some generators. During this period the imbalance between power-in and power-out for these generators is particularly severe, and the

machines are rapidly accelerated (or decelerated) away from the pre-fault SEP. At clearing, the post-fault system configuration is established, resulting in restorative forces that draw the generators toward their post-fault SEP. The system seeks this post-fault SEP, starting from a condition at clearing, where the machines are in motion and not at equilibrium. Some machines may have very advanced angles and may be moving rapidly. To reach a post-fault stable equilibrium condition, these machines must decelerate and reach zero velocity at a time when the forces tend to return the generator to the SEP.

The process by which the restoring forces slow the moving rotors is primarily one of converting kinetic energy (KE) into potential energy. (A relatively small amount of KE is converted into dissipative losses; as is common in the literature, this dissipative component is included when using the term potential energy.) If the restoring forces everywhere succeed in slowing the generators and returning them toward the SEP, stability will be achieved; in such cases the kinetic energy is successfully converted into potential energy.

It is possible, however, that the high velocities and advanced rotor positions existing at clearing may be large enough to cause one or more generators to be subjected to forces that are no longer in the direction of the SEP, but are

in a direction to accelerate those generators away from the rest of the system. In this case, not all of the kinetic energy is successfully converted into potential energy, and synchronism is not maintained, causing instability.

Assessing Stability by Energy Accounting

In assessing the stability of the transient response, we inspect the transition between the pre-fault SEP and the post-fault SEP and attempt to ascertain that no generators would lose synchronism with the rest of the system. As an alternative, we can ascertain whether the system will successfully convert the kinetic energy into potential energy.

To assess the stability of the transient response by direct methods, current research has focused on techniques that account for system energy. A disturbance is seen as an event that injects energy into the system. The energy at the instant of clearing is the fault transient energy, V_{cl}. For the system to remain stable, this fault energy must be absorbed as potential energy. The post-disturbance system, however, is seen as having a limit to its ability to absorb potential energy. Direct methods of stability analysis attempt to compute this limit, called the critical energy (V_{cr}), and compare it with the energy introduced by the fault (V_{cl}). The system is stable if the fault energy is within the system's potential-energy-absorbing capacity:

$$V_{cr} > V_{cl}$$

On the other hand, the system is unstable if the fault energy exceeds the potential-energy-absorbing capacity:

$$V_{cr} < V_{cl}$$

The Equal-Area Criterion

Direct methods of assessing transient stability by accounting for system energy can be illustrated by using the well-known equal-area criterion for a one-machine-infinite-bus system. Figure 2-1 shows the power-angle curve with pre-fault, faulted, and post-fault networks represented. The rotor position θ^{s1} represents the pre-fault SEP. The angle θ^{s2} is the post-fault SEP that the system is attempting to reach. The angle θ^{u} is the unstable equilibrium point (UEP) at which the restorative forces are zero and beyond which power-in exceeds power-out; θ^{u} is the point-of-no-return beyond which the system goes unstable.

The area of the power angle curve represents energy; the area A_2+A_3, between the SEP (θ^{s2}) and the UEP (θ^{u}), represents the maximum potential energy storage capacity of the post-fault system. If θ^{cl} is the fault clearing angle, area A_1 represents the transient kinetic energy stored in the motion of the disturbed generator (at the clearing instant), while A_3 represents the potential energy stored by virtue of the advanced rotor position (at clearing). The area A_2 is the potential energy storing capacity of the system remaining at

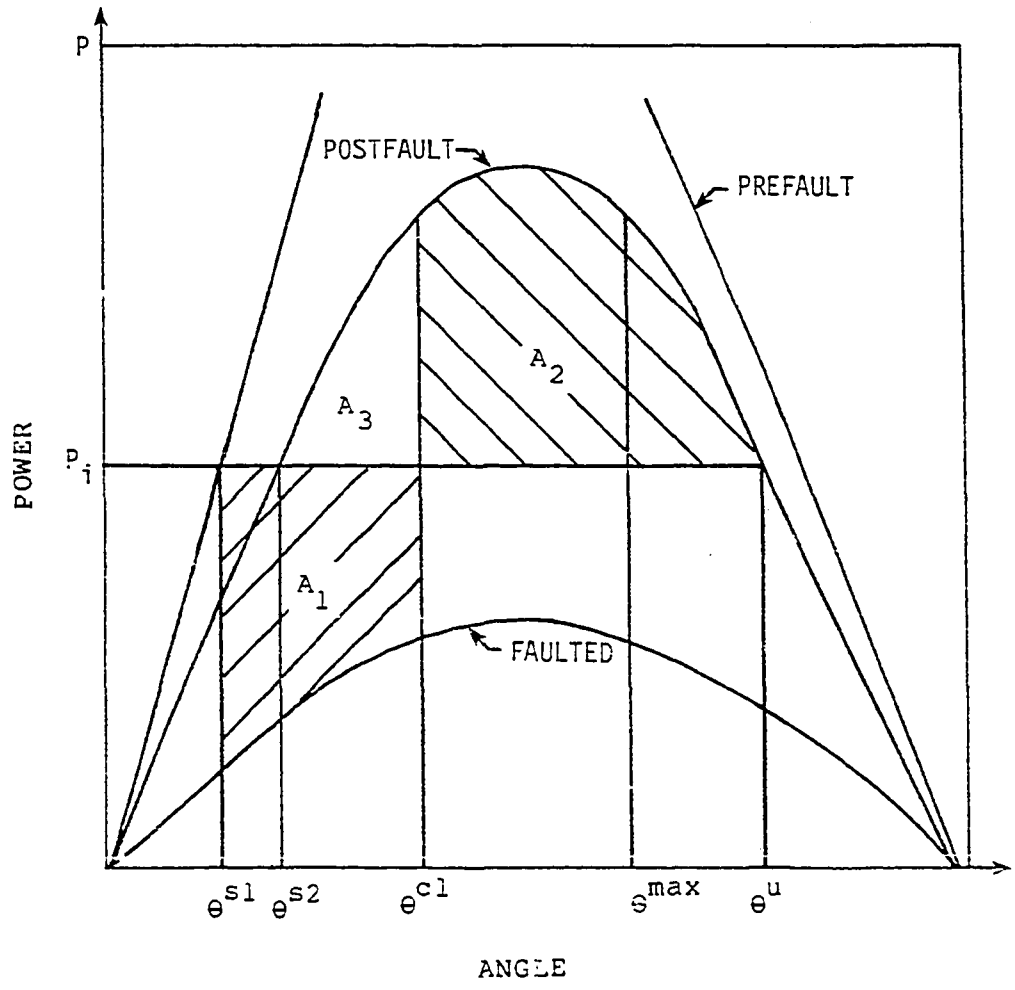

Figure 2-1. Energy margin for one-machine-infinite-bus system

the instant of clearing. As the rotor velocity decreases (but the angle increases) after clearing, kinetic energy is converted into potential energy. That is, the kinetic energy, A_1, is stored as potential energy, A_2. The maximum angle θ^{max} occurs when all of the kinetic energy is converted to potential energy (i.e., when A_2, between θ^{cl} and θ^{max}, equals A_1). The limiting case for transient stability is reached when θ^{max} and the UEP, θ^{u}, coincide.

Direct energy methods of stability analysis attempt to compute the fault transient energy (V_{cl}) at clearing, A_1+A_3, and the critical energy (V_{cr}), A_3+A_2 (extending to θ^{u}); if the fault energy is less than the critical energy, the system is stable.

This simple qualitative picture is the basis for many attempts to analyze power system stability using direct methods. The quantitative description of the system energy, particularly the critical energy, has been the subject of extensive investigation for many years (31).

More Complex Systems

To assess the transient stability of more complex systems, using direct methods, it is necessary to extrapolate the one-machine-infinite-bus concepts to larger dimensions. This extrapolation, it seems, is quite difficult to accomplish. The n-machine system will introduce n angles in

the angle space and n velocities in the velocity space. Therefore, the extrapolation from one machine to n machines will introduce 2n degrees of freedom (including time). This introduces the conceptual complexities of 2n-dimensional space; it is difficult to visualize the physical meaning behind the 2n-dimensional mathematics. Direct methods require proper accounting of energy in this 2n-space, as well as proper interpretation of the meaning attached to this energy.

Transient Kinetic Energy and the Inertial Center

One fundamental step in accounting for the energy contributing to system separation is the so-called center-of-inertia formulation of the system equations. (This formulation is also referred to in the literature as center-of-angle.) In the center-of-inertia formulation, the equations describing the motion of the synchronous machines are formulated with respect to a fictitious inertial center; this is in contrast to the usual situation where the machine's equations are formulated with respect to a synchronously moving frame of reference. The effect is to describe only the excursions of the generators with respect to a central grouping (i.e., the center-of-inertia). The importance of this formulation lies in clearly focusing on the motion that tends to separate one or more generators from the rest of the system, and thus removing a substantial component of system

transient energy that does not contribute to instability, namely, the energy that accelerates the inertial center (38,39). With the center-of-inertia formulation, the forces tending to separate some generators from the rest of the system (and the energy associated with these forces) can be easily identified (34,35).

Potential Energy Surfaces and the Critical Energy

The process of extrapolating the equal-area criterion from the one-machine-infinite-bus system into an n-bus system is a task of significant complexity. The following simplified picture seems to emerge from recent research (34,40,41,42). In the one-machine-infinite-bus system, the position of the machine rotor had a specific corresponding potential energy. In the n-machine system, each rotor position likewise corresponds to a specific energy, but with n machines, the energy becomes a function of n dimensions. The total system potential energy is visualized as an n-dimensioned potential energy terrain. The stable equilibrium point is the minimum energy point in this n-dimensioned space. Every point in the angle space has an energy associated with it. The entire space represents all possible positions of the generators.

Three-Dimensional Energy Terrain

To help visualize the energy in an n-dimensioned space, the introduction of a three-dimensional case is useful. A

three-machine energy terrain is depicted in Figure 2-2. In the horizontal plane, one axis shows the relative angle between machines one and three, and the other axis shows the relative angle between machines two and three; the vertical axis shows potential energy. The energy contours are lines of equal potential energy. The point marked "SEP" is the post-disturbance stable equilibrium position (corresponding to θ^{s2} in Figure 2-1). It is also taken as the zero energy datum. The energy terrain appears as a valley with the SEP at the lowest point. The valley is surrounded by hills of varying elevation. The energy terrain represents the energy values of all possible rotor positions that the system could have.

The ability of the post-disturbance system to convert fault energy into potential energy depends on the particular trajectory a disturbance produces, that is, the potential energy that the system absorbs depends upon the particular segment of the terrain that the trajectory traverses. As the trajectory passes parallel to the energy contours, little or no fault energy is converted to potential energy by the change in rotor positions. As the trajectory moves up a steep terrain, a greater amount of fault energy is absorbed as potential energy. As the trajectory climbs the steep walls of the valley, it converts fault kinetic energy into potential energy. When all of the kinetic energy is converted into

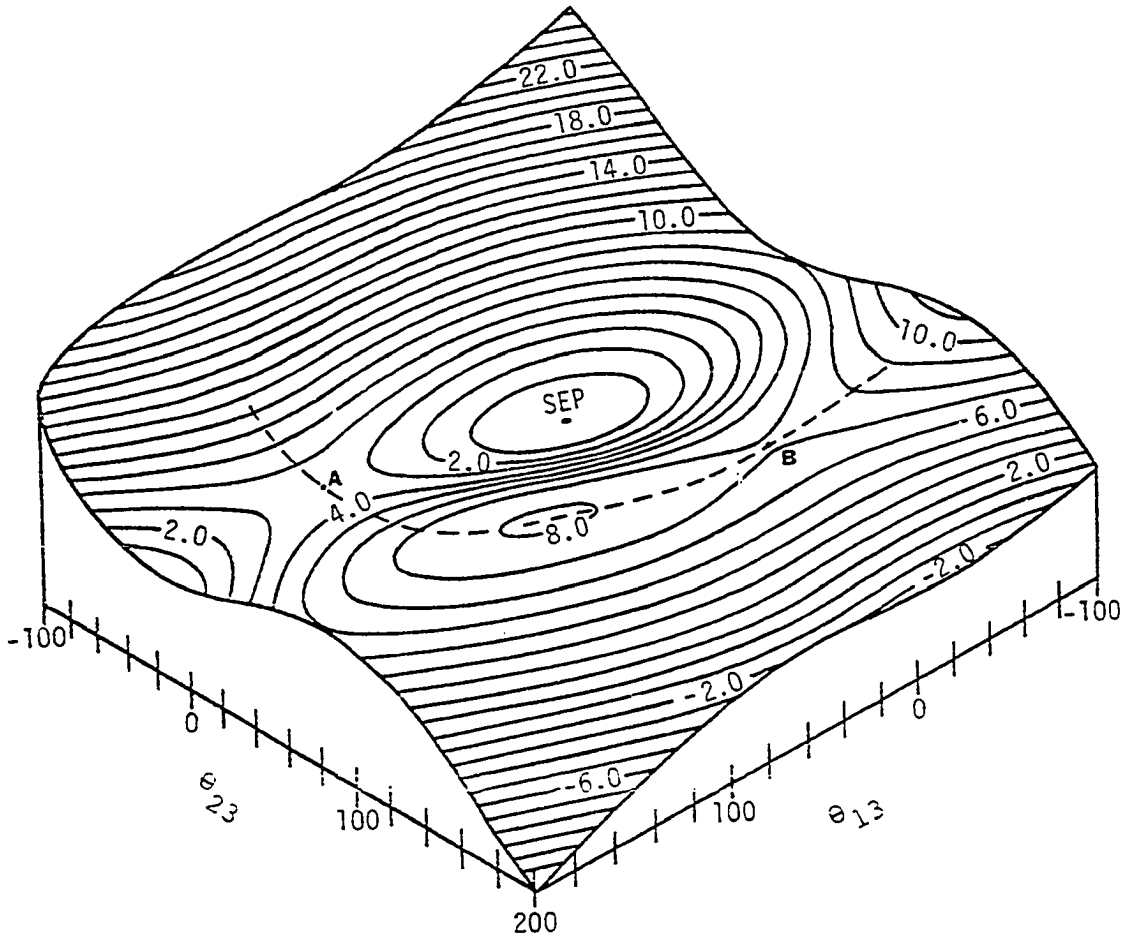

Figure 2-2. Potential energy function for a 3-machine system (from reference 35)

potential energy the trajectory will stop its ascent and will not climb higher. Thus, the faulted trajectory is analogous to a particle climbing up the hills around this valley. The disturbance imparts kinetic energy into the particle; the particle moves up the hill converting kinetic energy into potential energy. The trajectory is stable if the particle eventually settles at the SEP. An unstable trajectory, on the other hand, is one in which the particle manages to breach the summit and escape from the valley. The escape energy is the energy of the summit *at the point of escape.* It is evident that the escape energy is dependent upon the point where the particular trajectory breaches the summit.

All possible escape points are indicated on Figure 2-2 by the dotted line. These energy values represent the maximum energy of a trajectory escaping the valley and are *points-of-no-return* on any escape trajectory. Thus, the dotted line represents a locus of all of the possible escape energies.

The Unstable Equilibrium Points

We note that there are two local minimum escape points, marked "A" and "B" on Figure 2-2. These are *unstable equilibrium points* (and are the focus of the direct methods). Point "A" represents a local minimum escape energy of about 3.5 units of energy, while point "B" represents a local

minimum escape energy of about 7 units of energy. The maximum amount of fault energy that the system can absorb (as potential energy) in a worst-case trajectory would correspond to Point "A". If escape in the direction of Point "A" is not a physical possibility then Point "B" may be the worst-case point of escape. The smallest amount of fault energy that could drive the system unstable is that of the lowest energy UEP that is physically realizable.

The points "A" and "B" are UEPs and, as seen in Figure 2-2, represent local minimum escape points on the ridge of the energy terrain. It should be noted that the UEPs represent minimum/maximum points (e.g., are saddle points): these UEPs are a maximum in that they represent points on the ridge, and a minimum in that they are minimum points on the ridge.

A critical fault trajectory is seen as a trajectory that climbs the energy terrain, converting all of its kinetic energy into potential energy at the instant the particle arrives at the summit. This trajectory arrives at the escape point with zero velocity; it is undetermined as to whether or not the trajectory will become unstable. Theoretically, there is an infinite number of critical trajectories, but it is clear that the lowest energy critical trajectories will be ones that pass through the UEP. The UEPs are recognized as local minimum-energy escape points available to trajectories. The energy associated with the relevant UEP identifies the

critical energy V_{cr} for a given trajectory.

n-Dimensional Energy Terrains

The energy terrain of the multi-machine power system is visualized in a fashion similar to the three-machine system of Figure 2-2. A disturbance injects energy into the system and sets the generators into motion; the trajectory is visualized as a particle moving through n-dimensional space, converting kinetic energy into potential energy. The energy terrain, as reflected by potential energy contours, account for the amount of potential energy per unit of rotor displacement in the n-space. The amount of rotor motion (and corresponding potential energy absorbed) necessary to achieve instability will vary from one trajectory to another. If the system trajectory moves through a segment of high potential energy, then the network's ability to convert kinetic energy into potential energy is high, and a severe disturbance (as reflected in the amount of transient energy injected in the system clearing the fault) can be withstood. On the other hand, if a fault trajectory moves in a region where the potential energy surfaces are shallow, the network's ability to absorb transient energy is reduced, and instability occurs with a smaller disturbance.

The locus of all possible escape points forms a hypersurface in the n-dimensional space. The UEPs are local

minimum-energy escape points on this hypersurface. A UEP that is the local minimum for a given trajectory is considered the relevant or controlling UEP for that trajectory; that is, the UEP closest to the trajectory of the disturbed system is thought to decide the stability of the transient response. The critical energy (i.e., the maximum amount of energy a disturbance can safely inject) is the energy which corresponds to this relevant or controlling UEP.

If the n-machine system is faulted and the fault is cleared before the critical clearing time t_c, the system trajectory peaks before reaching the limiting hypersurface. For a clearing time exceeding t_c, the hypersurface is crossed (usually at a point other than the UEP) and instability results. A truly critical trajectory is one that reaches the hypersurface at a UEP with zero velocity.

The Energy Function

Power System Representation

The mathematical model used to describe the power system transient behavior is the classical model (see Chapter 2 of reference 43). This model is based on the following assumptions:

1. Mechanical power into each generator is constant
2. Damping is negligible
3. Constant-voltage-behind-transient-reactance generator representation

4. Mechanical rotor angles correspond to the angle of the internal generator voltage

5. Loads are represented by passive impedances

The classical model is useful for the study of the transient response during the "first swing" of a disturbance, when the motion of the machine rotors are determined primarily by the electrical synchronizing forces and the inertial forces.

For the classical model, the equations of motion for machine i are:

$$\begin{aligned} M_i\ddot{\delta}_i &= P_i - P_{ei} \\ \dot{\delta}_i &= \omega_i - 1 \end{aligned} \qquad i = 1,2,\ldots,n \tag{2-1}$$

where

$$P_{ei} = \sum_{\substack{i=1 \\ i\neq j}}^{n} E_i E_j [B_{ij}\sin(\delta_i - \delta_j) + G_{ij}\cos(\delta_i - \delta_j)]$$

$$P_i = P_{mi} - E_i^2 G_{ii}$$

and, for unit i

P_{mi} = mechanical power input

G_{ii} = real part of the driving point admittance for the internal generator node

B_{ij} = transfer susceptance between nodes i and j

E_i = constant voltage behind transient reactance

δ_i = generator rotor angle

ω_i = generator rotor speed

M_i = moment of inertia constant = $2H_i/\omega_r$

ω_r = rated synchronous speed

The Center of Inertia Formulation

Equation 2-1 is written with respect to an arbitrary, synchronously rotating frame of reference. The equation must be re-formulated with respect to the center-of-inertia for all machines (34).

For an n-generator system with rotor angles δ_i and inertia constants M_i, i=1, 2,...., n (where $M_i = 2H_i/\omega_r$), the position θ_o and speed ω_o of the inertial center are given by

$$\theta_o = (1/M_t) \sum_{i=1}^{n} M_i \delta_i$$

$$\omega_o = (1/M_t) \sum_{i=1}^{n} M_i \dot{\delta}_i \qquad (2\text{-}2)$$

where

$$M_t = \sum_{i=1}^{n} M_i$$

The motion of the center-of-inertia is given by

$$M_t\dot{\omega}_o = \sum_{i=1}^{n} [P_i - P_{ei}] \triangleq P_{coi}$$

and

$$\dot{\theta}_o = \omega_o$$

(2-3)

The generators' angles and speeds with respect to the center-of-inertia are defined by

$$\theta_i = \delta_i - \theta_o$$
$$\omega_i = \dot{\delta}_i - \omega_o$$

(2-4)

The equations for the motion of the individual machines, with respect to the center-of-inertia, become (34)

$$M_i\dot{\omega}_i = P_i - P_{ei} - (M_i/M_t)P_{coi}$$
$$\dot{\theta}_i = \omega_i$$

(2-5)

The Energy Function

The expression for the system transient energy is formulated from equation 2-5. First, the swing equation is multiplied by $\dot{\theta}_i$ and the sum is formed:

$$\sum_{i=1}^{n} [M_i\dot{\omega}_i - P_i + P_{ei} + (M_i/M_t)P_{coi}]\ \dot{\theta}_i$$

Recognizing that

$$\sum_{\substack{i=1\\ i\neq j}}^{n}\sum_{j=1}^{n} E_i E_j B_{ij}(\sin\theta_{ij})\dot{\theta}_i = \sum_{i=1}^{n-1}\sum_{j=i+1}^{n} E_i E_j B_{ij}(\sin\theta_{ij})\dot{\theta}_{ij}$$

and

$$\sum_{\substack{i=1\\ i\neq j}}^{n}\sum_{j=1}^{n} E_i E_j G_{ij}(\cos\theta_{ij})\dot{\theta}_i = \sum_{i=1}^{n-1}\sum_{j=i+1}^{n} E_i E_j G_{ij}(\cos\theta_{ij})(\dot{\theta}_i+\dot{\theta}_j)$$

we integrate 2-5 with respect to time; chosing the limits arbitrarily as "a" and "b". The expression for the system transient energy V becomes the function:

$$V\Big|_{\theta^a}^{\theta^b} = (1/2)\sum_{i=1}^{n}[M_i[(\omega_i^b)^2 - (\omega_i^a)^2]$$

$$-P_i(\theta_i^b - \theta_i^a)]$$

$$-\sum_{i=1}^{n-1}\sum_{j=i+1}^{n} E_i E_j [B_{ij}(\cos\theta_{ij}^b - \cos\theta_{ij}^a)$$

$$-\int_{(\theta_i^a+\theta_j^a)}^{(\theta_i^b+\theta_j^b)} \cos\theta_{ij}\, d(\dot{\theta}_i + \dot{\theta}_j)] \qquad (2\text{-}6)$$

This function defines the system energy between any two points in the state space. We use the notation

$$V\Big|_{\theta^a}^{\theta^b}$$

as a shorthand for the energy function. The superscripted

terms θ^a and θ^b imply both the angles and velocities of the points a and b in the state space (44,45). In the usual application, θ^a is the SEP, where the angles are θ^{s2} and the velocities are zero.

The components of the energy function are readily identifiable in familiar terms. The first term is the kinetic energy, the second term is the position energy which is part of the system potential energy. The third term is the magnetic energy, which is also part of the system potential energy. The fourth term is the dissipation energy, which is the energy dissipated in the network transfer conductance (which represents both transmission network conductance and system loads) and is also considered part of the system potential energy. Following the terminology common in the literature, the term potential energy will be used to include the last three energy components. Furthermore, this dissertation refers to the potential energy being "absorbed" by the system even though a portion is dissipative.

Approximating the Dissipative Term

It is noted that the last term of equation 2-6 (the dissipative term) can be evaluated only if the system trajectory is known. Various methods of approximating this term, without prior knowledge of the trajectory, have been suggested in the literature (33,34,40,41,42,46). The method

used in this investigation is suggested by Athay et al. (34,35). Their expression for the energy function is

$$V\Big|_{\theta^a}^{\theta^b} = \sum_{i=1}^{n} [(1/2)M_i(\omega_i^b)^2 - (1/2)M_i(\omega_i^a)^2 - P_i(\theta_i^b - \theta_i^a)] - \sum_{i=1}^{n-1}\sum_{j=i+1}^{n} E_i E_j B_{ij}(\cos\theta_{ij}^b - \cos\theta_{ij}^a) + I_{ij}\Big|_{\theta_a}^{\theta_b} \qquad (2\text{-}7)$$

where

$$I_{ij}\Big|_{\theta^a}^{\theta^b} = \text{an approximated term to account for transfer conductances,}$$

$$= E_i E_j G_{ij}\left[\frac{(\theta_i^b+\theta_j^b)-(\theta_i^a+\theta_j^a)}{(\theta_{ij}^b-\theta_{ij}^a)}\right](\sin\theta_{ij}^b - \sin\theta_{ij}^a)$$

Transient Fault Energy

In examining equation 2-7, we see that if the SEP angle θ^s is taken as the lower limit of integration θ^a (e.g., θ^s is the zero energy datum), the transient energy at any instant is

$$V = V\Big|_{\theta^s}^{\theta^b}$$

The expression evaluates the transient energy in the system at point θ^b in the state space. When θ^a represents the

post-fault SEP and θ^b represents the speeds and angles immediately after clearing, the energy function calculates the energy injected into the system by the disturbance, i.e., the fault transient energy, V_{cl}.

$$V_{cl} = V\Big|_{\theta^{s2}}^{\theta^{cl}}$$

Critical Energy

According to the energy function method, the critical energy is that energy associated with the appropriate UEP (θ^u) for the particular disturbance under consideration. A critical trajectory is assumed to start at the SEP and reach the appropriate UEP with zero velocities. For such a trajectory, the critical energy is the energy at the appropriate UEP (θ^u) calculated with respect to the post-fault SEP (θ^{s2}):

$$V_{cr} = V\Big|_{\theta^{s2}}^{\theta^{u}}$$

Since the kinetic energy at both θ^u and θ^{s2} is assumed zero, the critical energy is potential energy only.

Stability Analysis via Direct Methods

The approach used by direct methods of transient stability assessment (34) is to compare the transient fault energy V_{cl} with the critical V_{cr}. For the system to be stable,

the fault energy must be successfully absorbed as potential energy during the trajectory. This is taken to mean that all kinetic energy is converted to potential energy, and thus stability is predicted when $V_{cr} > V_{cl}$, which requires:

$$V\Big|_{\theta^{s2}}^{\theta^{u}} > V\Big|_{\theta^{s2}}^{\theta^{cl}}$$

Analogy with the Equal-Area Criterion

The energy function can easily be illustrated on the one-machine-infinite-bus system with zero transfer conductances (47). This is useful in that it illustrates the various features of the energy function and provides physical insight as to what the energy function actually represents. The power angle curves for the one-machine-infinite-bus system, neglecting transfer conductance, are shown in Figure 2-3. The angles indicated as θ^{s1}, θ^{s2}, θ^{cl} and θ^{u} are respectively: pre-fault SEP, post-fault SEP, clearing angle, and UEP.

Consider the situation at clearing. The energy function, using the post-fault network, evaluates the energy between the post-fault SEP (θ^{s2}) and clearing (θ^{cl}) by:

$$V_{cl} = V\Big|_{\theta^{s2}}^{\theta^{cl}}$$

$$= 1/2(\omega^{cl})^2 - E_1E_2B_{12}(\cos\theta^{cl} - \cos\theta^{s2})$$

$$- (P_m - E_1^2 G_{11})(\theta^{c1} - \theta^{s2})$$

The first term of equation 2-8 is the transient kinetic energy and, according to the well-known equal-area criterion, represents area oabf in Figure 2-3. The second and third terms represent the potential energy of area cdf, and is familiar as the potential energy gained during the disturbance.

It should be noted, incidentally, that fault transient energy V_{c1} is often computed with respect to the pre-fault SEP θ^{s1}. This calculation uses θ^{s1} as the reference and the energy at clearing would include the area oed, which represents the energy between θ^{s1} and θ^{s2}:

$$\text{Area oed} = V\Big|_{\theta^{s1}}^{\theta^{s2}}$$

The velocity at either stable point is assumed to be zero. The total system potential energy absorbing capacity, V_{cr}, is represented by the area cdfg and is the energy between the SEP θ^{s2} and the UEP θ^{u}.

$$V_{cr} = \text{Area cdfg} = V\Big|_{\theta^{s2}}^{\theta^{u}}$$

In evaluating the critical energy, the velocity at both the SEP (θ^{s2}) and the UEP (θ^{u}) is assumed zero, so that V_{cr}

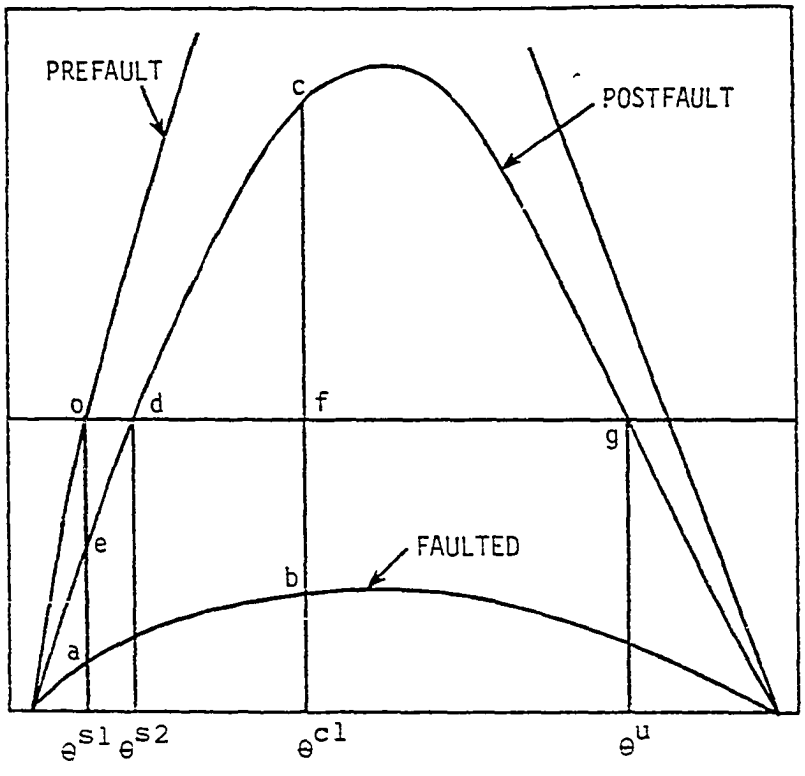

Point o: pre-fault operating point; $\theta = \theta^{s1}$, $t = t_o^-$

Point a: electrical power at $t = t_o^+$, $\theta = \theta^{s1}$

Point b: electrical power at $t = t_{cl}^-$, $\theta = \theta^{cl}$

Point c: electrical power at $t = t_c^+$, $\theta = \theta^{cl}$

Point d: post-fault operating point, i.e., operating point then transient subsides, $t \to \infty$, $\theta = \theta^{s2}$

Figure 2-3. Power angle curves for one-machine-infinite-bus system (transfer conductances neglected)

is purely potential energy. If θ^{cl} is the critical clearing angle, then

$$V_{cl} = V_{cr}$$

(provided that V_{cl} is computed with respect to θ^{s2}). This equality corresponds to the equal area criterion where

$$\text{area oabf} + \text{area cdf} = \text{area dgcd}$$

or

$$\text{area oabf} = \text{area cfg}$$

CHAPTER 3. THE TEST POWER NETWORKS USED FOR VALIDATION

The Two Test Systems

This research used the energy function to analyze several faults on two test systems; the result is a detailed accounting of the system energy involved in a disturbance. The two power systems are a 4-generator system and a 17-generator equivalent of the power system serving the State of Iowa[1].

The 4-Generator Test System

The 4-generator test system, shown in Figure 3-1, is a modified version of the 9-bus, 3-machine, 3-load system widely cited in the literature and referred to as the WSCC system (43). Two changes were made to the WSCC system:

- Changing the rating of the transmission system from 230 kV to 161 kV to avoid an excess VAR problem. (The R and X values in per unit remain unchanged.)
- Adding a fourth generator, connected by a step-up transformer and a double-circuit 120-mile, 161-kV line. (The new generator has the same rating as one of the original generators, giving a new system generating capacity of 680 MW.)

The generator data and initial operating conditions,

---

[1]While the networks were used in this research, their development and testing was not part of the work done for this dissertation. The networks were developed by Dr. K. Kruempel, Iowa State University.

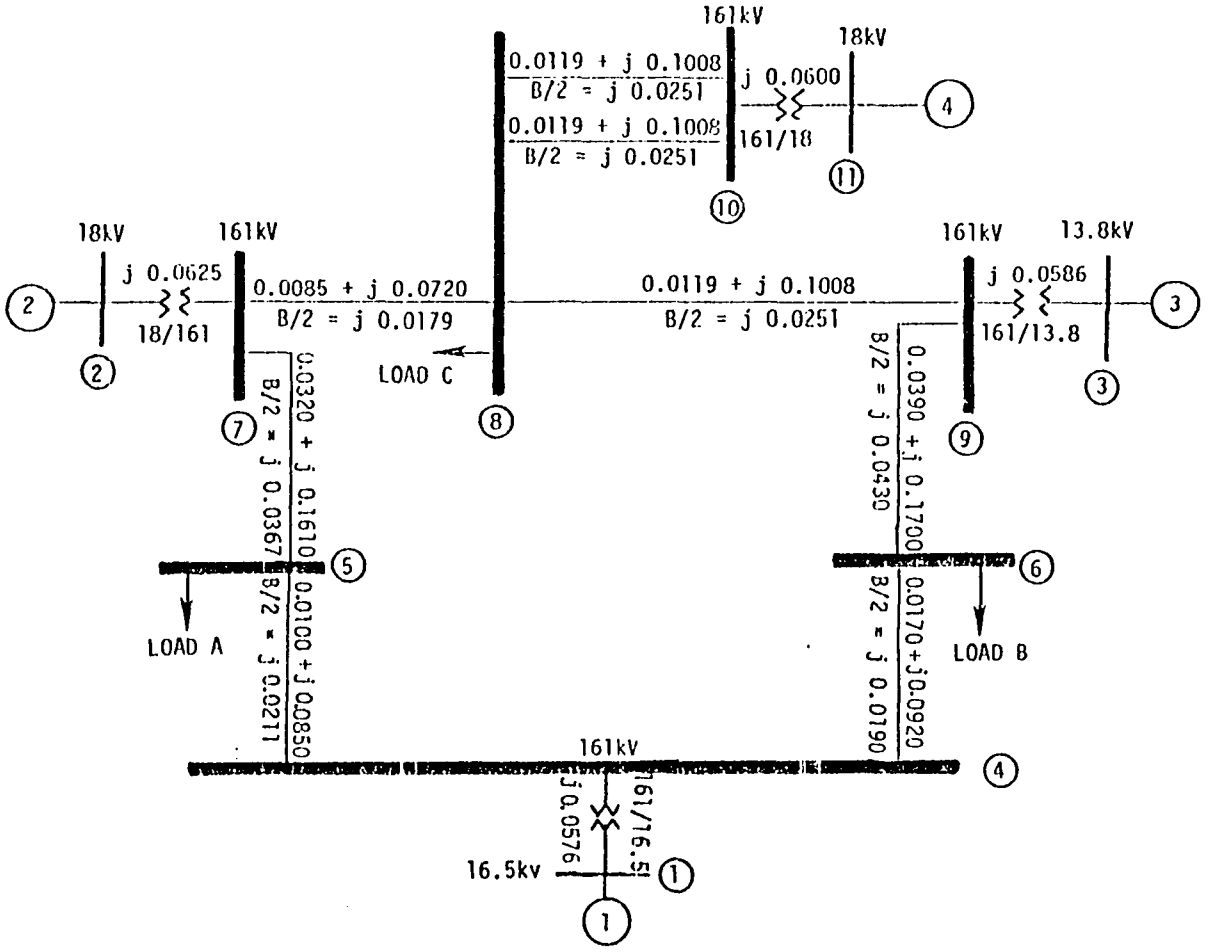

Figure 3-1. The 4-generator test network

including the internal generator voltages, are given in Table 3-1. The 4-generator system was primarily used for initial validation of new procedures and computer programs developed in the project. For faults near generator No. 4, the mode of instability is simple and the system's transient behavior is rather predictable.

17-Generator, Reduced Iowa System

The Power System Computer Service of Iowa State University has been involved in several full-scale stability studies for new generating units in the Iowa area. The Philadelphia Electric Transient Stability Program was used in these studies. The base data and the results of one of these studies, the NEAL 4 stability study, were used to develop a Reduced Iowa System model. Figure 3-2 shows the main study region and Figure 3-3 shows a partial one-line diagram of the area. The base load-flow system is modeled with 862 busses and 1323 lines and transformers. Most of the transmission lines are 345 kV and 161 kV; some of the lines are 230 kV, 115 kV, or 69 kV. The base load-flow model was reduced by a load-flow network reduction program to a network with 163 busses and 304 lines and transformers. Of the 163 busses, 30 are terminal busses of the equivalent networks; of the 304 lines and transformers, 69 are equivalent lines. The resulting system is referred to as the Reduced Iowa System.

Table 3-1. Generator data and initial conditions

No.	Generator* Parameters H MWs/MVA	x'_d pu	Initial Conditions P_m pu	Internal Voltage E pu	Internal Voltage deg.	θ^{sl} deg.
	4-generator system					
1	23.64	0.0608	2.269	1.0967	6.95	-4.08
2	6.40	0.1198	1.600	1.1019	13.49	2.45
3	3.01	0.1813	1.000	1.1125	8.21	-2.76
4	6.40	0.1198	1.600	1.0741	24.90	13.91
	17-generator system					
1	100.00	0.0040	20.000	1.0032	-27.92	-6.26
2	34.56	0.0437	7.940	1.1333	-1.37	20.28
3	80.00	0.0100	15.000	1.0301	-16.28	5.38
4	80.00	0.0050	15.000	1.0008	-26.09	-4.42
5	16.79	0.0507	4.470	1.0678	-6.24	15.41
6	32.49	0.0206	10.550	1.1235	-26.95	-5.29
7	6.65	0.1131	1.309	1.0163	-23.02	-1.35
8	2.66	0.3115	0.820	1.1235	-26.95	-5.29
9	29.60	0.0535	5.517	1.1195	-12.41	9.25
10	5.00	0.1770	1.310	1.0652	-11.12	10.53
11	11.31	0.1049	1.730	1.0777	-24.30	-2.64
12	19.79	0.0297	6.200	1.0609	-10.10	11.55
13	200.00	0.0020	25.709	1.0103	-28.10	-6.44
14	200.00	0.0020	23.875	1.0206	-26.76	-5.10
15	100.00	0.0040	24.670	1.0182	-21.09	0.56
16	28.60	0.0559	4.550	1.1243	-6.70	14.95
17	20.66	0.0544	5.750	1.1160	-4.35	17.30

*To 100 MVA base.

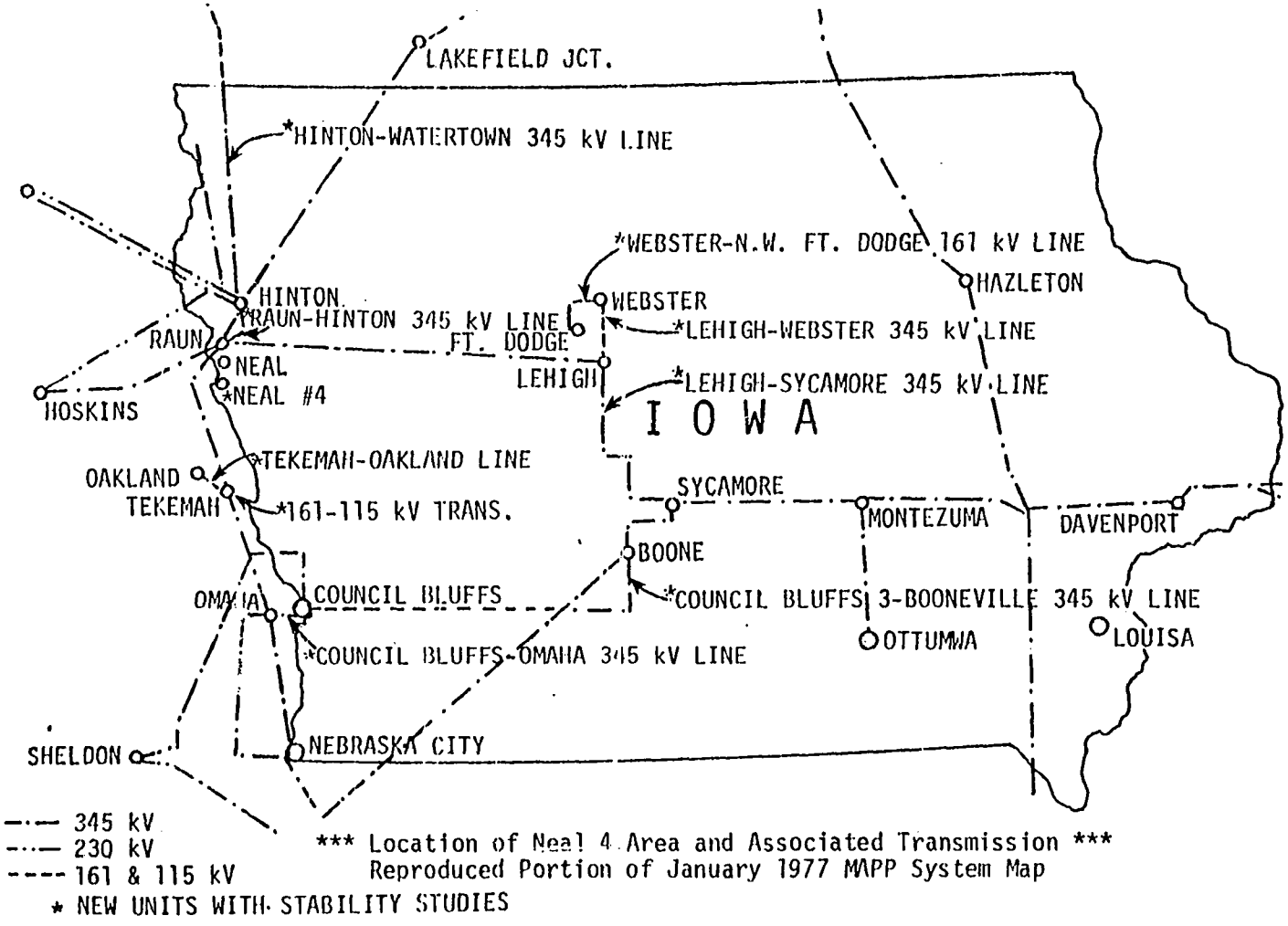

Figure 3-2. The main study region for the 163-bus Reduced Iowa System

Figure 3-3. One-line diagram of the study area

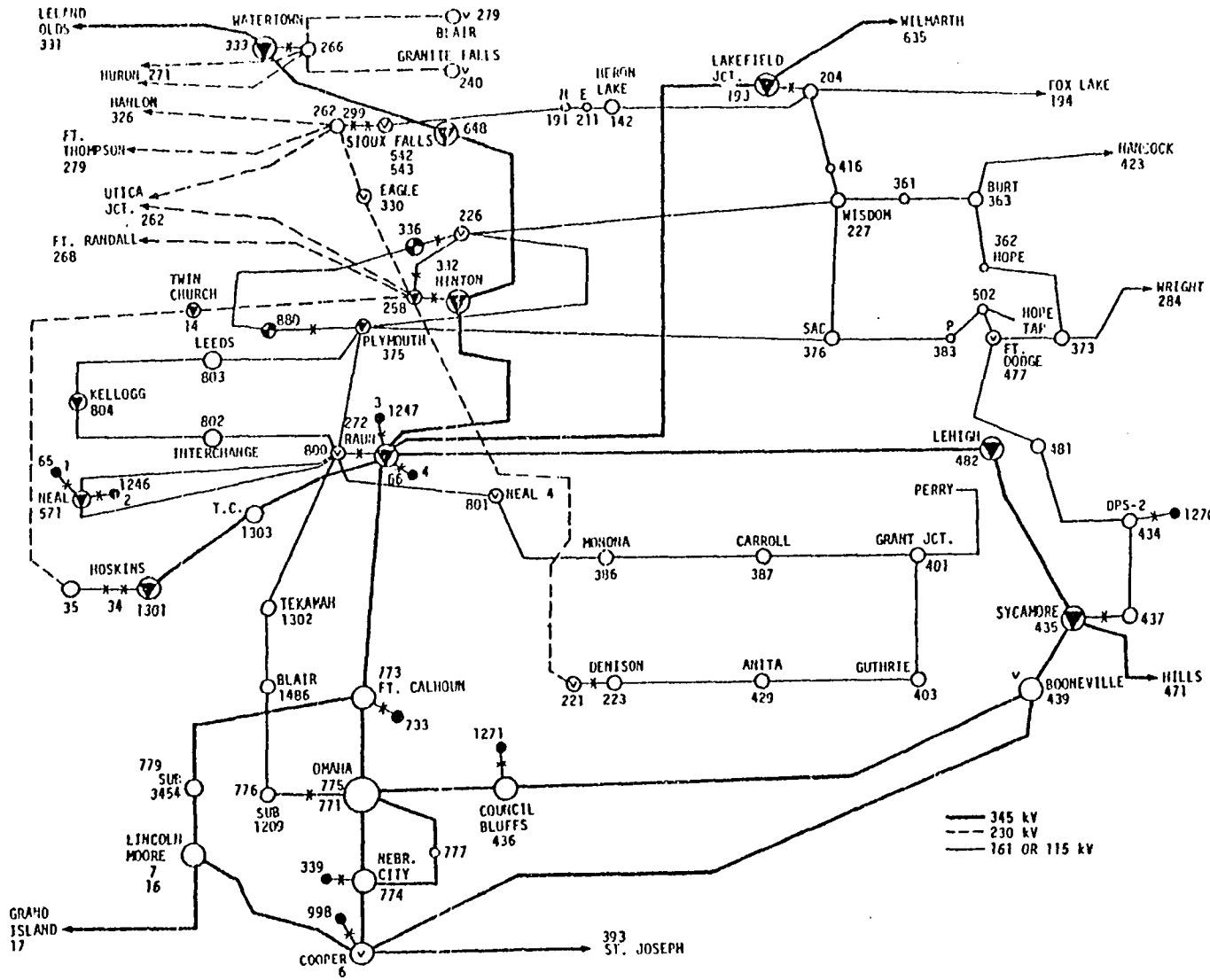
LELAND OLDS 331
WATERTOWN 333
266
279 BLAIR
GRANITE FALLS 240
HURON 271
HAHLON 326
FT. THOMPSON 279
UTICA JCT. 262
FT. RANDALL 268
262 299
SIOUX FALLS 542 543
648
EAGLE 330
336
226
332 HINTON
258
TWIN CHURCH 14
880
PLYMOUTH 375
LEEDS 803
KELLOGG 804
802 INTERCHANGE
800
272 RAUN
3 1247
65 1
NEAL 571
1246 2
66 4
T.C. 1303
HOSKINS 35 34 1301
TEKAMAH 1302
BLAIR 1486
773 FT. CALHOUN
733
779 SUB 3454
776
OMAHA 775 771
SUB 1209
1271
COUNCIL BLUFFS 436
LINCOLN MOORE 7 16
339
NEBR. CITY 774
777
998
COOPER 6
GRAND ISLAND 17
393 ST. JOSEPH
NEAL 4
801
HERON LAKE
N E 191 211 142
LAKEFIELD JCT. 193
204
WILMARTH 635
FOX LAKE 194
416
361
BURT 363
HANCOCK 423
WISDOM 227
362 HOPE
502
HOPE TAP
WRIGHT 284
SAC 376
P 383
FT. DODGE 477
373
LEHIGH 482
481
PERRY
DPS-2 1270
434
MONONA 386
CARROLL 387
GRANT JCT. 401
DENISON 221 223
ANITA 429
GUTHRIE 403
SYCAMORE 435
437
BOONEVILLE 439
HILLS 471
345 kV
230 kV
161 OR 115 kV

The Reduced Iowa System was selected to reproduce the "first swing" characteristics of the original 862 bus model. This was done using 17 generators. Seven of these generators correspond directly to generators in the original system, four generators are single generator equivalents of 2-machine pairs at the same generating plants, and six generators are equivalent machines that represent the inertia of machines eliminated by the load-flow network reduction. The value of inertia constants of these six machines was reduced from very large values to values of 100 or 200 s (on a 100-MVA base). The resulting 17-generator Reduced Iowa System is shown in Figure 3-4.

Testing the Model

Testing the Transient Response

The transient response of the Reduced Iowa System was compared to the response data of the original NEAL 4 stability study. The NEAL 4 study included 43 generators modeled by the one axis model (including exciters and governors) and 80 generators modeled classically.

The first swing characteristics of the Reduced Iowa System compare rather well with the first swing characteristics from the NEAL 4 study. Rotor swings and power surges on the local area generators and key 345 kV transmission lines are similar. Examples of power surges on a

Figure 3-4. 17-generator system (Reduced Iowa System)

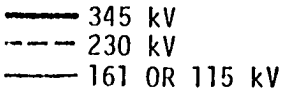

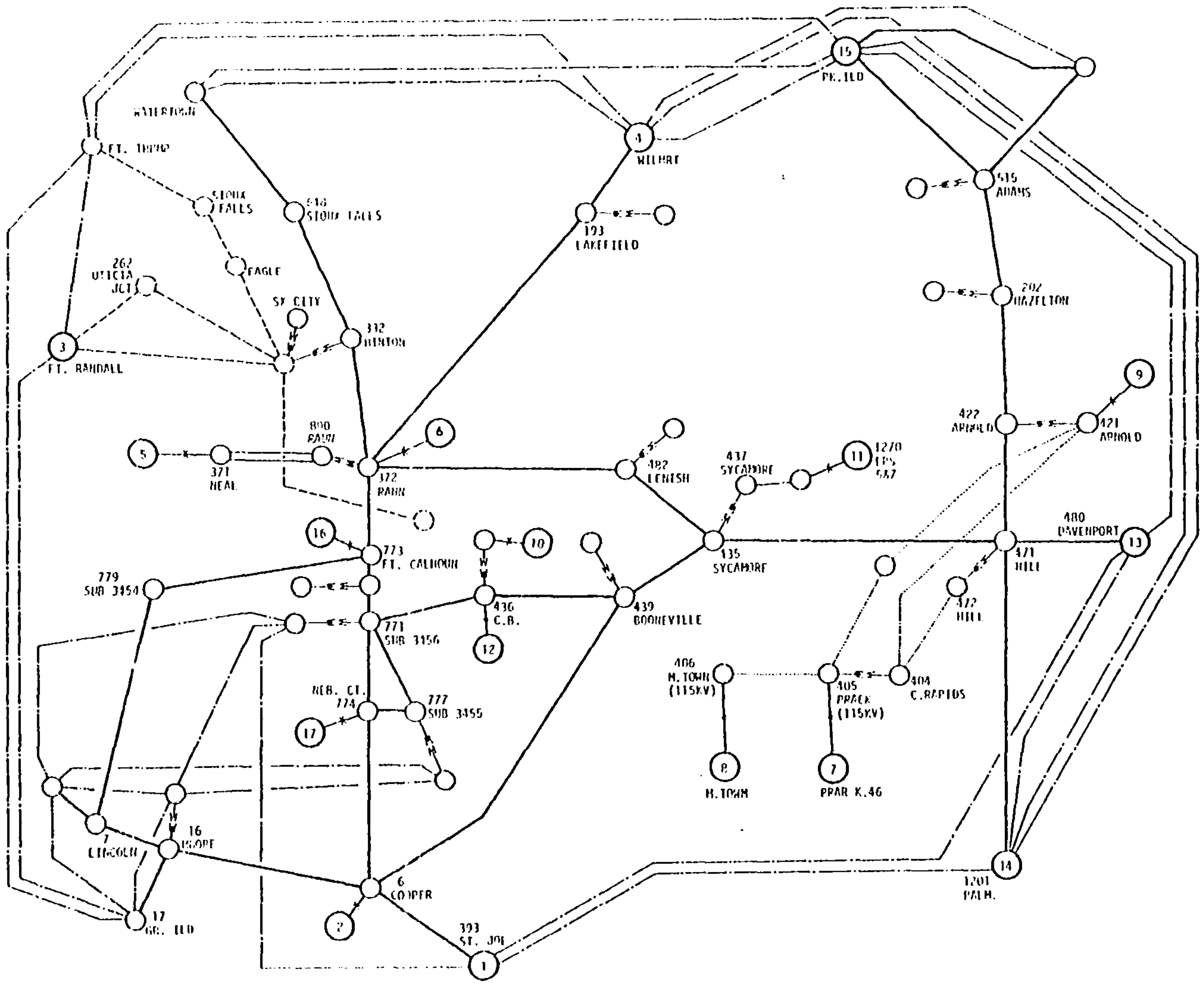

WATERTOWN
FT. THOMP
SIOUX FALLS
616 SIOUX FALLS
EAGLE
262 UTICIA JCT
SX CITY
312 HINTON
3 FT. RANDALL
5
371 NEAL
800 RAUN
6
372 RAUN
16
773 FT. CALHOUN
779 SUB 3454
771 SUB 3156
NEB. CT. 774
777 SUB 3455
17
7 LINCOLN
16 HOPE
17 GR. ILD
6 COOPER
2
393 ST. JOE
1
15
PK. ILD
4
WILMRT
193 LAKEFIELD
515 ADAMS
202 HAZELTON
9
422 ARNOLD
421 ARNOLD
480 DAVENPORT
13
471 HILL
472 HILL
482 LENISH
437 SYCAMORE
11
1270 EPS 5A7
135 SYCAMORE
10
436 C.B.
12
439 BOONEVILLE
406 H. TOWN (115KV)
405 PRACK (115KV)
404 C.RAPIDS
8
H. TOWN
7
PRAR K.46
14
1201 PALM.

345 kV line and a faulted generator are shown in Figure 3-5a and 3-5b, respectively. (This particular disturbance is a three-phase fault on the 345 kV bus at Neal, cleared by removing the Raun-Lakefield 345 kV line.)

The generator data and initial operating conditions, including the internal generator voltages, are given in Table 3-1. Line and transformer data and load-flow data for the operating condition analyzed in this project are given in reference (42).

The Missouri River Transmission Corridor

The Reduced Iowa System was used to simulate faults primarily in the western part of the network along the Missouri River. Of particular interest is a major 345 kV transmission corridor, shown in Figure 3-6. This transmission corridor, referred to in this dissertation as the Missouri River transmission corridor, connects Raun, Ft. Calhoun, SUB 3456, Nebraska City, Cooper, and Council Bluffs. In all, seven generators are astride the Missouri River transmission corridor: Numbers 2, 5, 6, 10, 12, 16, and 17 in Figure 3-4. This transmission corridor represents a relatively strong connection between these seven generators; a disturbance along the corridor significantly disturbs all seven generators. A wide variety of very complex modes of instability occur, offering a severe test for any transient stability analysis

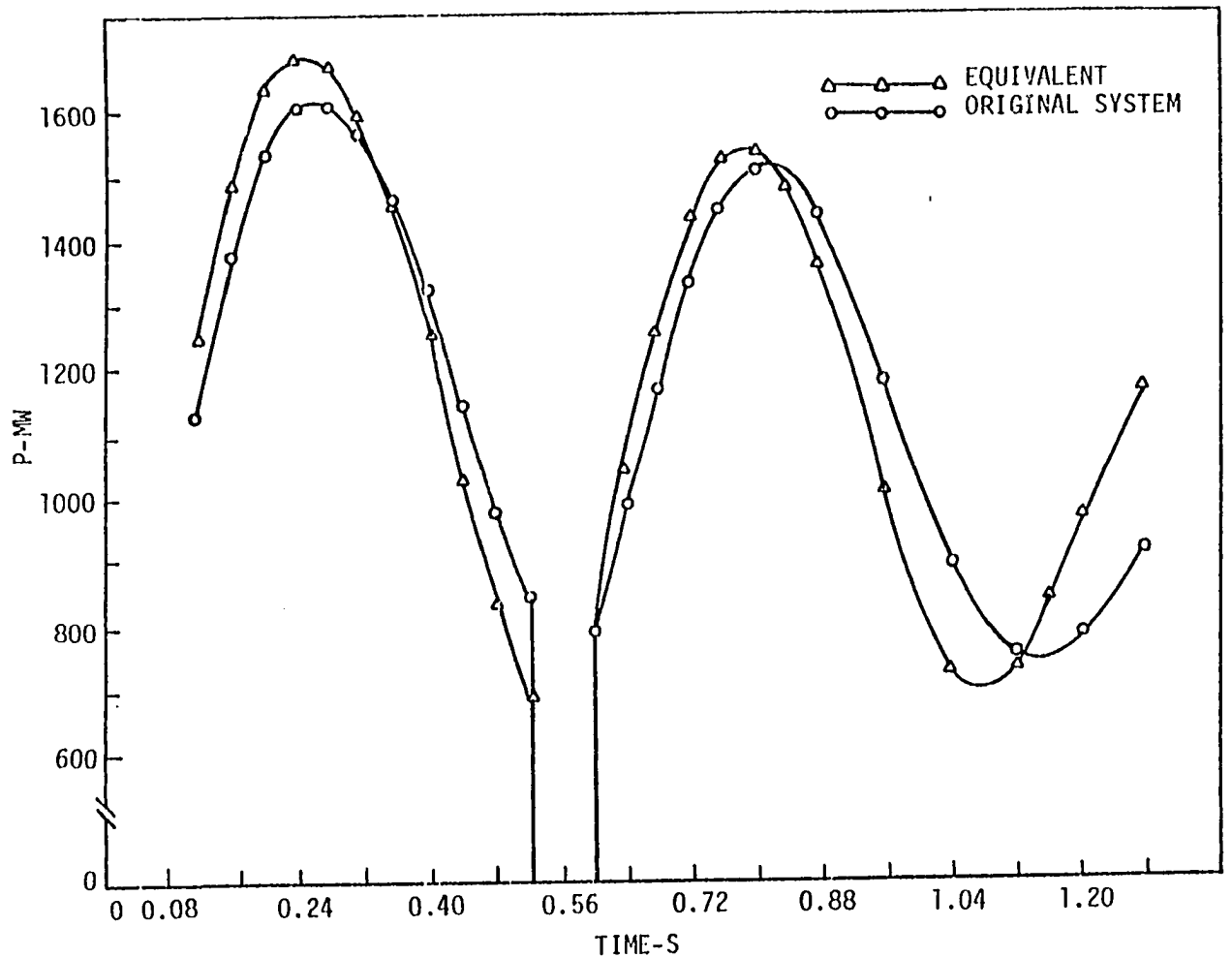

Figure 3-5(a). Flow in line 372-773 for original and Reduced Iowa System (Case T8Ø-RM-RU-Ø)

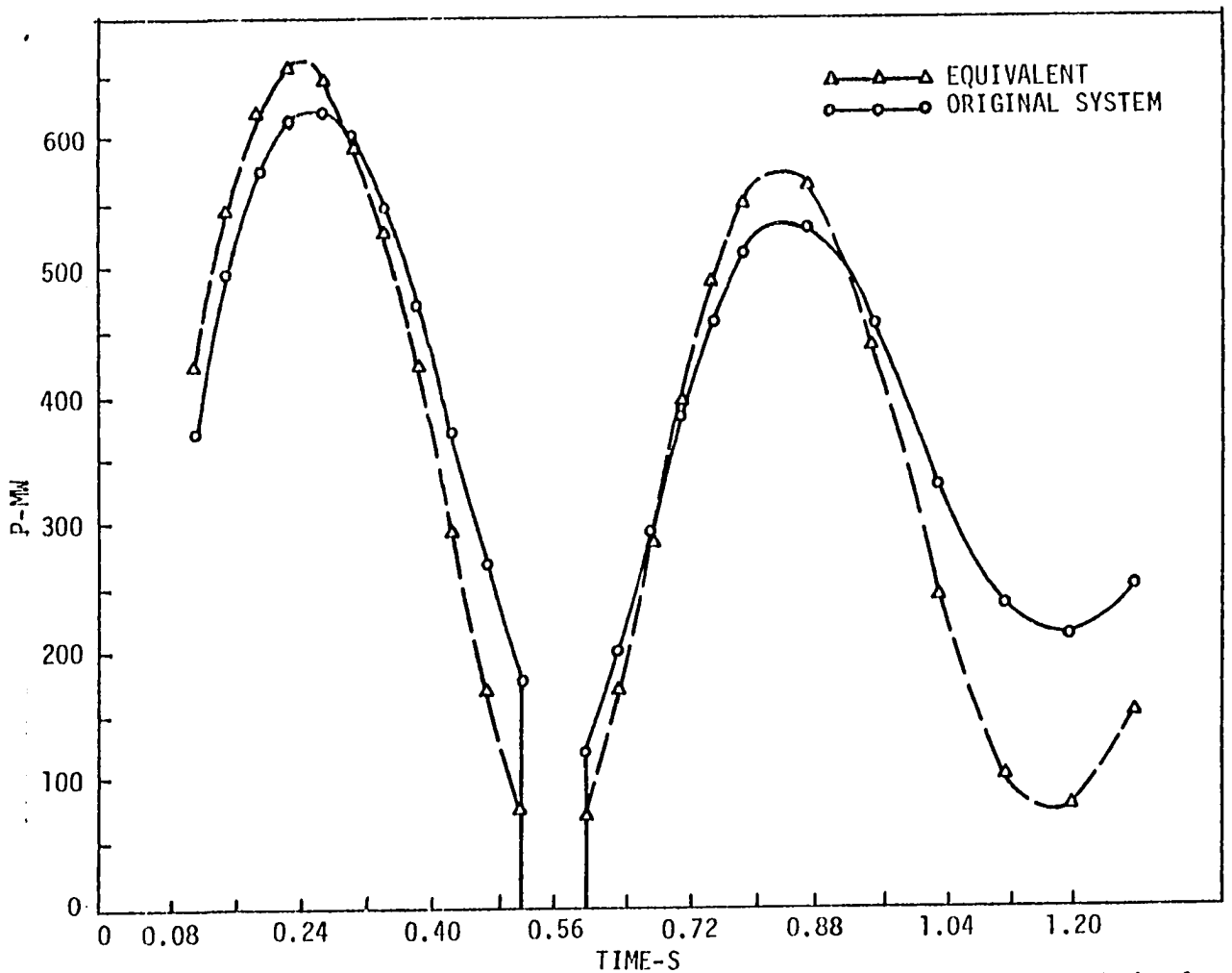

Figure 3-5(b). Power of generator No. 6 (Neal 3,4 units) for original and Reduced Iowa System (Case T8Ø-RM-RU-Ø)

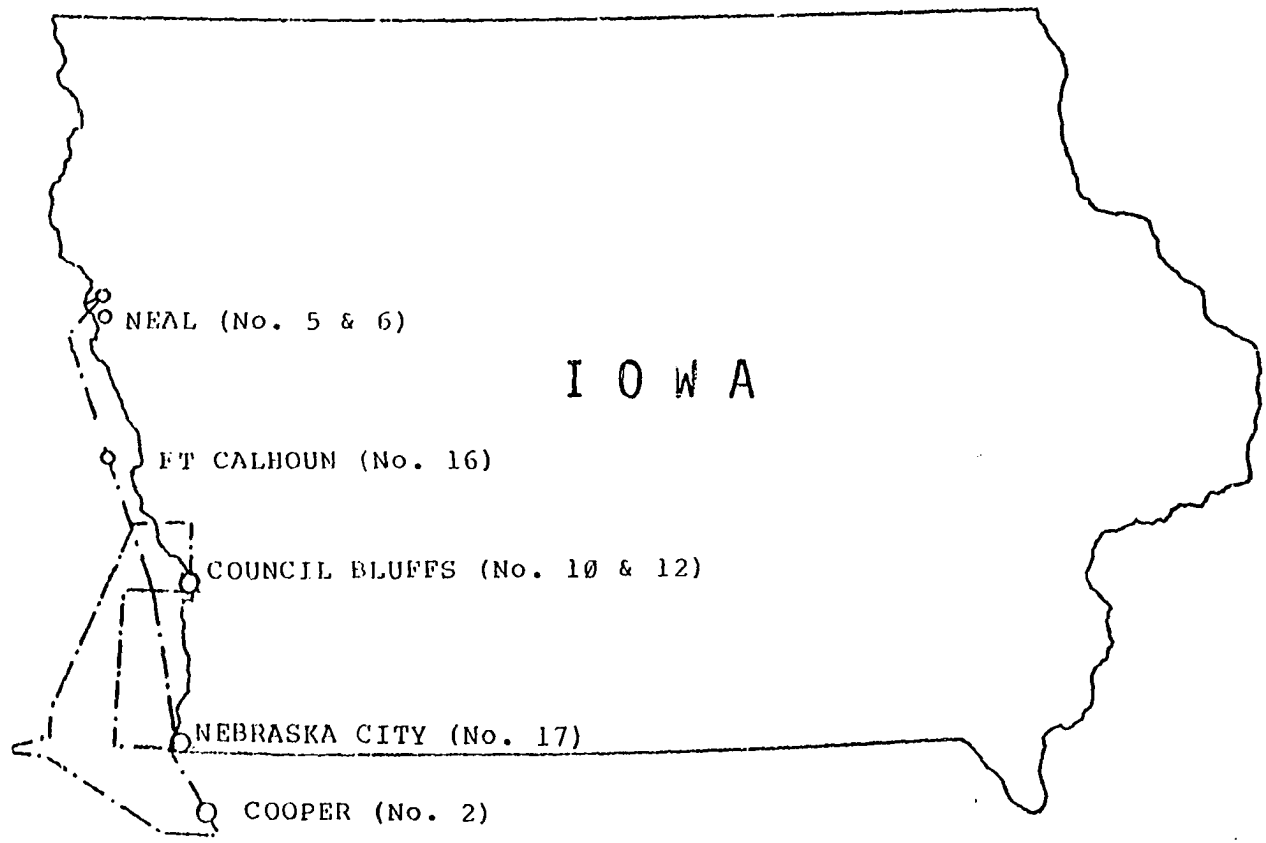

Figure 3-6. The Missouri River transmission corridor

procedure. The Reduced Iowa System is both a severe test environment and a practical, real-world system. It represents the 1980 power system for the State of Iowa, operating at an 80% load level.

CHAPTER 4. INVESTIGATION OF THE ENERGY FUNCTION BY SIMULATION STUDIES

Introduction

In the course of the investigation conducted in this research, some of the basic questions concerning the energy function method had to be dealt with. Among these are: the validity of the concept of the relevant UEP; analysis of the components of the system transient energy, and developing an understanding of the mechanism by which some generators separate from the rest of the system. This was accomplished by detailed simulation studies.

This research carefully investigated disturbances applied to the two test networks described in the previous chapter. In the 4-generator system, a three-phase fault was applied at bus 10 and was cleared by opening one of the lines between bus 10 and bus 12. In the 17-generator system, faults on the Missouri River transmission corridor were investigated, e.g., a three-phase fault applied at Raun (bus 372) and cleared by opening the Raun-Lakefield 345 kV line (bus 372 to bus 193).

In both cases, the energy function was used to evaluate the energy at each step in the simulation. This provided a means of inspecting the energy of the system during a disturbance.

The relevant UEPs were carefully determined, and the

trajectories of the disturbed system were examined to determine the influence of the relevant UEPs (if any). In addition, the predicted value of the critical energy V_{cr} was computed.

Computing the Unstable Equilibrium Points

The unstable equilibrium point (UEP) is the solution to the equations:

$$M_i\dot{\omega}_i = \emptyset = P_i - P_{ei} - (M_i/M_t)P_{coi} \qquad i=1,2,\ldots,n \tag{4-1}$$

The solution to these equations is similar to the solution of the load-flow problem, except that the mismatch power (P_{coi}) is distributed amongst the generators in proportion to the inertias, rather than being attributed to a swing machine. Mathematically there are an infinite number of solutions to equation 4-1. We are interested only in those solutions within the space

$$\theta < 2\pi$$

In that space there are $(2^n - 1)$ such solutions that represent unstable equilibrium points (of which we are only interested in a few).

The UEPs are computed in this research using a Davidon-Fletcher-Powell (DFP) minimization routine provided by Systems Control Inc. (34) (also see the Appendix for a brief

description of the DFP technique). Rewriting equation 4-1 as:

$$f_i \triangleq P_i - P_{ei} - (M_i/M_t)P_{coi}$$

or

$$f_i = \emptyset$$

a power mismatch function is defined as

$$F(\theta) = \sum_{i=1}^{n}(f_i)^2$$

This power mismatch equation is the objective function whose minimization, via the DFP technique, yields the UEP. The equilibrium points are those sets of generator angles for which the power mismatch is everywhere zero; consequently, $F(\theta)$ is minimum.

It is noted that the DFP routine does not assure convergence to a physically meaningful equilibrium point. To quote Athay et al. (35), "given an initial set of angles inside the principal singular surface an algorithm based on the minimization of $F(\theta)$ will converge to the SEP; given initialization outside it will converge to the closest, in terms of $F(\theta)$, UEP." The angles to which this routine will converge may include physically absurd values (i.e., some angles may be in the order of several thousand degrees). In order to accomplish convergence to a physically meaningful

UEP, the initial angles must be close to the actual UEP values. The UEPs used in this research are obtained by starting the DFP procedure at the point where the highly disturbed machines (as seen by speeds and angles of clearing) are at advanced angles (typically 3.Ø radians) and the remaining machines are at their SEP angles.

UEP Values

The UEPs obtained for the faults on the 4-generator and 17-generator systems agreed with the mode of instability actually realized. Table 4-1 shows the predicted UEPs and their potential energy.

Examination of the data in Table 4-1 shows which machines are those tending to separate from the system. In the 4-generator system, θ_4 is well-advanced; this is the generator that goes unstable (for a fault on bus 1Ø). In the 17-generator system, generators 5 and 6 are well-advanced and these two generators actually go unstable. Additionally, machines 2, 1Ø, 12, 16 and 17 are somewhat advanced; these are the remaining machines on the Missouri River transmission corridor. These data are reasonable since the fault is quite close to generator No. 4 in the 4-generator system and to generators 5 and 6 in the 17-generator system, and is astride the Missouri River transmission corridor.

Table 4-1. Predicted UEP angles

a) 4-generator system, fault at bus 10, line 8-10 cleared

$\theta_1^u = -27.7^\circ$ $\theta_3^u = -11.3^\circ$

$\theta_2^u = -5.5^\circ$ $\theta_4^u = 113.2^\circ$

V_u = 0.6260 pu (with respect to θ^{s1})

V_u = 0.5703 pu (with respect to θ^{s2})

b) 17-generator system, fault at bus 372, line 372-192 cleared

$\theta_1^u = -1.4^\circ$ $\theta_7^u = -16.0^\circ$ $\theta_{13}^u = -25.8^\circ$

$\theta_2^u = 46.6^\circ$ $\theta_8^u = -8.0^\circ$ $\theta_{14}^u = -23.6^\circ$

$\theta_3^u = 9.7^\circ$ $\theta_9^u = -6.6^\circ$ $\theta_{15}^u = -17.6^\circ$

$\theta_4^u = -24.0^\circ$ $\theta_{10}^u = 47.8^\circ$ $\theta_{16}^u = 63.6^\circ$

$\theta_5^u = 163.6^\circ$ $\theta_{11}^u = 10.3^\circ$ $\theta_{17}^u = 50.1^\circ$

$\theta_6^u = 144.9^\circ$ $\theta_{12}^u = 49.6^\circ$

V_u = 16.66 pu (with respect to θ^{s1})

V_u = 17.18 pu (with respect to θ^{s2})

System Trajectories and System Energy

The computer program used to simulate the three-phase disturbances provided rotor positions and speeds at each time increment Δt. Additionally, at each time increment the system energy was computed. Each energy component (kinetic, position, magnetic, and conductance) was displayed in order to give a mapping of where the system energy resides during the trajectory. It should be noted, incidentally, that the energy is calculated using the initial machine positions as reference; the energy is thus calculated with respect to the pre-fault stable equilibrium θ^{s1}.

4-Generator System

Figures 4-1 and 4-2 show some of the results obtained for the 4-generator system; the first shows the case of the fault cleared at Ø.148 s (stable) and the latter shows the fault cleared at Ø.159 s (unstable). The two cases, therefore, bracket the critical clearing instant t_c. The rotor trajectories for all four generators are shown; additionally, the system kinetic energy and potential energy are shown. It is evident, from inspection of Figure 4-1, that the maximum potential energy corresponds in time with the minimum kinetic energy, and that this correspondence in turn approximately corresponds to the peak of the trajectory of machine 4. This appears to confirm the notion that kinetic energy is being

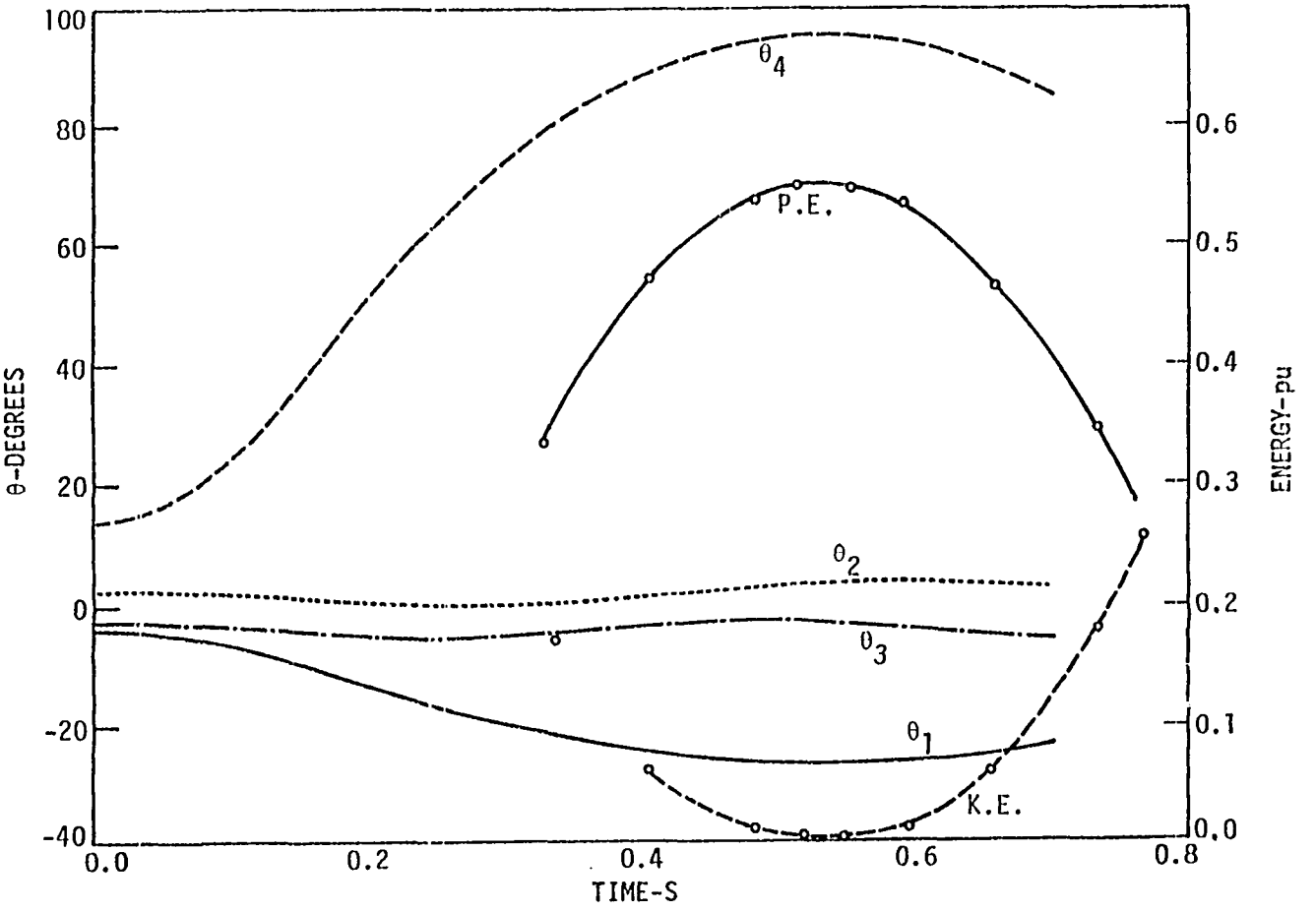

Figure 4-1. 4-generator system, fault at Bus 10 cleared at 0.148s

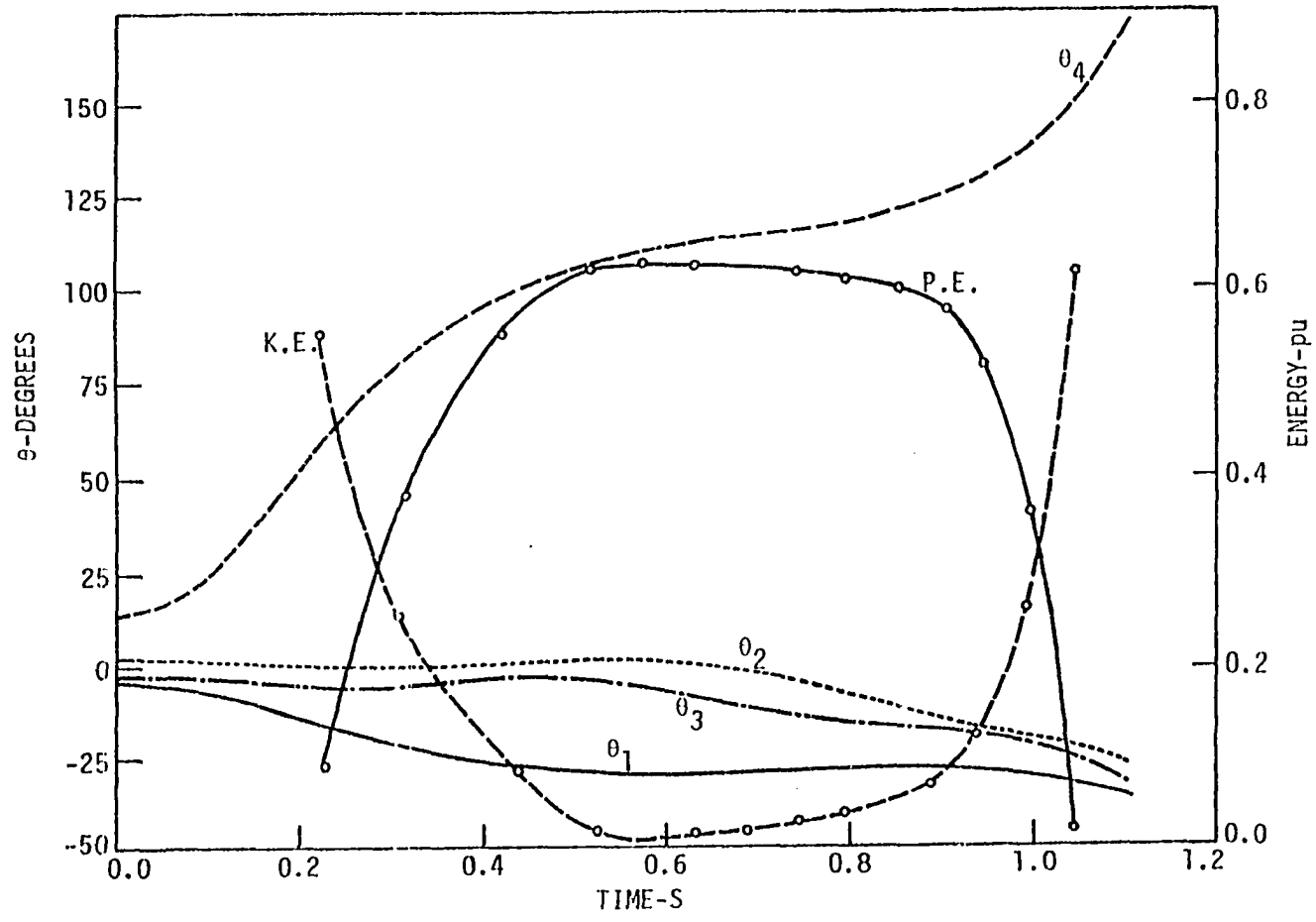

Figure 4-2. 4-generator system, fault at Bus 10 cleared at 0.159s

converted to potential energy, and that, at the peak of the swing of generator 4, nearly all the kinetic energy has successfully been absorbed by the system. The maximum potential energy is 0.57 pu. The kinetic energy minimum is near, (but not equal to), zero.

In Figure 4-2, the point of inflection of generator 4 (beyond which machine 4 accelerates into instability) is seen to occur somewhat near the maximum potential energy, minimum kinetic energy point. This occurs when

$$\theta_4 = 112^\circ \quad \text{and} \quad \theta_1 = -28^\circ,$$

which are almost identical to the values predicted by the UEP of

$$\theta_4 = 113.2^\circ \quad \text{and} \quad \theta_1 = -27.7^\circ$$

We note, however, that the values of θ_2 and θ_3 at that instant are

$$\theta_2 = 1.9^\circ \quad \text{and} \quad \theta_3 = -6.1^\circ.$$

These differ from the predicted value of

$$\theta_2 = -5.5^\circ \quad \text{and} \quad \theta_3 = 11.3^\circ$$

by a few degrees (see Table 4-1). The maximum potential energy is about 0.63 pu; we conclude that the critical energy is between 0.57 pu and 0.63 pu:

$$0.57 < V_{cr} < 0.63$$

The data suggest that the critical trajectory of the

critical machine seems to reach the position predicted by the UEP, while other machines may be off a little from their UEP values. It is not immediately clear from this case whether the critical energy (evidently between .57 pu and .63 pu) is specified by the maximum potential energy, minimum kinetic energy point or by the peak of the swing of θ_4. Nonetheless, the critical energy compares well with the energy predicted by the UEP of Ø.57 pu (with respect to θ_{s1}. See Table 4-1).

17-Generator System

The fault on the 17-generator system is located on the high voltage side of the transformer at generator No. 6 (bus 372). The location is also electrically close to generator No. 5. Although the fault is quite close to both of these machines, their responses differ significantly, peaking at substantially different instants. This is attributed to the fact that the inertias and synchronizing forces of the two machines differ substantially. Though the fault significantly disturbs the entire Missouri River corridor (Generators 2,5,6,10,12,16, and 17), a critical trajectory ultimately sends only machines 5 and 6 unstable.

To investigate the instability of the 5,6 group, a series of stability runs was made near the critical clearing time: at t_c = Ø.189 s, Ø.192 s and Ø.1932 s. Plots of θ_5, θ_6, and

the system kinetic energy, potential energy, and total energy are shown in figures 4-3 through 4-5. Additionally, since the gross motion of the 5,6 group is of particular interest, the motion of the inertial center of this 2-generator group is also indicated as $\theta_{5,6}$. Upon examining these data, we note the following:

- The swings of generators 5 and 6 peak about Ø.3 s apart. The motion of the inertial center of the 5,6 group peaks between the peaks of the swing of generator 5 and generator 6.
- For the disturbance cleared at t_c = Ø.189 s, the peak potential energy and minimum kinetic energy coincide with the peak of the inertial center $\theta_{5,6}$.
- For clearing just under the critical clearing value (i.e., t_c = Ø.192 s), the peak of $\theta_{5,6}$ coincides with the system potential energy, which is nearly equal to that of the UEP. (P.E. = 16.2, V_u = 16.6, see Table 4-1). At that instant,

  $$\theta_5 = 156^\circ \qquad \theta_6 = 141^\circ \qquad \theta_{5,6} = 145^\circ$$

  These are very close to the angles predicted by the UEP:

  $$\theta_5^u = 164^\circ \qquad \theta_6^u = 145^\circ \qquad \theta_{5,6}^u = 150^\circ$$

  Note that actual motion of the 5,6 group falls 5 degrees short of the value predicted by the UEP in this stable trajectory.
- The system trajectory continues toward maximum potential energy, minimum kinetic energy at a later instant.
- The point of inflection is the point on an unstable trajectory that corresponds to the peak of the swing of a stable trajectory. This point of inflection for the unstable case (t_c = Ø.1932 s) shows

  $$\theta_5 = 156^\circ \qquad \theta_6 = 156^\circ \qquad \theta_{5,6} = 156^\circ$$

Note that the inertial center is only 6 degrees beyond the inertial center specified by the UEP. It appears that the gross motion of the critical group approached the UEP for the critical trajectory.

- From the computer runs (not shown in the figures), we note that at the instant of the peak of $\theta_{5,6}$ the angles of the four highest-inertia machines (which are equivalent machines remote from the disturbance) are given by:

$$\theta_1 = 6.6^\circ \qquad \theta_{13} = -31.5^\circ \qquad \theta_{14} = -30.4^\circ$$
$$\theta_{15} = -21.1^\circ$$

while the UEP predicts:

$$\theta_1^u = -1.4^\circ \qquad \theta_{13}^u = -25.8^\circ \qquad \theta_{14}^u = -23.6^\circ$$
$$\theta_{15}^u = -17.6^\circ$$

- Therefore, the system trajectory seems to be passing near, but not exactly through, the controlling UEP. While the generators tending to separate from the rest of the system pass at or very near their UEP values, the rotors of the other generators are at positions off by a few degrees from their corresponding UEP values.

- The degree of group separation indicated by the UEP (i.e., $\theta_{5,6}^u$) is more or less the degree of separation required for instability to accur. Still, it is not clear whether the UEP is "approached" in terms of the individual (critical) machines or in the sense of the gross motion of the machines.

- The kinetic energy minimum is not zero for either the stable or unstable case. This is a significant point that will be discussed later in this chapter.

- For t_c greater than critical (t_c = 0.1932 s), the system crossed the maximum potential energy "ridge" at a point different than the UEP. For this trajectory, the system peak potential energy is close to that of the UEP. However, the maximum

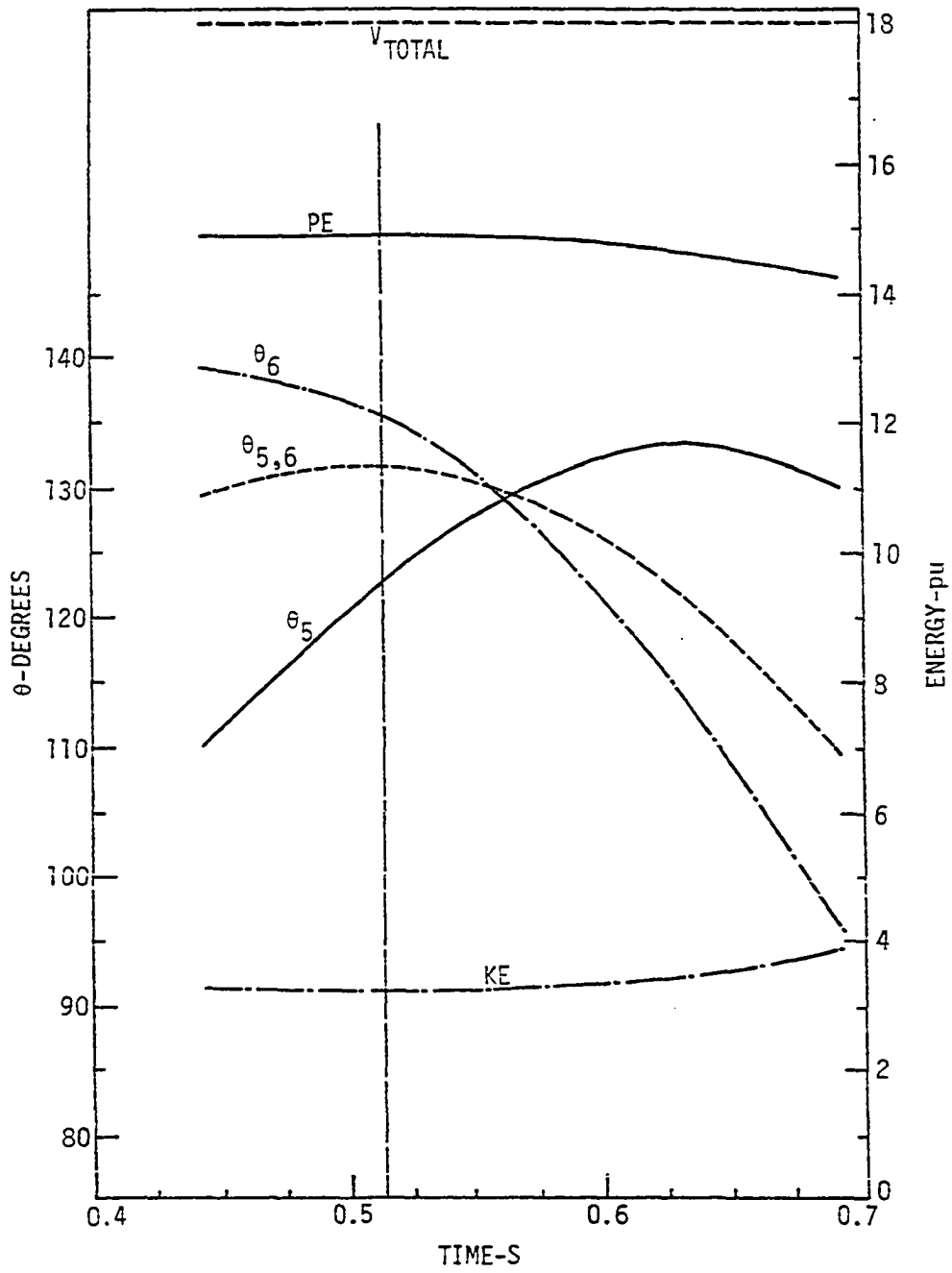

Figure 4-3. 17-generator system, fault at Bus 372 cleared at Ø.189s

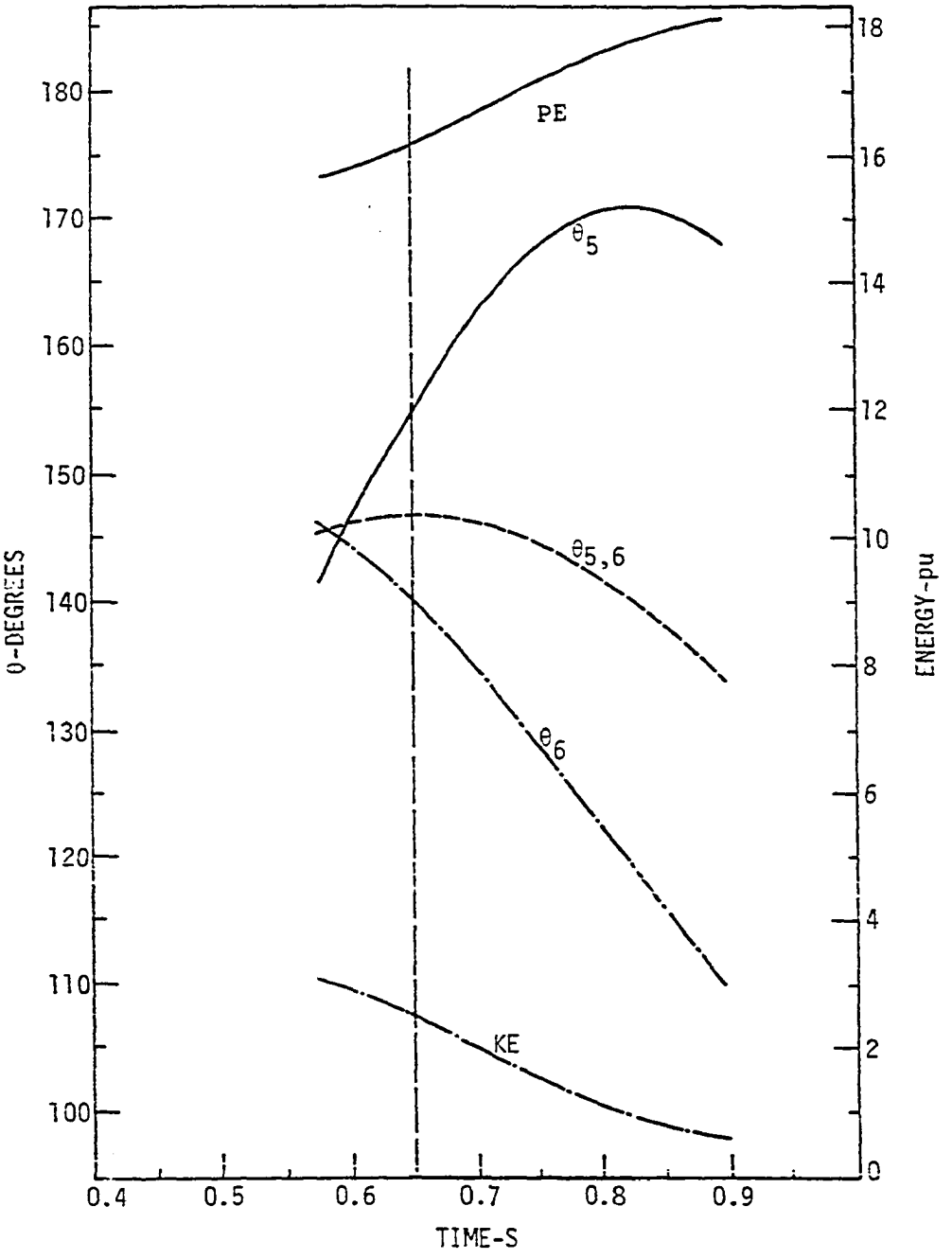

Figure 4-4. 17-generator system, fault at Bus 372 cleared at 0.192s

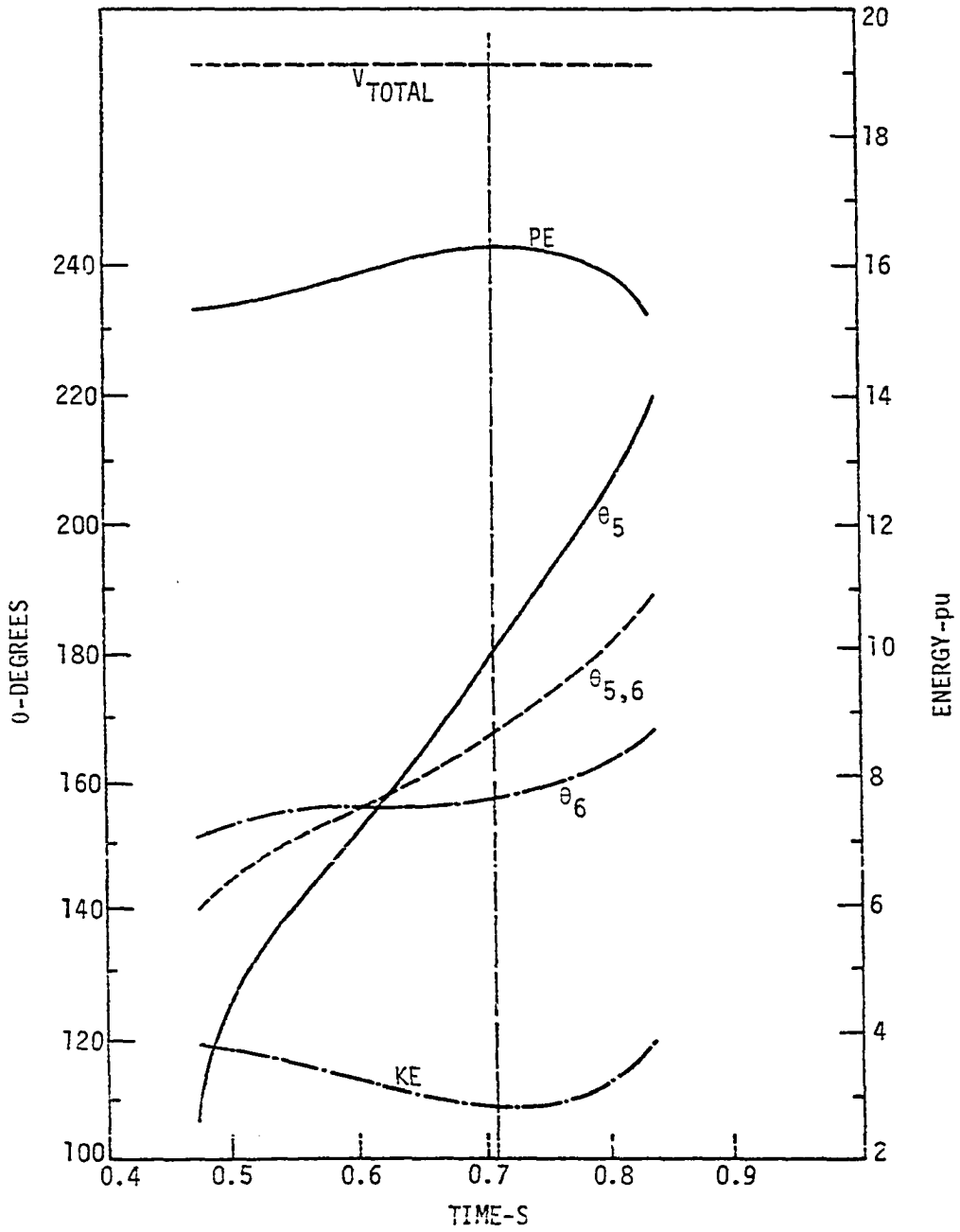

Figure 4-5. 17-generator system, fault at Bus 372 cleared at 0.1932s

> potential energy, minimum kinetic energy instant is not established as a point of significance in establishing V_{cr}. Stability seems to be decided, instead, between the peak of the swing of the 5,6 group (for the stable case) and the point of inflection of the 5,6 group (in the unstable case). In both cases, the maximum potential energy, minimum kinetic energy point does not occur until a later instant.

The data presented in Figures 4-3 through 4-5 show that the concept of a particular UEP controlling the fault trajectory is a valid one. The "critical machines" appear to be the highly-advanced machines; these approach very near to the UEP values on the critical trajectory and give a system potential energy that is very close to that of the UEP. There are two additional points of significance to be noted: the system minimum kinetic energy is not zero, and the generators other than the critical ones may be off by a few degrees from their UEP values.

Energy Analysis

A more detailed analysis of the transient energy of the 17-generator system is carried out by plotting the various components of energy along the system trajectory. The same fault (at Raun, cleared by opening the Raun-Lakefield line) is investigated. In one case, the fault is cleared at Ø.15 s to represent a very stable disturbance. In the other two cases, clearing is carefully chosen to bracket the critical clearing instant as closely as the computer programs will allow: t_c =

Ø.1923 s and t_c = Ø.1926 s.

Clearing at Ø.15s

In this trajectory the system is significantly disturbed, but system stability is not endangered. The data for this disturbance are displayed in Figure 4-6(a) and 4-6(b). The first figure shows selected rotor trajectories (generators 2,5,6,1Ø,13 and 16) and the inertial center of 5 and 6 ($\theta_{5,6}$). All of these machines, except generator 13, represent generators on the Missouri River transmission corridor; generator 13 is a machine with a very high inertia constant (2ØØ s) located outside the study area. The fault splits the system into two groups; the seven generators of the Missouri River transmission corridor swing with respect to the remaining 1Ø generators. Figure 4-6(b) shows the system transient energy for this case, displayed as four components (position, magnetic, conductance, and kinetic energy) as well as potential energy and total energy. The plot of total energy clearly shows that the transient energy increases up to the point of clearing. After clearing, no additional energy is injected into the system and the total energy remains

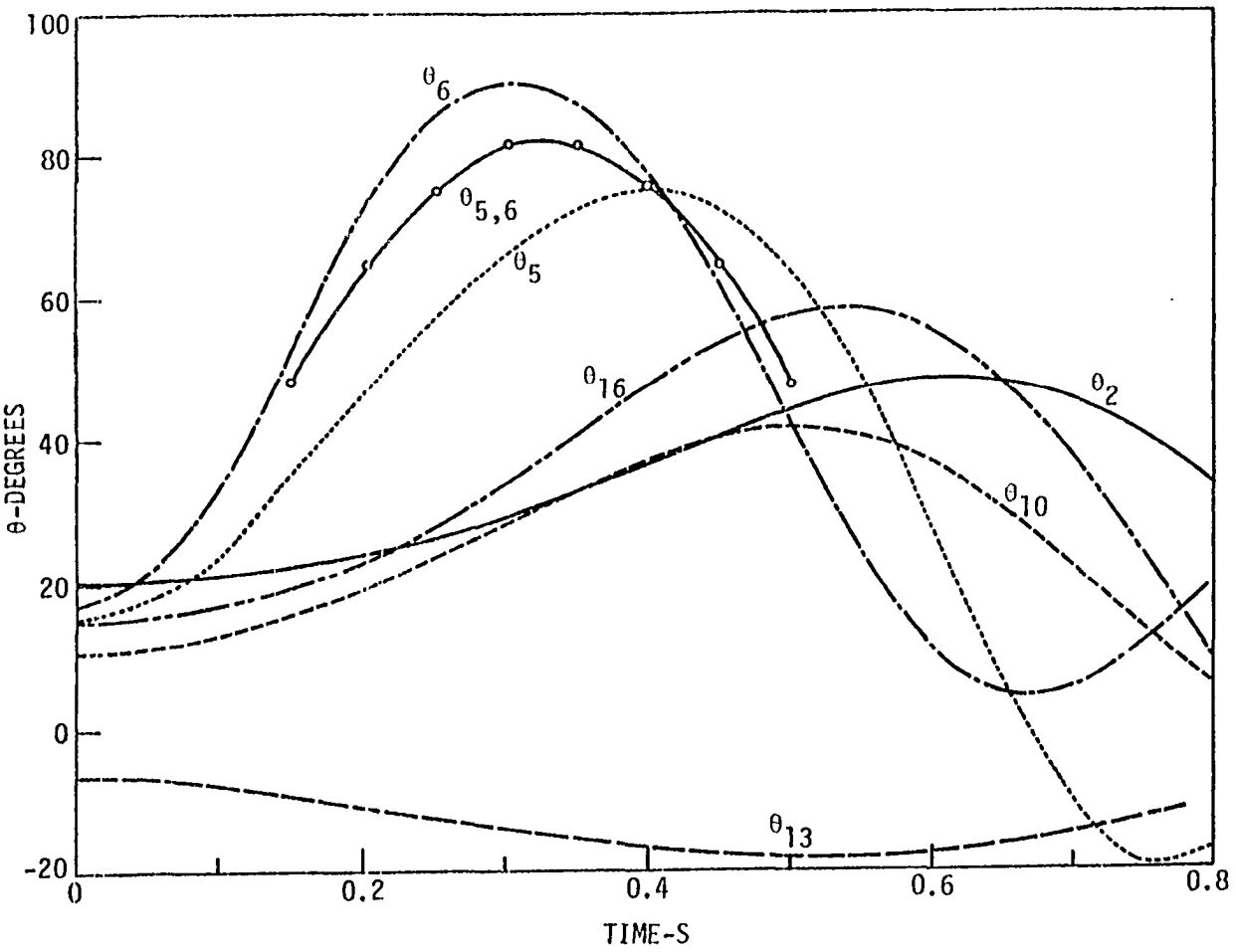

Figure 4-6(a). Rotor angles of 17-generator system, fault at Bus 372 cleared at Ø.15Øs

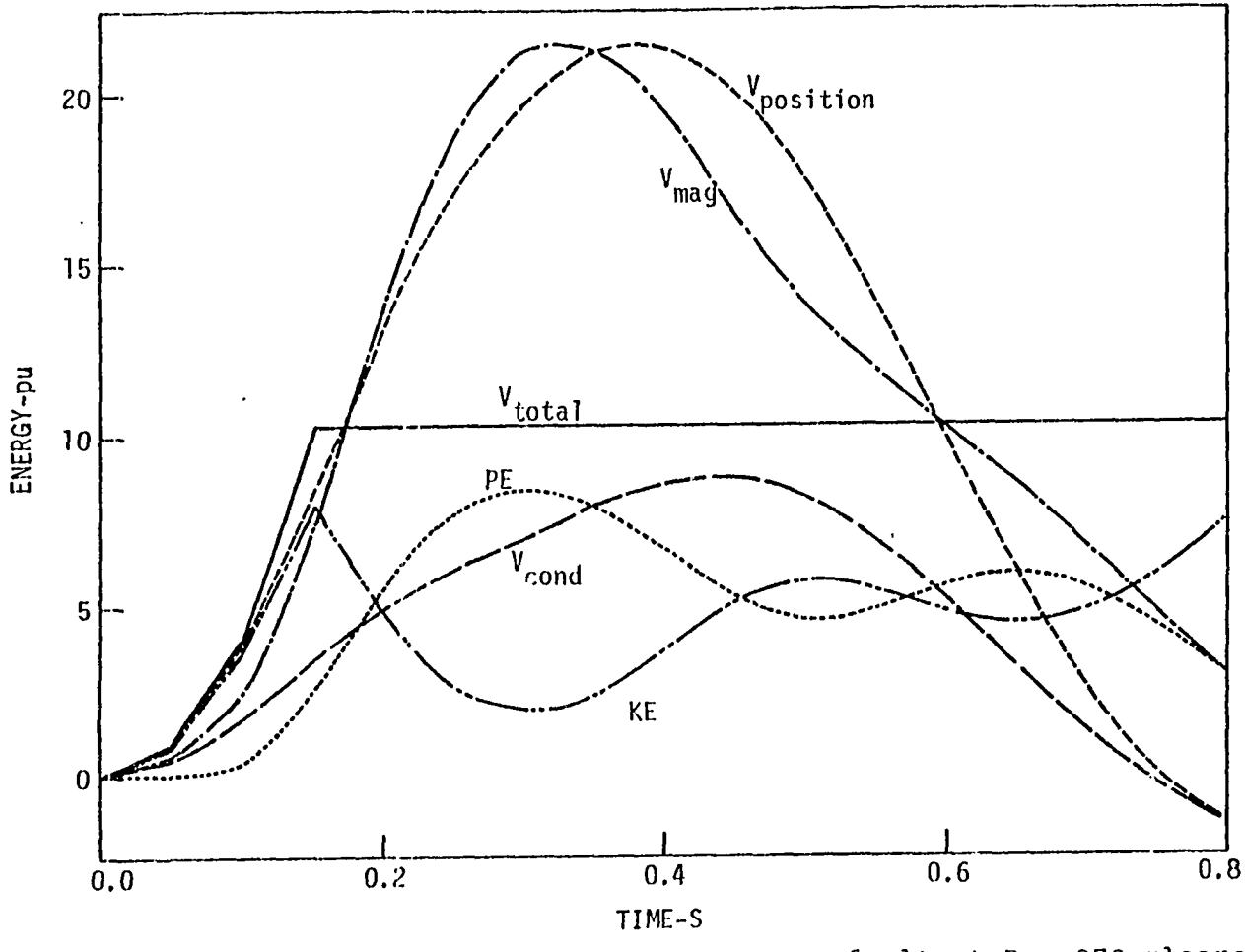

Figure 4-6(b). Energy of the 17-generator system, fault at Bus 372 cleared at Ø.15Øs

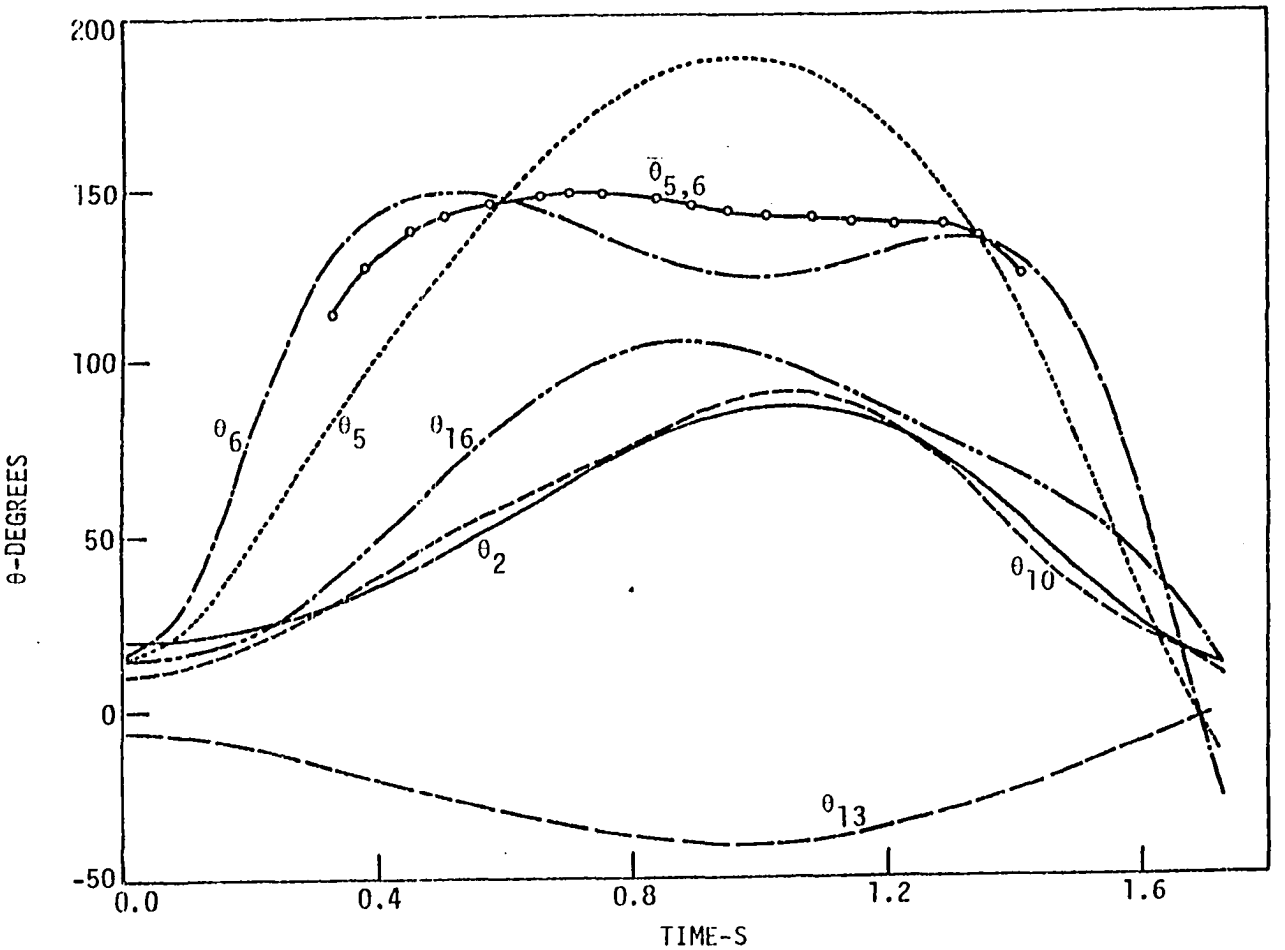

Figure 4-7(a). Rotor angles of the 17-generator system, fault at Bus 372 cleared at 0.1923s

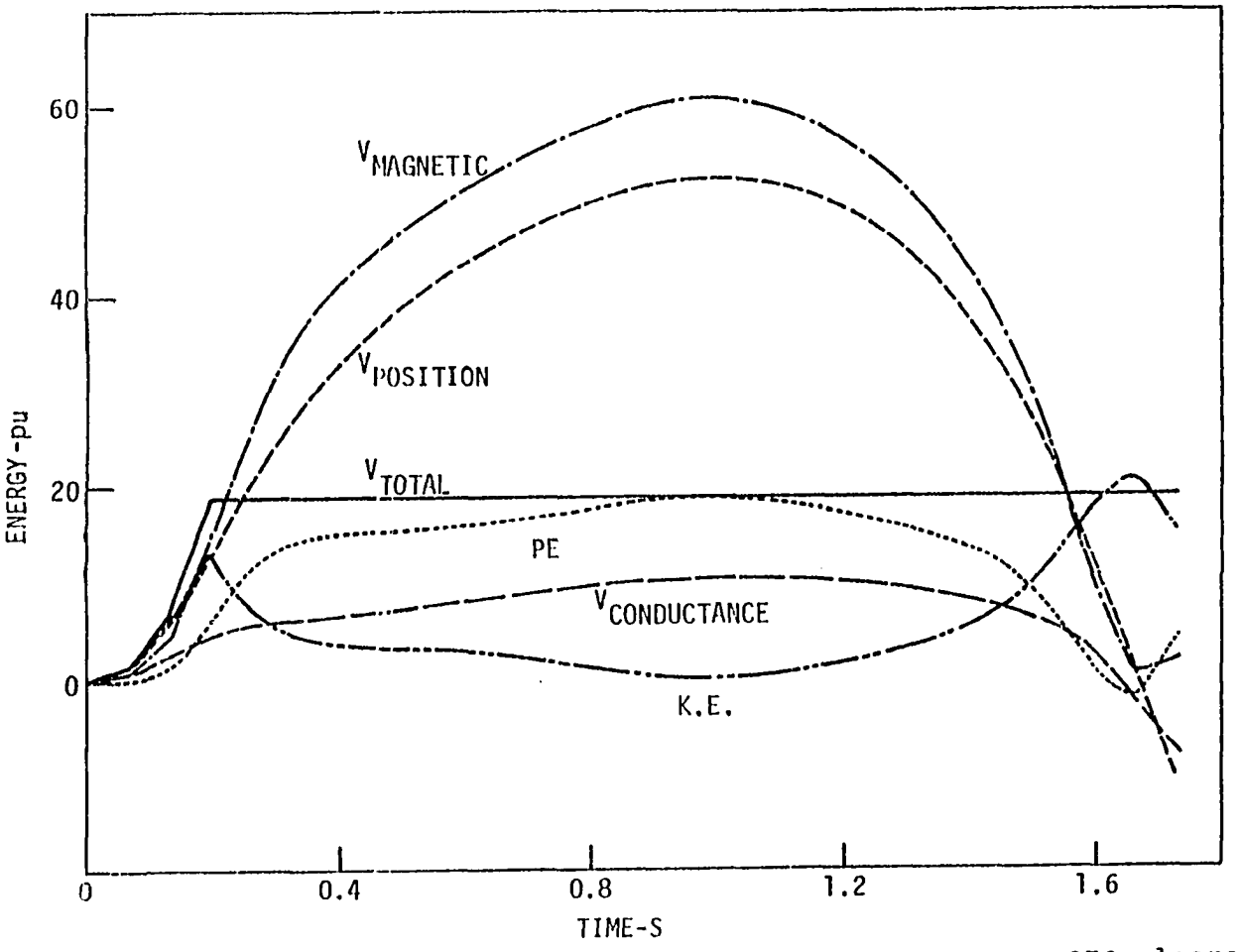

Figure 4-7(b). Energy of the 17-generator system, fault at Bus 372 cleared at Ø.1923ε

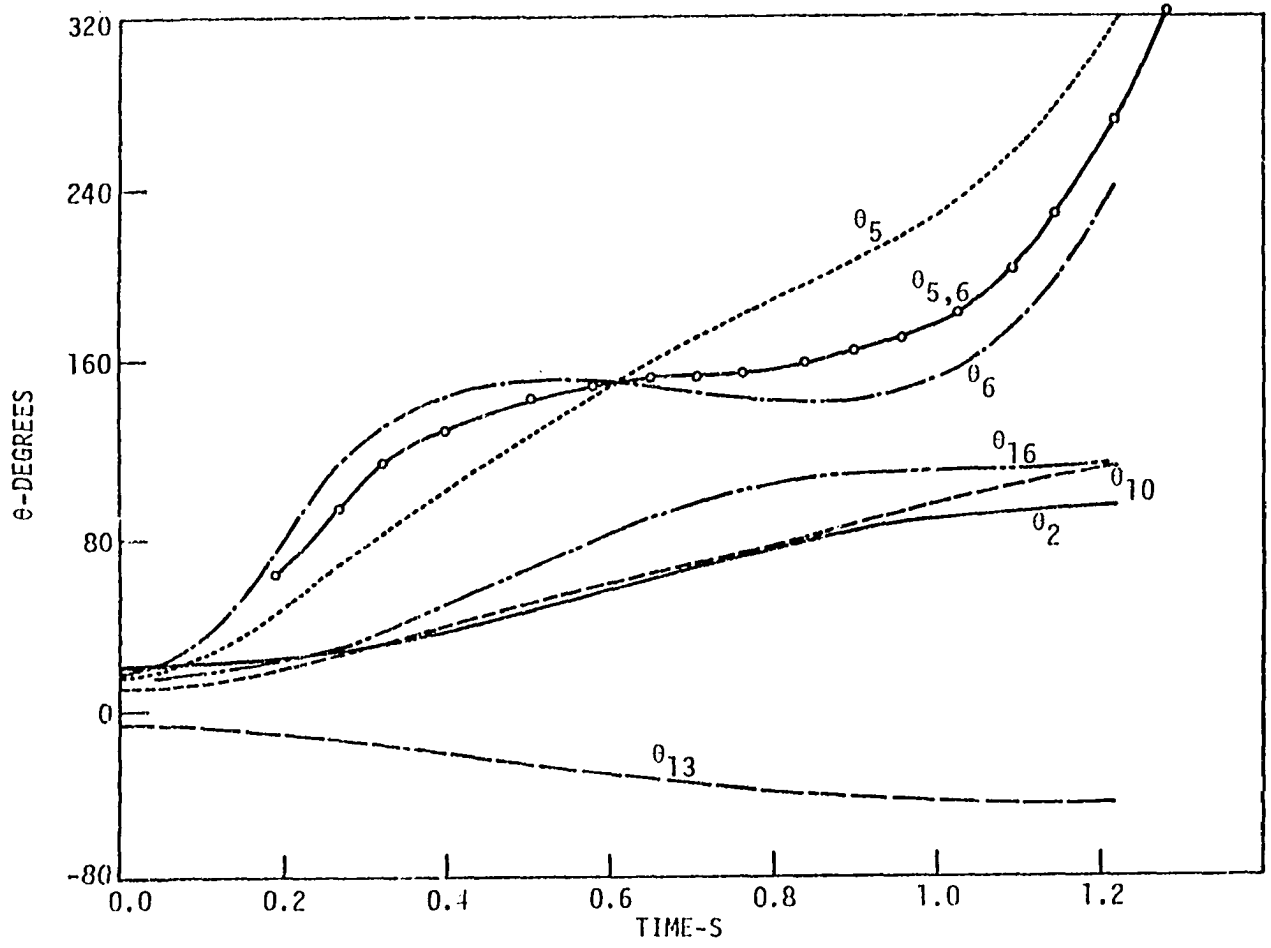

Figure 4-8(a). Rotor angles of the 17-generator system, fault at Bus 372 cleared at 0.1926s

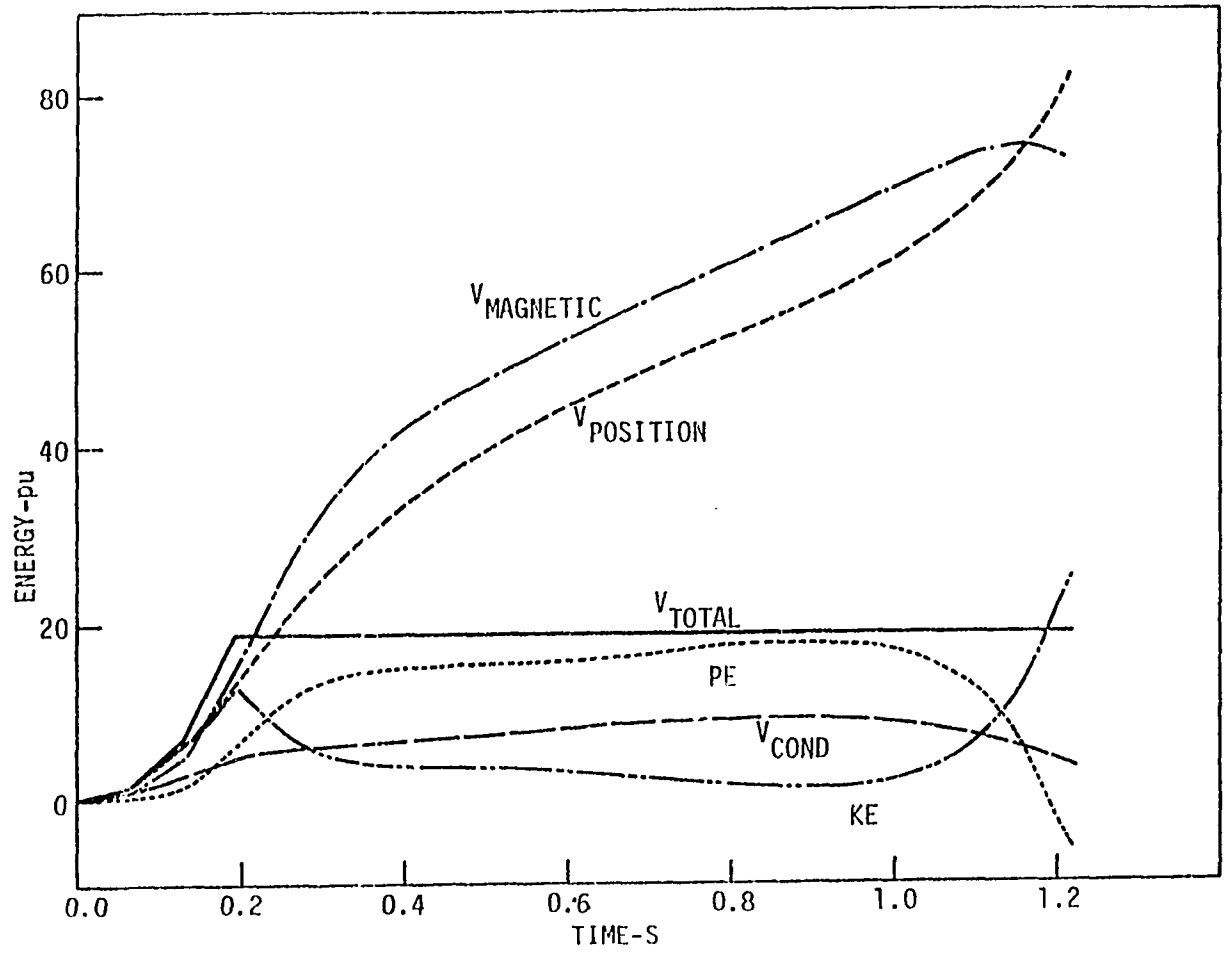

Figure 4-8(b). Energy of the 17-generator system, fault at Bus 372 cleared at Ø.1926s

constant. It is particularly interesting to note the interaction between potential energy and kinetic energy. System energy is exchanged back and forth between the two energy forms, with the maximum potential energy corresponding in time to the minimum kinetic energy (and vice versa). The first maximum potential energy, minimum kinetic energy point corresponds to the peak of the swing of $\theta_{5,6}$, i.e., where the critical group acquires zero velocity.

Fault Cleared at Ø.1923 s and Ø.1926s

These two cases bracket the critical clearing instant as closely as possible. The stable case, with t_c = Ø.1923 s, is shown in Figure 4-7(a) (selected rotor trajectories) and Figure 4-7(b) (energy). Data for the unstable case, with t_c = Ø.1926 s, are similarly displayed in Figures 4-8(a) and (b). The stable case is very close to the case with t_c = Ø.192Ø s, presented in Figure 4-4. We note that the trajectories pass very near the UEP at about Ø.7Ø s. The rotor angles at this instant are:

$$\theta_5 = 166^\circ \qquad \theta_6 = 144^\circ \qquad \theta_{5,6} = 149.8^\circ$$

These compare to the UEP angles of

$$\theta_5^u = 164^\circ \qquad \theta_6^u = 145^\circ \qquad \theta_{5,6}^u = 150^\circ$$

This point corresponds to the instant where $\theta_{5,6}$ reaches its peak (or zero velocity instant). In the unstable case, the point of inflection occurs at an only slightly later time and at an angle of $\theta_{5,6} = 151.3^\circ$.

For the stable case, simple interpolation identifies the point $\dot{\theta}_{5,6} = 0$, which occurs at 0.70 s when

$$PE = 16.73 \text{ pu}$$

For the unstable trajectory, the point is indicated by the point of inflection (i.e., $\ddot{\theta}_{5,6} = 0$) which occurs at 0.7353 s where

$$PE = 16.97 \text{ pu.}$$

We conclude from these data that the maximum transient energy that the system can absorb (i.e., the critical energy V_{cr}) must lie between these two values:

$$16.73 < V_{cr} < 16.97$$

This compares to the value predicted by the UEP of

$$V_u = 16.66 \text{ pu (see Table 4-1)}$$

This also suggests that the point on the critical

trajectory, corresponding to this energy, satisfies the criterion:

$$\dot{\theta}_{5,6} = \emptyset$$
$$\ddot{\theta}_{5,6} = \emptyset$$

As with the previous cases, the positions of the generators other than the critical machines are off by a few degrees from their UEP values.

Figures 4-7(b) and 4-8(b) reveal a very important aspect of the energy distribution along the system trajectory. It is sometimes reported in the literature that the critical energy, which is the network's maximum ability to absorb the transient energy, is the maximum potential energy along the trajectory. We have already seen that the critical energy V_{cr} is less than 17 units. Figure 4-7(b) shows, however, that the maximum potential energy is 18.75 pu and occurs at t = Ø.96 s. That this is <u>not</u> V_{cr} is evident from Figure 4-8(b), where the system becomes unstable when less than this amount of transient energy is injected into the system. Indeed, for that case, when the energy is 17.9 pu (at t = Ø.9 s) $\theta_{5,6}$ is already accelerating toward instability.

The point of maximum potential energy (and minimum kinetic energy) does not represent the V_{cr} associated with the instability of the 5,6 group. Though it is not shown in the figure, careful examination of the data shows that the instant of maximum potential energy and minimum kinetic energy is the peak of the swing of all seven machines on the Missouri River transmission corridor, i.e., the inertial center of generators 2,5,6,10,12,16, and 17 (taken with respect to the remaining 10 machines: 1,3,4,7,8,9,11,13,14,15). Since that 7-machine group is not the critical group, the value of V_{cr} is not defined by the energy at the peak of the swing of that 7-machine group. Instead, it is the energy at the peak of the 5,6 group (i.e., the critical group) that identifies V_{cr}.

An additional observation concerning the kinetic energy is in order. The instant at which the critically stable trajectory comes close to the UEP and $\theta_{5,6}$ reaches its peak, the kinetic energy of the system is not zero; rather, at that instant, K.E. = 2.17 pu. In the unstable trajectory, the instant at which $\theta_{5,6}$ reaches its inflection point corresponds to K.E. = 1.967 pu.

Implications of the Data

These data are of considerable significance to transient stability analysis by direct methods. It clearly indicates that:

- The critical transient energy occurs when the critical machines in the system (i.e., the generators tending to separate from the rest) pass at (or very near to) their value at the UEP. This amount of critical transient energy appears to be the same as the value of V at the UEP. The extensive investigations, conducted in the course of this work, seem to indicate that for all practical purposes the value of V_u (at θ^u) can be used with sufficient accuracy as V_{cr}.
- A certain amount of kinetic energy, between 1.967 and 2.17 units, is not absorbed by the system at the UEP. This indicates that not all transient energy created by the fault contributes to the instability of the system. This component is associated with the intermachine motion, not with separating the critical machines from the others (e.g., at the instant where $\dot{\theta}_{5,6} = 0$, not every machine velocity will be zero; this is motion around the inertial centers and represents kinetic energy that does not contribute to the instability of the 5,6 group).

Discussion and Conclusions

The results presented in this chapter merit the following conclusions:

1. The concept of a controlling UEP for a particular system trajectory is a valid concept.
2. From the values of θ_i, i = 1,2...n, the critical machines are those tending to separate from the rest and having the largest values of θ_i.
3. At critical clearing, the system trajectory is such

that only the critical machines need pass at, or very near to, their values at the UEP. Other generators may be off from their UEP values.

4. If more than one generator tends to lose synchronism, instability is determined by the gross motion of these machines, i.e., by the motion of their center of inertia.
5. The critical energy V_{cr} (e.g., the maximum potential energy that the system can absorb and stay stable) is the potential energy at the peak of the swing of the inertial center of the critical group during the critical trajectoy.
6. The value of the energy at the UEP (V_u) is, for all practical purposes, equal to the critical energy V_{cr}.
7. Not all the fault kinetic energy (at t_c) contributes directly to the separation of the critical machines from the rest of the system; some of that energy accounts for intermachine swings. For stability analysis, that component of kinetic energy does not contribute to instability and should be subtracted from the energy that needs to be absorbed by the system for stability to be maintained.
8. First-swing transient stability can be accurately

assessed by the energy function if it is evaluated using the controlling UEP and the energy function is modified to include a correction for the kinetic energy not contributing to instability. The method, then, is:

- o determine the correct critical group and, thus, the controlling UEP; compute the critical energy V_{cr}.
- o determine the transient energy at the end of the disturbance (V_{cl}) and correct it for the kinetic energy that does not contribute to instability.
- o compare V_{cr} to V_{cl}; stability requires that

$$V_{cr} < V_{cl}$$

CHAPTER 5. THE TRANSIENT ENERGY MARGIN

Defining the Transient Energy Margin

Chapter 2 introduced the energy function. Athay et al. (34) defined the system transient energy to be given by this energy function, evaluated (using the post-fault Y-bus) between θ^{s2} and any angle θ on the disturbed trajectory:

$$V = V\Big|_{\theta^{s2}}^{\theta}$$

Using θ^{s2} as reference, the transient <u>fault energy</u> V_{cl} is defined as:

$$V_{cl} = V\Big|_{\theta^{s2}}^{\theta^{cl}} \tag{5-1}$$

The <u>critical energy</u> V_{cr} is assumed to be the energy of the UEP with zero velocities:

$$V_{cr} = V\Big|_{\theta^{s2}}^{\theta^{u}} \tag{5-2}$$

The system stability is determined by comparison between V_{cl} and V_{cr} (provided that they are both computed with the same reference, θ^{s2}). Stability is predicted if

$$V_{cr} > V_{cl}$$

or

$$V_{cr} - V_{cl} > 0$$

This research considered the difference between V_{cr} and V_{cl} to be the transient energy margin ΔV:

$$\Delta V = V_{cr} - V_{cl} \tag{5-3}$$

Substituting equation 5-1 and 5-2 in equation 5-3:

$$\Delta V = V\Big|_{\theta^{s2}}^{\theta^{u}} - V\Big|_{\theta^{s2}}^{\theta^{cl}}$$

$$= V\Big|_{\theta^{cl}}^{\theta^{u}} = \text{Transient Energy Margin} \tag{5-4}$$

Thus,

$$\Delta V = \sum_{i=1}^{n} [(1/2)M_i(\omega_i^{cl})^2 - P_m(\theta_i^u - \theta_i^{cl}) - \sum_{i=1}^{n-1}\sum_{j=i+1}^{n}[E_iE_jB_{ij}(\cos\theta_{ij}^u - \cos\theta_{ij}^{cl}) + I_{ij}\Big|_{\theta^{cl}}^{\theta^{u}}] \tag{5-5}$$

where the last term is the approximation to account for transfer conductances:

$$I_{ij}\Big|_{\theta^{cl}}^{\theta^{u}} = E_i E_j G_{ij}\left(\frac{(\theta_i^u+\theta_j^u)-(\theta_i^{cl}+\theta_j^{cl})}{(\theta_{ij}^u-\theta_{ij}^{cl})}\right)(\sin\theta_{ij}^u - \sin\theta_{ij}^{cl}) \qquad (5\text{-}6)$$

Thus, by knowing the values of rotor angles and speeds at clearing and the position of the relevant UEP, the transient energy margin can be evaluated directly, using the post-disturbance network. In other words, there is no need to compute the value of the energy function at θ^c, and its value at θ^u (with each referred to the same θ^s), and then to compute the difference.

The transient energy margin defined directly as

$$\Delta V = V\Big|_{\theta^{cl}}^{\theta^{u}}$$

has several advantages over subtracting V_{cl} from V_{cr}:

- The need for computing the post-fault SEP is avoided altogether, eliminating the need for one load-flow solution for each line cleared.
- The energy function is computed only once (for ΔV) rather than twice (for V_{cl} and V_{cr}).
- The question of reference (θ^{s1} vs θ^{s2}) never arises.
- Computation of the term I_{ij} involves less approximation, since only one approximation is used (for ΔV) rather than two (for V_{cr} and V_{cl}), and since the approximation is over a smaller segment of the trajectory (e.g., between θ^{cl} and θ^u, rather than between θ^{s2} and θ^u).
- Assessment of system stability is accomplished by

> examining the degree of stability. Thus, by focussing on the system's ability to absorb the faulty transient energy, a more important question is addressed: "What is the margin of safety?"

Kinetic Energy Correction Applied to the Energy Margin

As pointed out in Chapter 4, a correction must be made to compute the "true" system transient energy at clearing which actually contributes to instability. The kinetic energy, associated with intermachine motion about the inertial centers, which is not contributing to instability, must be corrected for.

The kinetic energy which is responsible for the separation of the critical generators from the rest of the system is the kinetic energy associated with the gross motion of the critical generators, i.e., that kinetic energy associated with the motion of the inertial center of the critical machines taken with respect to the inertial center of all other generators. The remaining portion of the kinetic energy need not be absorbed by the system for stability to be maintained; this kinetic energy is associated with the relative motion of each group of machines about their centers of inertia and does not represent a contribution to the gross motion of the group.

The kinetic energy associated with the gross motion of k machines having angular speeds (with respect to their center of inertia) of

$$\omega_i, \qquad i = 1, 2, 3, \ldots\ldots k$$

is the same as the kinetic energy of their inertial center. The speed of the inertial center, and its kinetic energy, is given by

$$\omega_{coi} = \left(\sum_{i=1}^{k} M_i\omega_i\right) / \left(\sum_{i=1}^{k} M_i\right) \tag{5-7}$$

$$K.E. = (1/2)M_t(\omega_{coi}^2) \tag{5-8}$$

Essentially, we see a disturbance splitting the generators of the system into two groups: the critical machines and the rest of the generators. Each group has a kinetic energy associated with its gross motion, as indicated by the motion of each inertial center; the total kinetic energy is the sum of two expressions similar to equations 5-7 and 5-8:

$$K.E. = (1/2)M_{cr}\omega_{cr}^2 + (1/2)M_{sys}\omega_{sys}^2$$

This same result is obtained by a different approach, which is somewhat more physically meaningful. We can consider the gross motion of the two groups as equivalent to that of a

two-machine system. The kinetic energy causing separation of the two groups is the same as that of an equivalent one-machine-infinite-bus system (see reference 47) having an inertial constant M_{eq} and angular speed ω_{eq} given by:

$$M_{eq} = (M_{cr})(M_{sys})/(M_{cr}+M_{sys})$$

and

$$\omega_{eq} = (\omega_{cr} - \omega_{sys}) \tag{5-9}$$

The kinetic energy is given by

$$K.E. = (1/2)M_{eq}(\omega_{eq})^2 \tag{5-10}$$

The kinetic energy correction ΔKE_{corr} is, thus

$$\Delta KE_{corr} = (1/2)\sum_{i=1}^{n} M_i\omega_i^2 - (1/2)M_{eq}(\omega_{eq})^2 \tag{5-11}$$

Notice that ΔKE_{corr} will always be positive. Again, the kinetic energy term in the margin should be corrected accordingly. We, therefore, define the corrected energy margin by

$$\Delta V_c \triangleq V\Big|_{\theta^a}^{\theta^b} + \Delta KE_{corr} \tag{5-12}$$

Since the kinetic energy correction is always positive, it

will always serve to increase the margin.

The kinetic energy contributing to system separation is illustrated in the following examples.

4-generator System

For the three-phase fault at bus 10 cleared at 0.1 s by opening one of the lines between busses 10 and 12, the critical machine is generator number 4, which tends to separate from the system. Data for calculating the kinetic energy correction at clearing are shown in Table 5-1. From this table we note that the total kinetic energy equals 0.2703 pu. Generator No. 4, which represents about 16% of the total system inertia, is accelerated. The 3-generator group (1, 2, and 3), representing 84% of the system inertia, is decelerated. The kinetic energy associated with the gross motion of each group is to be calculated. Since the accelerating group consists of only one generator, the kinetic energy is found from Table 5-1 to be 0.2187 pu. This number needs no adjustment. The kinetic energy of the 3-machine decelerating group is the kinetic energy of the inertial center of that group. We obtain the following data:

$M_{cr} = 0.0340$ $\quad \omega_{cr} = 0.00951$ $\quad KE_{cr} = 0.2187$ pu

$M_{sys} = 0.1754$ $\quad \omega_{sys} = -0.00184$ $\quad KE_{sys} = \underline{0.0424 \text{ pu}}$

$KE_{total} = 0.2611$ pu

Table 5-1. 4-generator system, fault at bus 10, cleared at 0.1s

Gen. No.	M_i	ω^c pu	K.E.
1	0.1254	-0.004	0.0507
2	0.034	-0.0005	0.0006
3	0.016	-0.0005	0.0003
4	0.034	0.0095	0.2187
			total = 0.2703 pu

The kinetic energy of the accelerating group is .2187 pu; the kinetic energy of the decelerating group is .0424 pu; the total kinetic energy of the gross motion is the sum of these numbers, and is .2611 pu.

This same number can be found by converting to an equivalent one-machine-infinite-bus system:

M_{eq} = 0.02848 ω_{eq} = 0.01136 KE_{total} = 0.2611 pu

Comparing this value to kinetic energy at clearing (.2703), the kinetic energy correction for this case is

$$\Delta KE_{corr} = 0.0082 \text{ pu}$$

17-Generator System

For a three-phase fault at bus 372 (near generator No.6) cleared at Ø.15 s by opening line 372-193, the generators which ultimately separate from the system are generators No. 5 and 6. These generators are taken as the critical group. The other five machines of the Missouri River transmission corridor (No. 2, 1Ø, 12, 16, and 17) are accelerated with generators 5 and 6, while the rest of the machines are either decelerated or not significantly disturbed. Generators 5 and 6, which represent only about 5% of the total inertia of the system, have a center of inertia velocity of .Ø1874 pu. The rest of the system (95% of the inertia) has a group velocity of .ØØØ95 pu. We obtain the following data:

M_5 = Ø.Ø89Ø7 ω_5 = Ø.Ø1142 pu KE_5 = Ø.83 pu

M_6 = Ø.17236 ω_6 = Ø.Ø2252 pu KE_6 = 6.22 pu

KE_5+KE_6 = 7.Ø5 pu

For the inertial center of the 5,6 group:

$M_{5,6}$ = Ø.26143 $\omega_{5,6}$ = Ø.Ø1874 $KE_{5,6}$ = 6.53 pu

For all other machines:

M_{other} = 4.87442 ω_{other} = -.ØØØ954 KE_{other} = Ø.32 pu

Total kinetic energy for the gross motion is:

$$KE_{total} = 6.53 + 0.32 = 6.839 \text{ pu.}$$

To calculate the same kinetic energy from the equivalent one-machine-infinite-bus system, we obtain:

$$M_{eq} = 0.24312 \qquad \omega_{eq} = 0.0197 \qquad KE_{total} = 6.839 \text{ pu}$$

The total kinetic energy for this case is 7.97 pu. Thus, the energy correction at clearing is:

$$\Delta KE_{corr} = 1.131 \text{ pu}$$

which is a 14% adjustment in the kinetic energy. That is, at the instant of clearing, 14% of the kinetic energy is involved in intermachine motion around the inertial centers and that 14% does not contribute to separation of the critical group from the rest of the system.

Other Corrections Applied to the Energy Margin

While the major correction in the energy margin is the kinetic energy correction, other minor corrections may be in

order. This dissertation defines the transient energy margin as the energy function properly evaluated between clearing and the UEP. Other researchers, familiar with the transient energy function as offered by SCI, might define the margin as being the difference between V_{cr} and V_{cl}. As stated previously, the transient energy margin defined as between θ^{cl} and θ^{u} is not exactly the same as the margin computed as the difference between V_{cl} and V_{cr}. Two points must be considered to reconcile the two definitions.

-- V_{cr} and V_{cl} must be computed using a common reference (e.g., θ^{s1} vs θ^{s2}). It is common to compute V_{cr} with respect to the post-fault SEP, θ^{s2}, and V_{cl} with respect to the pre-fault SEP, θ^{s1}. In Chapter 3, we stated that in such cases the correction

$$V\Big|_{\theta^{s1}}^{\theta^{s2}}$$

must be applied. This must be subtracted from V_{cl} to refer it to θ^{s2}:

$$V\Big|_{\theta^{s2}}^{\theta^{cl}} - V\Big|_{\theta^{s1}}^{\theta^{s2}} = V\Big|_{\theta^{s2}}^{\theta^{cl}}$$

In the 17-generator system, for example, the correction is computed as:

$$V\Big|_{\theta^{s1}}^{\theta^{s2}} = 0.142 \text{ pu}$$

-- The approximation term,

$$I\Big|_{\theta^{cl}}^{\theta^{u}}$$

that accounts for the network transfer conductances in the energy function is defined as by equation

5-6. This approximation for the conductance term does not give the same value for the margin when computed as

$$\Delta V = V_{cr} - V_{cl} \tag{5-13}$$

as it does when computed directly as

$$\Delta V = V\Big|_{\theta^{cl}}^{\theta^{u}} \tag{5-14}$$

Being specific, this is because the margin computed via equation (5-14) will contain the terms

$$I_{ij}\Big|_{\theta^{cl}}^{\theta^{u}} = E_i E_j G_{ij} \left(\frac{(\theta_i^u+\theta_j^u)-(\theta_i^{cl}+\theta_j^{cl})}{(\theta_{ij}^u-\theta_{ij}^{cl})} \right) (\sin\theta_{ij}^u - \sin\theta_{ij}^{cl})$$

while the same margin calculated using equation (5-13), will contain the terms

$$I_{ij}\Big|_{\theta^{s2}}^{\theta^{u}} - I_{ij}\Big|_{\theta^{s2}}^{\theta^{cl}} = E_i E_j \left(\frac{(\theta_i^u+\theta_j^u)-(\theta_i^{s2}+\theta_j^{s2})}{(\theta_{ij}^u-\theta_{ij}^{s2})} \right) (\sin\theta_{ij}^u - \sin\theta_{ij}^{s2})$$

$$- E_i E_j \left(\frac{(\theta_i^{cl}+\theta_j^{cl})-(\theta_i^{s2}+\theta_j^{s2})}{(\theta_{ij}^{cl}-\theta_{ij}^{s2})} \right) (\sin\theta_{ij}^{cl} - \sin\theta_{ij}^{s2})$$

The two expressions, though intended to estimate the same conductance energy, clearly are not identical. The computation using equation (5-14) is taken to be more accurate. A correction equal to the difference between the two conductance approximations must be applied in order to reconcile the results obtained by the two computational techniques. For the 17-machine case, for example, this correction amounts to

$$I_{corr} = -\emptyset.356 \text{ pu}$$

The correction (of $I_{corr} = -.36$ pu) must be added to the margin obtained by equation (5-13) to reconcile it with results obtained via equation (5-14).

Thus, for the 17-machine system the $V_{cr} - V_{cl}$ definition may be expressed as

$$\Delta V_c = V\Big|_{\theta^{s2}}^{\theta^{u}} - V\Big|_{\theta^{s1}}^{\theta^{cl}} + V\Big|_{\theta^{s1}}^{\theta^{s2}}$$

$$+ \; I_{corr}$$

where the last two terms will represent a total correction for the 17-generator system of:

$$V_{corr} = -\emptyset.142 - \emptyset.356$$

$$= \quad -\emptyset.496$$

Of course, use of the equation (5-14) avoids these corrections altogether, as they are embedded in the basic definition. However, to assure completeness in this dissertation, we used the energy terms, V_{cl}, V_u, and ΔV_c; we use the term V_u to denote the corrected energy in order to facilitate reconciliation.

One other adjustment to the energy margin should be mentioned even though it cannot be quantified at this point. This adjustment, or correction, is applied to V_{cr} to account for the angular distance by which the critical trajectory misses the UEP. This energy can be thought of as consisting

of two parts: the energy associated with how far the non-critical generators miss their UEP positions, and the energy associated with how far the critical generators miss their UEP positions. In the former case, the energy seems consistently small (in the order of 0.5 pu) during the entire trajectory, while the latter is small when the critical generators approach the UEP on the critical trajectory. In chapter 4 we concluded that, for all practical purposes, the UEP energy can be taken as equal to the critical escape energy.

Procedure for Computing the Transient Energy Margin

The transient energy margin for a given post-fault system is the transient energy function evaluated between θ^u and θ^{cl} and corrected for kinetic energy not contributing to instability:

$$\Delta V_c = V\Big|_{\theta^{cl}}^{\theta^u} + \Delta KE_{corr}$$

The procedure for calculating the transient energy margin involves the following steps:

1. Identifying the critical machines, i.e., the generators tending to separate from the rest of the system.
2. Determining the specific post-disturbance network configuration to be considered.
3. Identifying the relevant UEP (θ^u) for the disturbance under investigation.

4. Computing the angle and speeds of the generators at fault clearing, i.e., θ_{cl} and ω_{cl}.

5. Computing

$$\Delta V = V\Big|_{\theta^{cl}}^{\theta^{u}}$$

6. Computing the kinetic energy at clearing which does not contribute to system separation (ΔKE_{corr}) and correcting ΔV to obtain ΔV_c.

7. If the procedure is to be repeated for other post-disturbance network configurations (i.e., other lines cleared), computing the changes in the Y-bus and the corresponding θ^u and ΔV_c.

These steps are outlined in order to identify the computational aspects encountered during implementation. In practice, however, steps 5 and 6 are combined.

The Computer Programs

In this research, the computations of the transient energy margin are actually performed by two computer programs or packages of programs.

Package I.

In this package, the following information is obtained:

- The generators' positions, velocities, and accelerations during the fault period
- The post-fault Y-bus

This package is based on programs received from SCI. It has been modified to include the following additional features:

- Plotting the rotor positions of individual generators
- Computing and plotting the positions of the inertial centers of a group of generators

- Computing and plotting the energy components during the trajectory

This package of computer programs, coupled with various plot routines, has been used extensively for investigating the transient energy in the system trajectories discussed in the various sections of this report.

Package II.

From information obtained from Package I (specifically from the angles and velocities at clearing, and the post-fault Y-bus), the mode of instability promoted by the fault is determined; the machines with large velocities and angles are used to "suggest" a UEP that may control the instability for the specific sequence of events. In our procedure, the Davidon-Fletcher-Powell process (DFP routine provided by SCI) is started from the initial positions available to us from the study of the system trajectory. In this research, the resulting UEP was considered a candidate and was subject to confirmation by simulation studies. Knowing the controlling UEP (θ^u) makes it possible to compute the value of the margin ΔV.

The package of programs calculates the transient energy margin as well as an estimate of additional power perturbations necessary to consume that margin. The information needed is obtained from the previous package;

θ_{cl}, ω_{cl}, Y-bus. In addition, the critical machines are identified.

The program accomplishes the following tasks:

- Computes $\Delta V = V\Big|_{\theta^{cl}}^{\theta^{u}}$
- Computes kinetic energy that does not contribute to instability, ΔKE_{corr}, and, consequently, the corrected margin ΔV_c
- When the post-fault network changes (i.e., when alternate lines are cleared), it recomputes θ^u, and the corrected margin ΔV_c
- For analytical purposes, computes V_{cr} and V_{cl}
- Estimates a power injection required to consume this margin ΔV_c

Except for the DFP routine, this entire package was developed specifically for this research project. A description of these programs is given in the Appendix.

Identifying the Critical Generators

A disturbance in a power system creates an imbalance between mechanical power into and electrical power out of each generator. If power-out exceeds power-in, the machine decelerates; if power-in exceeds power-out, the machine accelerates. The difference between power-in and power-out (that is, the accelerating power) is called mismatch. The rate of acceleration due to this mismatch depends upon the inertia constant of the machine. During the fault-on period, the mismatch imbalance is visualized as an injection of transient energy that splits the system, accelerating some

machines and decelerating others, depending on the system configuration during the disturbance. The result is that some machines (those most severely disturbed) will tend to separate from the rest of the system. The grouping promoted by this during-fault configuration may not be fully apparent at the end of the disturbance period. When the disturbance is removed (e.g., by clearing the fault), the post-disturbance configuration results in a new imbalance between power-in and power-out. This new mismatch produces synchronizing forces that tend to hold the system together and maintain system stability. Again, the forces vary in magnitude among the various machines. The post-fault trajectory and the resulting machine groupings reflect the combined effect of the disturbed system forces tending to separate some generators from the rest, and the post-disturbance forces tending to maintain synchronism.

In many situations encountered in power systems, the group of generators that tends to separate from the rest of the system is clearly identifiable. The grouping promoted by the disturbance is not altered by the post-disturbance synchronizing forces. If the disturbance is large enough, these generators will, as a group, lose synchronism with the rest of the system (as governed by the motion of their inertial center, as discussed in Chapter 4). There are situations, however, in which the group of generators

initially separated from the system by the disturbance may not lose synchronism as a group; instead, only some of the generators of the group actually go unstable. When the disturbance is removed, the synchronizing forces are such that some generators of the group will remain in synchronism with the rest of the system, while the others in the group go unstable. This situation may be encountered when a number of power plants are concentrated in a small area of the network.

The correct identification of the critical generators (and, hence, of the relevant UEP) for a particular sequence of events is essential in the determination of the transient energy margin. The critical generators seem to be those generators (within the significantly advanced group) that actually go unstable or are on the verge of going unstable. The selection must be made from the group of highly disturbed generators. The technique for choosing the critical generators, in this research, was to use the angles and speeds at clearing to suggest a UEP; the UEP was then used in computing the margin, but the UEP was subject to verification by inspection of the critical trajectory obtained in validating the results. In most cases, the relevant UEP coincided with the mode of instability actually encountered. The process of identifying the critical generators to obtain the relevant UEP will be illustrated by investigating faults on the 17-generator system.

Investigation of the 17-generator System

For this system, the following disturbances are investigated:

- A three-phase fault at Raun (Bus 372) cleared by opening line 372-193.
- A three-phase fault at Council Bluffs (Bus 436) cleared by opening line 436-771.
- A three-phase fault at Cooper (Bus 6) cleared by opening line 6-439.
- A three-phase fault at Ft. Calhoun (Bus 773) cleared by opening line 773-779.

Using the techniques and computer program packages described in the previous sections, the controlling UEP for each disturbance is determined. This particular UEP (e.g., the UEP shown in Table 4-1) identifies the so-called critical machines, i.e., the generators tending to separate from the rest of the system. This information is checked against time solutions to make certain the identity of the critical generators. In some cases, several modes of instability were found to be possible for the same initial disturbance.

For the Raun fault (near generator No. 6), the generators tending to separate from the system are generators No. 5 and 6. This checks with the time solution shown in Figure 5-1. The critical energy V_{cr} predicted by the computer program (Package II) shows the potential energy to be 16.66 pu (see Table 4-1). This is comparable to the corrected value of transient energy at critical clearing:

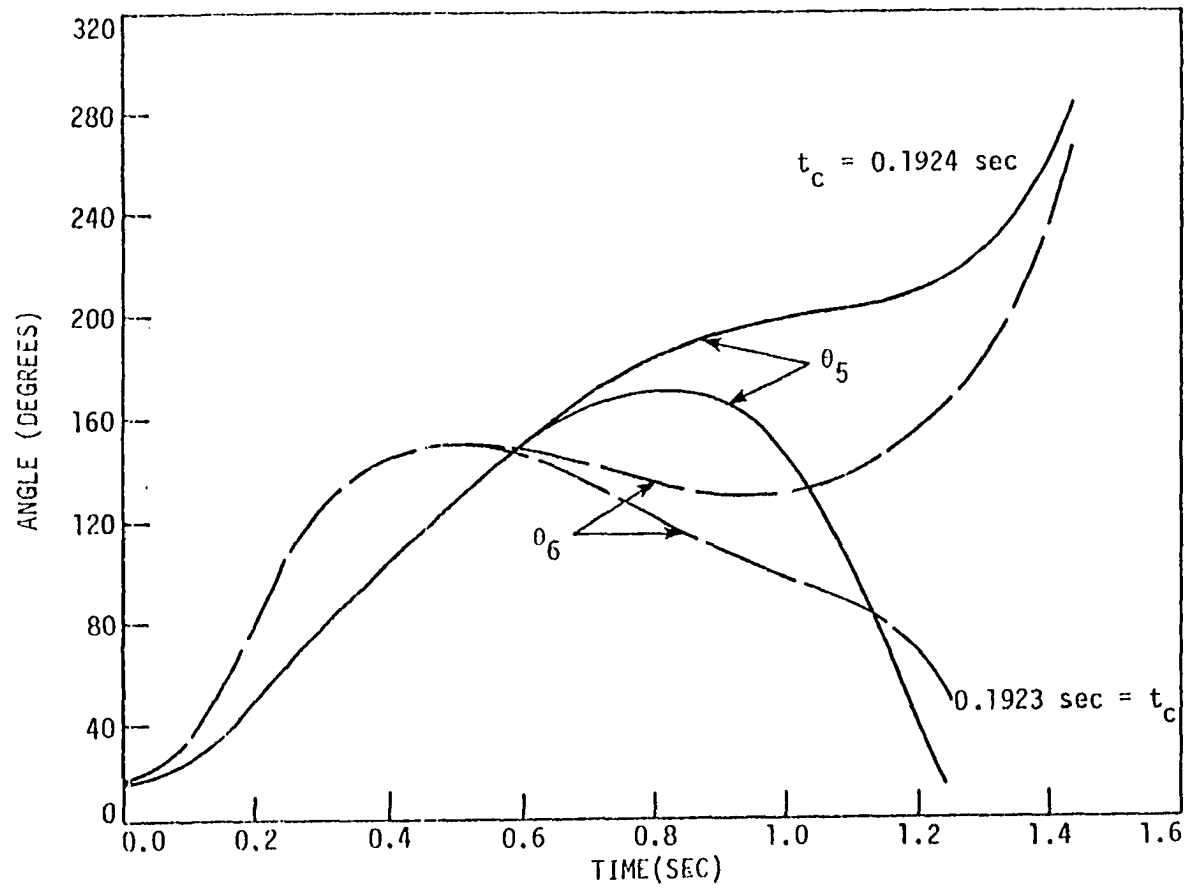

Figure 5-1. Swing curves of generators No. 5 and 6 for Raun fault; t_c = 0.1923s and 0.1924s

$$V\Big|_{\theta^{sl}}^{\theta^{cl}} + \Delta KE_{corr} = 17.10 \text{ pu}$$

For the fault at Council Bluffs (near generators No. 10 and 12), the critical machines are generators No. 10 and 12. The swing curves for clearing near the critical clearing instant are shown in Figure 5-2. While it is possible for generator No. 12 to lose synchronism alone (t_c = 0.204), the slightest additional transient energy causes both generator No. 10 and generator No. 12 to become unstable (t_c = 0.206s). The critical energy for $\theta^u_{10,12}$ is comparable to the corrected value of the transient energy at critical clearing. On the other hand, V_u for θ^u_{12} is much lower and would predict a rather conservative critical clearing. Thus, although the critical trajectory would realize an instability involving machine No. 12 alone, the critical generators are taken to be generators No. 10 and 12. Here we differentiate between the mode of instability and the critical group. The machines that make up the critical group are those machines that are so severely disturbed as to be on the verge of going unstable. The ones that actually separate from the system and lose synchronism will depend on the duration of the fault. Those machines determine the mode of instability. In the case under discussion, generator 10 and 12 form the critical group, while the mode of instability is No. 12 alone going unstable.

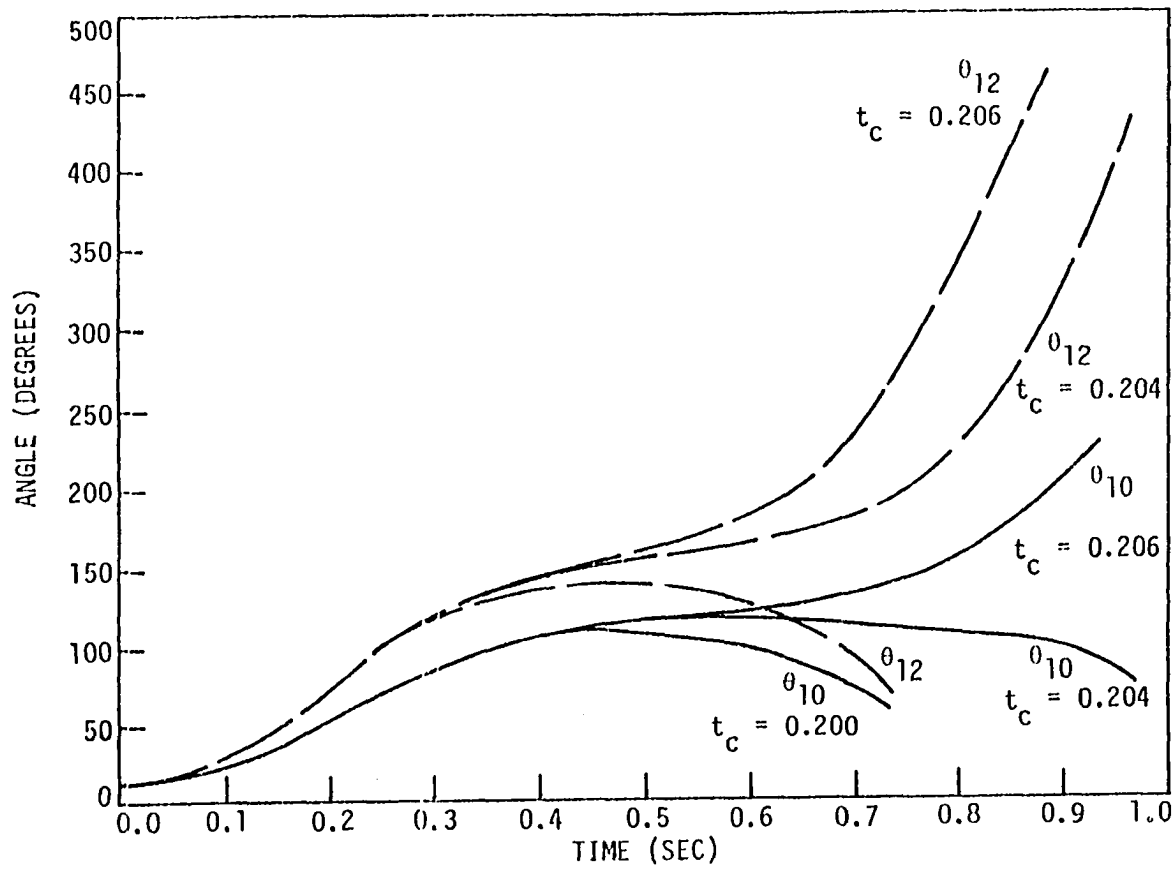

Figure 5-2. Swing curves of generators No. 10 and 12 for fault at Council Bluffs; t_c = 0.200s, 0.204s, and 0.206s

This visualizes a critical trajectory that approaches the UEP for 10 and 12, but in fact only No. 12 goes unstable while No. 10 recovers.

The fault at Cooper (near generator No. 2) exhibits a behavior similar to that of the fault at Council Bluffs. Figure 5-3 shows the swing curves for the different clearing times. Generator No. 2 loses synchronism alone, unless considerably more transient energy is injected to cause generator No. 17 to lose synchronism as well (as for t_c = 0.30 s). Thus, for practical purposes the critical group is that of No. 2 alone. This is confirmed by the fact that the critical energy V_u for θ_2^u is comparable to the transient energy at critical clearing.

The situation for the Ft. Calhoun fault (near generator No. 16) is more complex. Figures 5-4(a), 5-4(b), and 5-4(c) show the swing curves for six generators for t_c = 0.357 s, t_c = 0.4125 s, and t_c = 0.423 s, respectively. All three are unstable, but in (a) only No. 16 separates from the system; in (b) generators No. 2, 16, and 17 separate; in (c) all six generators lose synchronism (as does generator No. 6, which is not shown in the figure). Detailed investigation of the Ft. Calhoun fault shows that several modes of instability are possible, and each mode represents a critical group of machines (including generator No. 16, which is close to the fault). For each of these modes, a controlling UEP can be

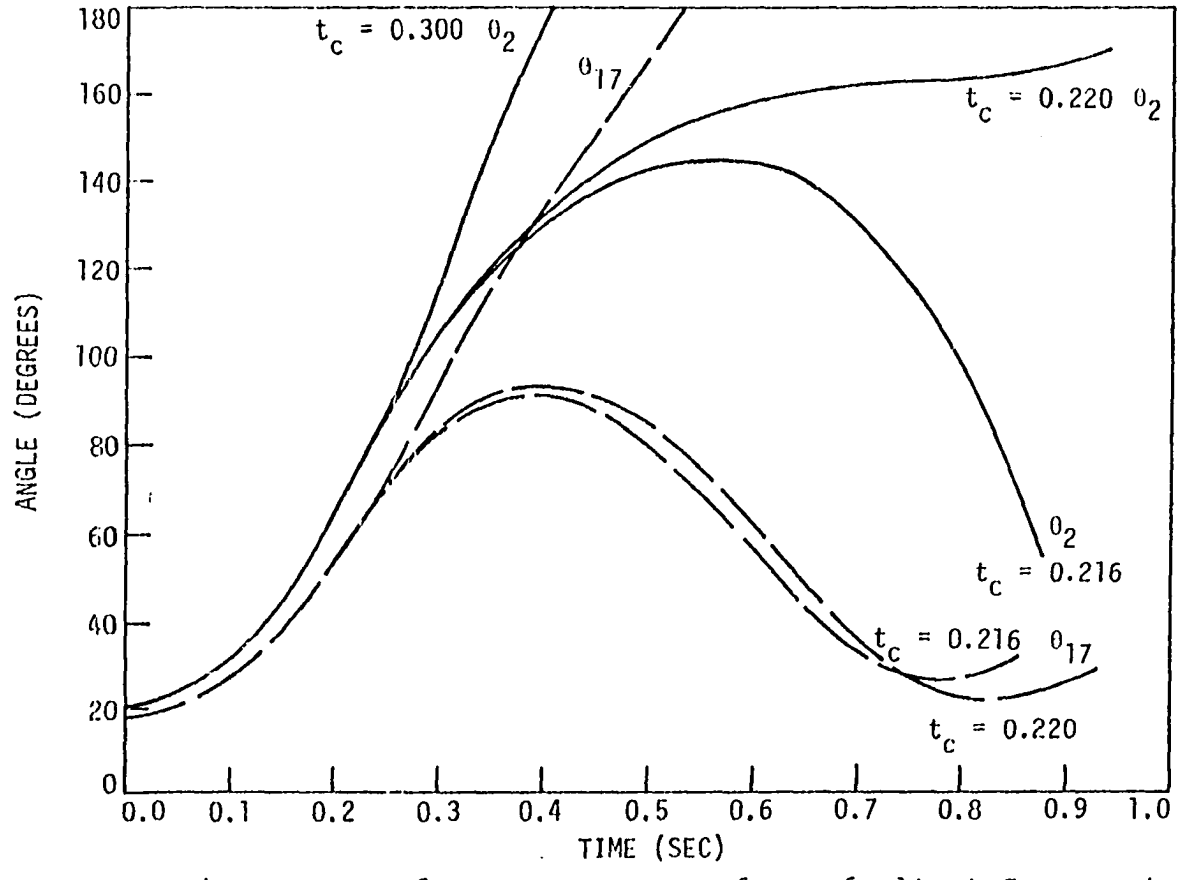

Figure 5-3. Swing curves of generator No. 2 for a fault at Cooper; t_c = 0.216s, 0.220s, and, 0.300s

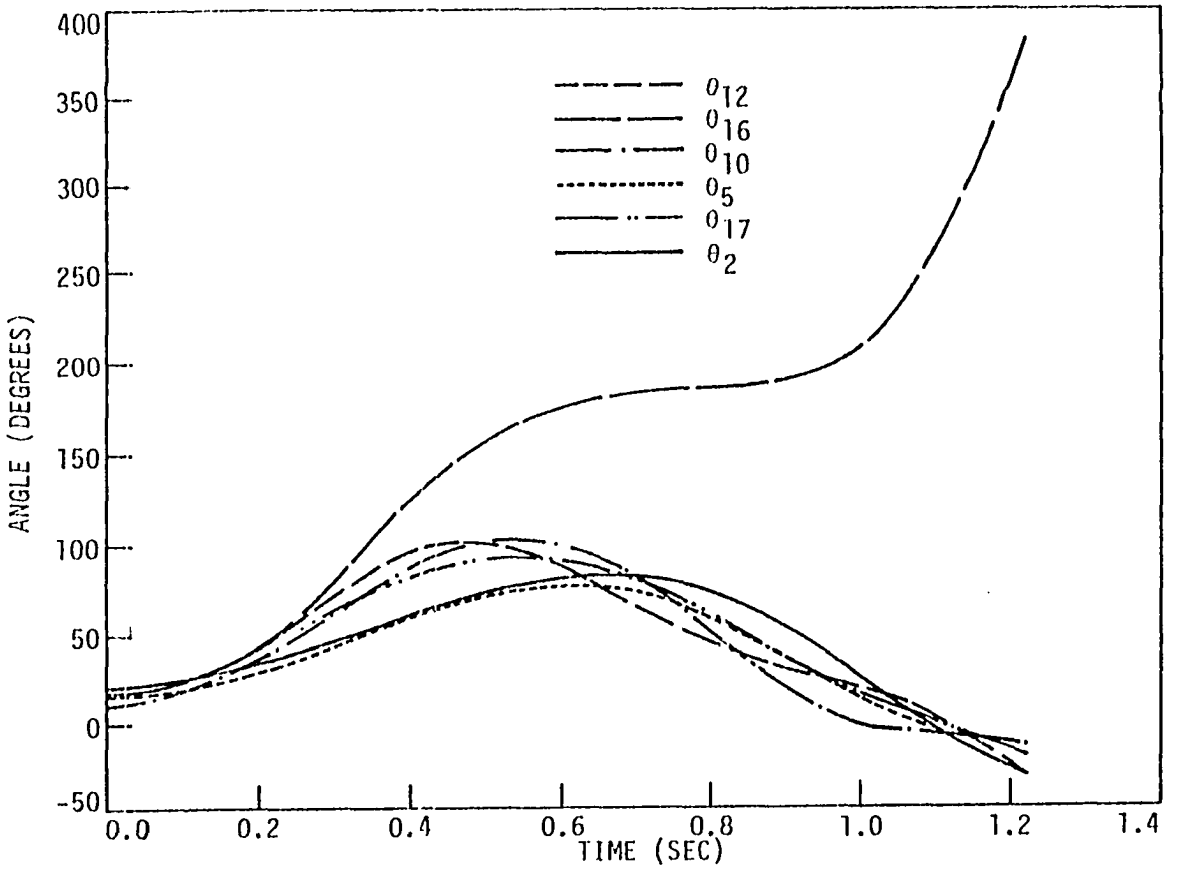

Figure 5-4(a). Swing curves of generators No. 2,5,10,12,16, and 17 for a fault at Ft. Calhoun; t_c = 0.357s

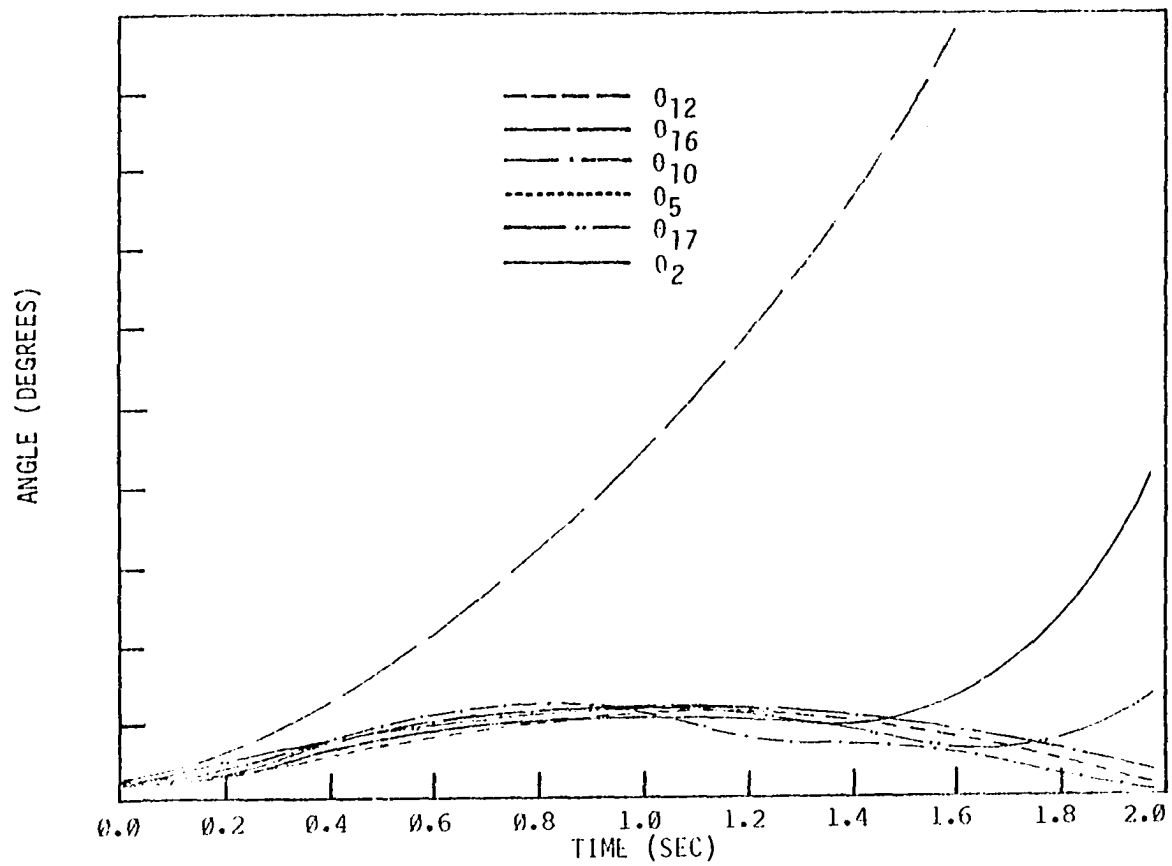

Figure 5-4(b). Swing curves of generators No. 2,5,10,12,16, and 17 for a fault at Ft. Calhoun; t_c = 0.4125s

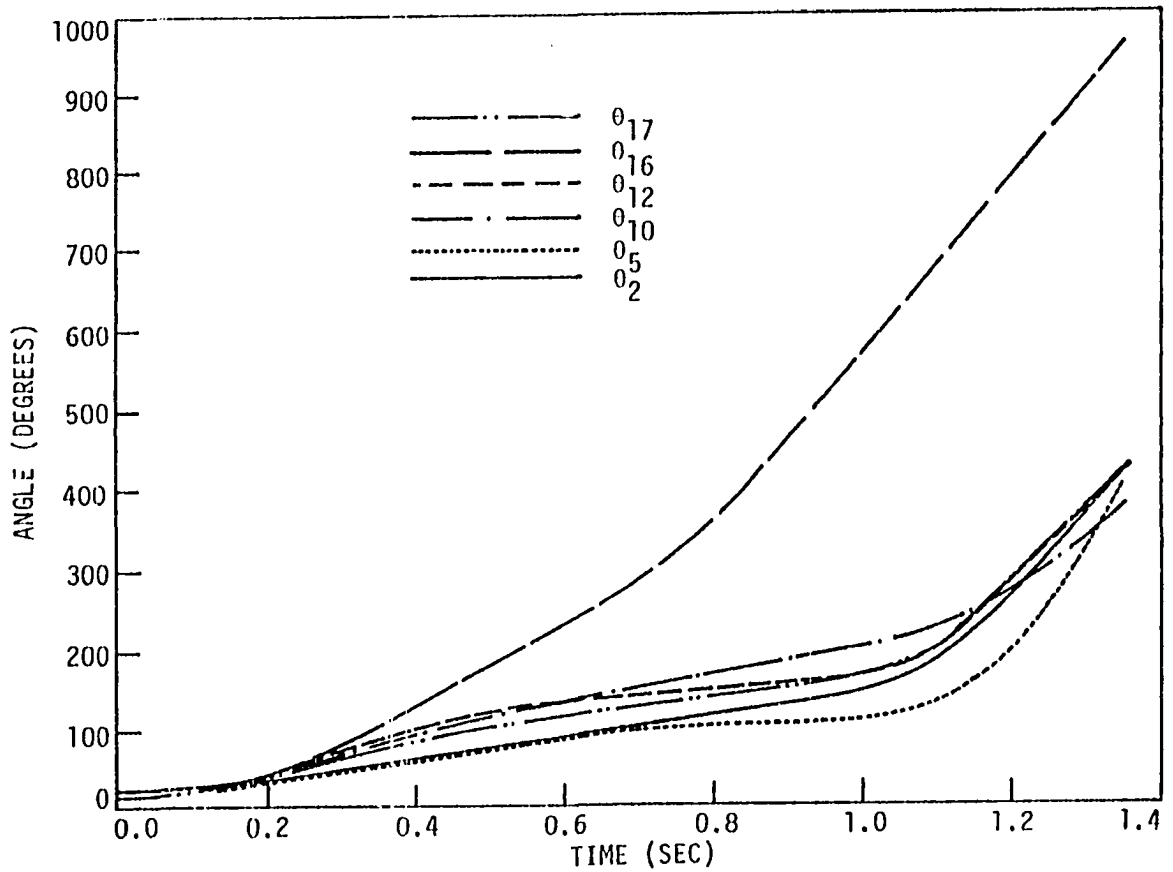

Figure 5-4(c). Swing curves of generators No. 2,5,10,12,16, and 17 for a fault at Ft. Calhoun; t_c = 0.4230s

identified, each with a corresponding critical energy. These UEPs have potential energies of similar magnitudes, i.e., in the range of 24.5 - 28.5 pu, and thus constitute a cluster of UEPs representing various possible modes. Therefore, identification of the controlling UEP is not an easy task. Only the most probable one, i.e., the UEP for which the critical energy most closely matches the energy values along the system trajectory, is selected based on the following reasoning: the disturbance tends to separate all of the generators on the Missouri River transmission corridor (generators No. 2,5,6,10,12,16, and 17) from the rest of the system. The energy level needed to separate this group is quite high (about 30 pu). As the system trajectory moves toward the UEP for this group, it encounters the cluster of UEPs with potential energy levels of 24.5-28.5 pu. This cluster controls the first swing stability for this disturbance. This is confirmed by the fact that the system trajectory of the critically unstable case (t_c = 0.357 s) has a potential energy of 24.6 at the point of inflection of θ_{16}.

Table 5-2 shows a summary of the cases for the four fault locations in terms of the critical generators, the critical energy predicted by the controlling UEP V_u, and the critical transient energy V_{cl} (obtained from the trajectory).

Table 5-2. Data for Critical Generators, 17-generator system

Fault	Critical Generators	Corrected V_u^* (V_{cr})	Corrected V_{cl}
Raun	5,6	16.66	17.10
C.B.#3	10,12	12.30	13.30
Cooper	2	11.56	13.40
Ft. Calhoun	16,2,10,12,17	28.25	24.90

* V_u with respect to θ^{sl}

Investigation of Critical Clearing Times

Results of studies of system stability are conventionally reported in terms of critical clearing times. To put the transient energy margin analysis into these terms is not difficult: the instant on the faulted trajectory when the transient energy margin ΔV_c becomes zero identifies the instant of critical clearing.

The transient stability of the two test systems has been investigated to determine the critical clearing time for each of the faults discussed so far: one fault on the 4-generator system and four faults on the 17-generator system. The results are compared to the trajectories obtained from time simulations. The results show in familiar terms how well the relevant UEP predicts stability.

Four-generator system

The procedure is first applied to the four-generator test system. The disturbance investigated is the same as previously discussed (a three-phase fault at bus 10 cleared by opening line 8-10). Several clearing times are selected and displayed in Table 5-3. For each value of t_c, the corrected values of the fault transient energy V_{cl} and the predicted critical transient energy V_u are computed, together with the energy margin ΔV_c. The last column in Table 5-3 contains this value of the transient energy margin ΔV_c for diffenent clearing times. This transient energy margin must not be less

Table 5-3. Fault transient energy for the 4-generator system, fault at bus 10.

t_c clearing s	V_{cl} corrected pu	V_u corrected pu	ΔV_c margin pu
0.1	0.2076	0.5703	0.3627
0.148	0.5258	0.5703	0.0445
0.150	0.5450	0.5703	0.0253
0.153	0.5671	0.5703	0.0032
0.156	0.5967	0.5703	-0.0264
0.159	0.6306	0.5703	-0.0603

than zero for stability to be maintained. The data indicate that the critical clearing time is between Ø.153 s and Ø.156 s (probably closer to Ø.153 s). The swing curves for some of the cases displayed in Table 5-3 are shown in Figure 5-5. The rotor trajectory for generator No. 4 is shown for different clearing times. The time solution data indicate that the critical clearing time is between Ø.156 and .159 s (probably closer to Ø.156 s). The UEP predicts a critical clearing time that is within Ø.ØØ6 s of the actual critical clearing time.

17-generator System

The corrected values of the transient energy margin for different values of clearing time (t_c) are computed. The results for faults at Raun, Council Bluffs, Ft. Calhoun, and Cooper are displayed in the last column of Table 5-4.

For the Raun fault, the results of Table 5-4 show that the critical clearing time which gives the zero transient energy margin is about t_c = Ø.191 s. Swing curves for different clearing times for this disturbance, shown in Figure 5-1, indicate that the clearing time of t_c = Ø.1924 is critically unstable. Therefore, the critical clearing time predicted by a direct method compares favorably to that obtained by the time solution, e.g., within .ØØ14 s.

For the fault at Council Bluffs, the predicted critical clearing time, having a transient energy margin equal to zero,

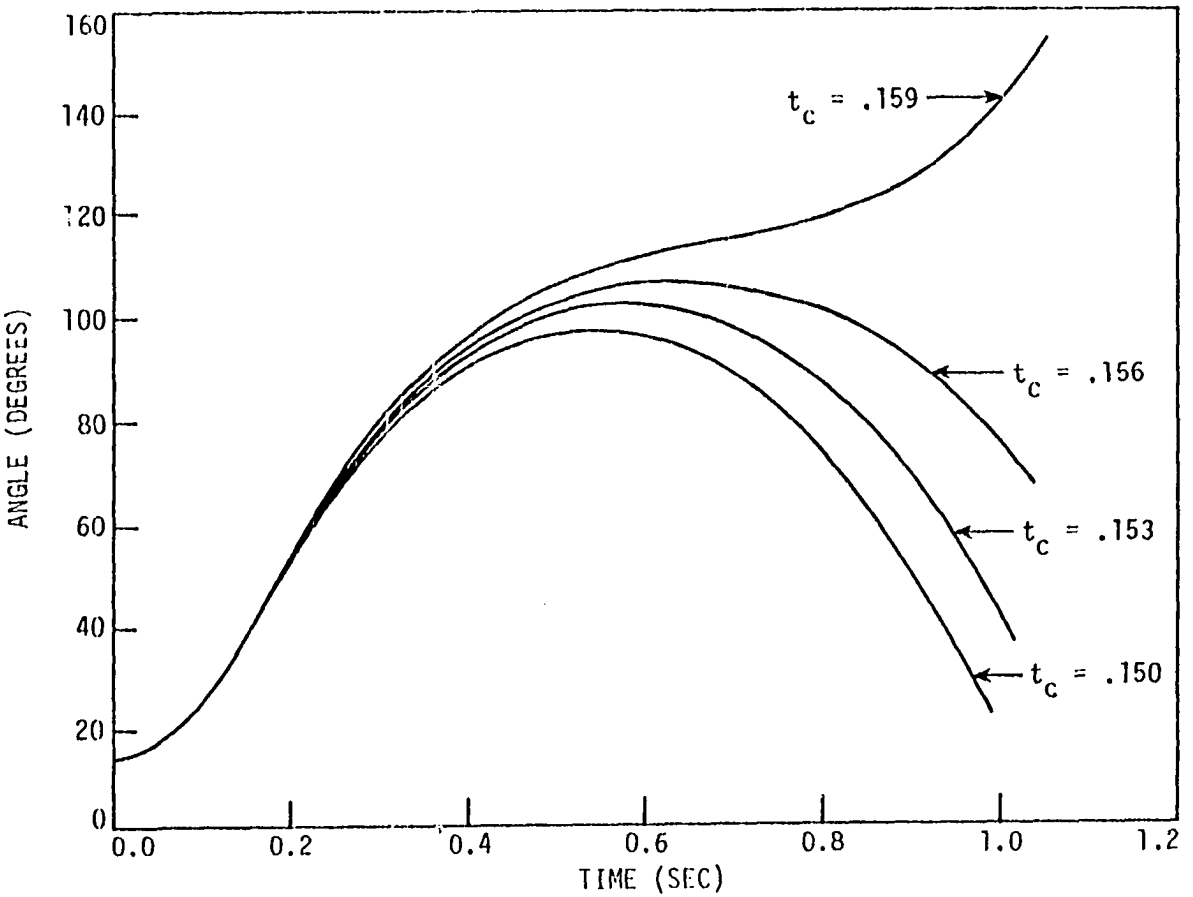

Figure 5-5. Swing curves of generator No.4 (4-generator system) for a fault at Bus 10; t_c = 0.150s, 153s, 156s, and 159s

Table 5-4. Fault transient energy for three-phase faults on the 17-generator system

t_c clearing s	ΔKE_{corr} pu	V_{cl} corrected pu	V_u corrected pu	ΔV_c margin pu
a) RAUN: critical generators 5,6				
0.15	1.119	9.167	16.664	7.497
0.189	1.801	16.269	16.664	0.395
0.1920	1.740	17.029	16.664	-0.365
0.1924	1.774	17.116	16.664	-0.452
0.1932	1.745	17.309	16.664	-0.645
b) COUNCIL BLUFFS: critical generators 10,12				
0.15	2.497	5.935	12.301	6.336
0.200	3.741	12.670	12.301	-0.369
0.204	3.807	13.360	12.301	-1.059
0.206	3.896	13.653	12.301	-1.352
c) FT. CALHOUN: critical generators 2,10,12,16,17				
0.300	3.145	17.757	28.016	10.259
0.350	3.938	23.874	28.016	4.142
0.357	3.909	24.893	28.016	3.123
0.400	4.526	30.344	28.016	-2.328
d) COOPER: critical generator 2				
0.150	3.094	4.999	11.558	6.559
0.204	4.765	11.763	11.558	-0.205
0.216	5.411	13.444	11.558	-1.886
0.220	5.553	14.112	11.558	-2.554

is just under t_c = Ø.2ØØ s. The time solutions, shown in Figure 5-2, give a critical clearing time of just under t_c = Ø.2Ø4 s. This case is within Ø.ØØ4 s of the correct value.

For the Ft. Calhoun fault, the predicted critical clearing time is about Ø.382 s. Time solutions, shown in Figure 5-6, give a critical clearing time of just under Ø.357 s. This case is within Ø.Ø25 s of the correct value.

For the fault at Cooper, the predicted critical clearing time is about Ø.2Ø4 s. The time solutions, shown in Figure 5-7, give a critical clearing time of about Ø.22Ø s. The predicted critical clearing time is within .Ø16 s of the correct value.

The discrepancies between actual and predicted clearing times are small; the worse case was Ft. Calhoun, with a 7% error in the predicted clearing time.

Summary and Discussion

Chapter 5 has introduced the transient energy margin function as computing the difference between the energy at clearing and the energy at the relevant UEP. When this function is properly evaluated (including a correction the kinetic energy that does not contribute to instability), the margin value is the value of the unused potential-energy-storage-capacity remaining after a fault has been completely absorbed. Stability can be assessed by inspecting this margin

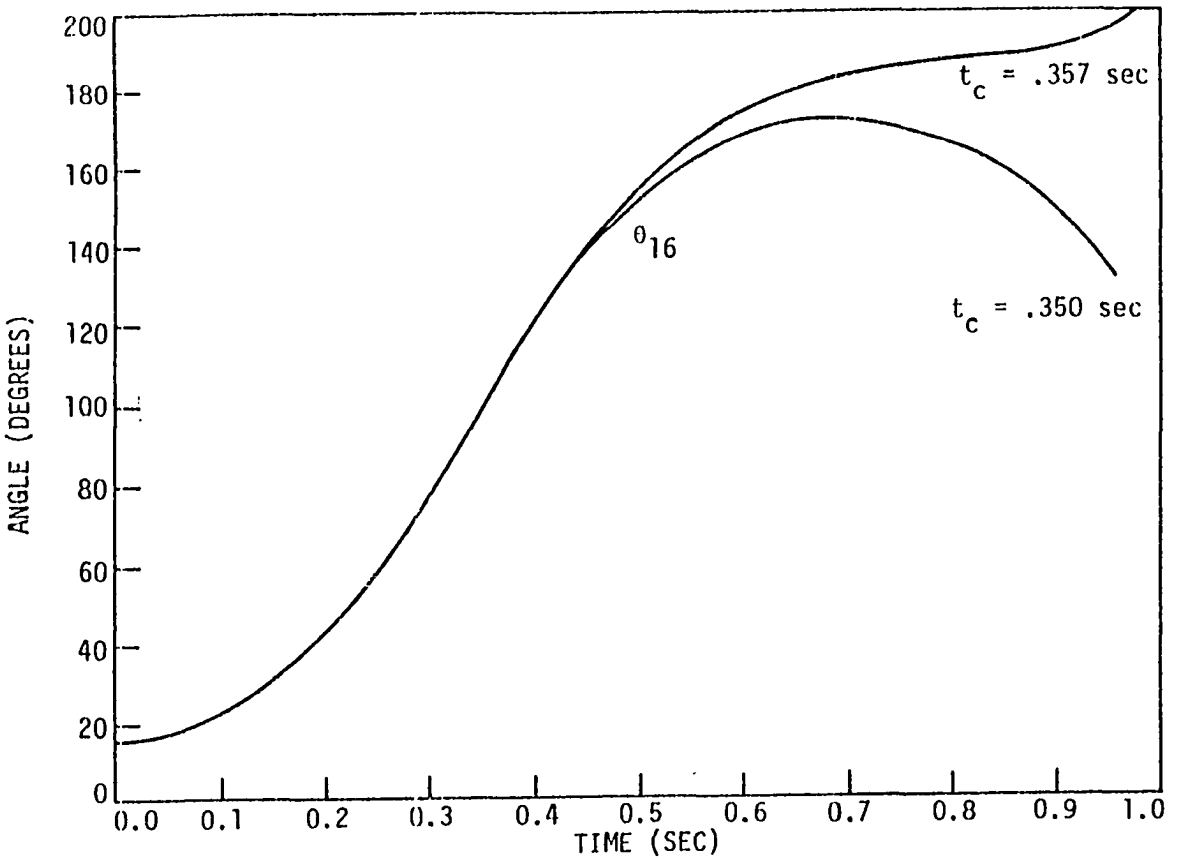

Figure 5-6. Swing curves for generator No. 16 (17-generator system) for a fault at Ft. Calhoun; t_c = Ø.35Øs and Ø.357s

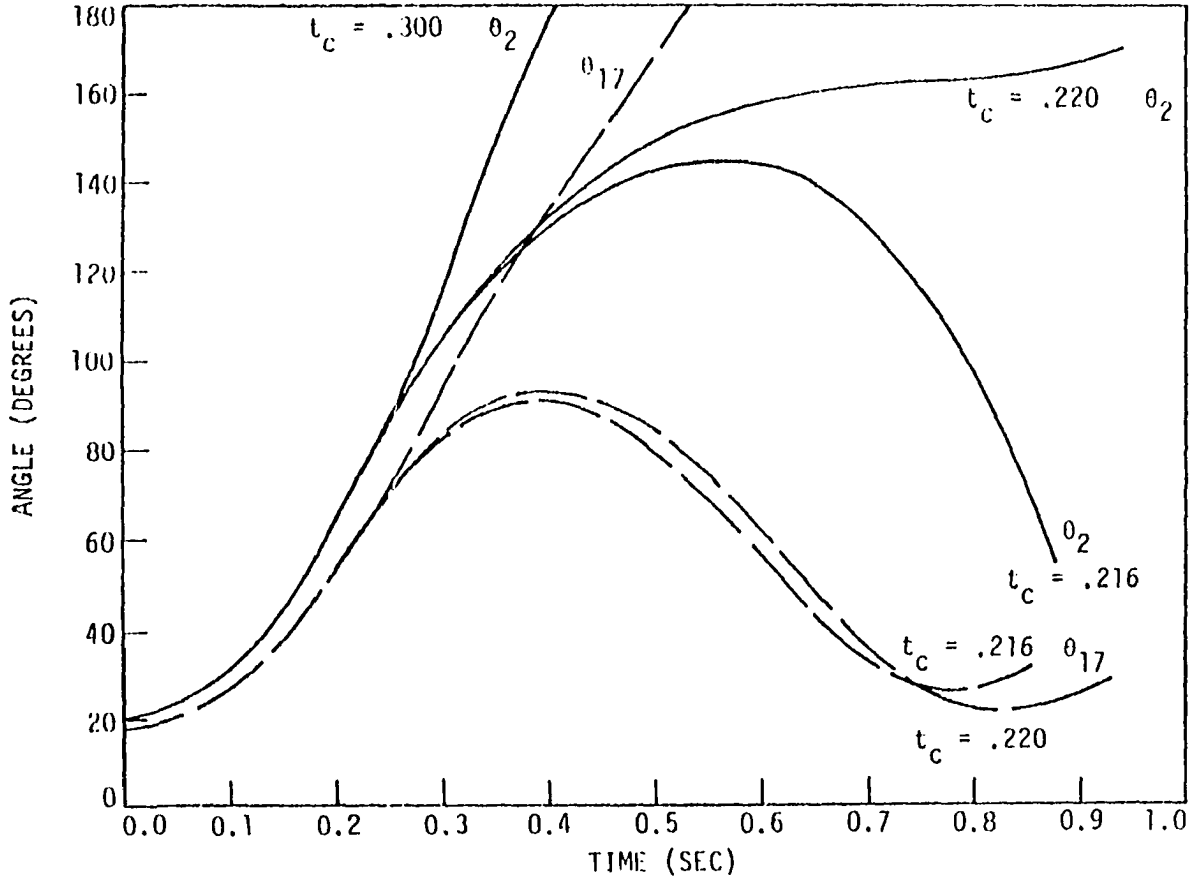

Figure 5-7. Swing curves for generator No. 2 (17-generator system) for a fault at Cooper; t_c = 0.215s, 0.220s, and 0.300s

value. The technique was successfully used to determine critical clearing times for four disturbances on the Missouri River transmission corridor. Maximum error was only 7%.

The results strongly suggest that the relevant UEP does provide a sufficiently accurate measure of critical energy and that the margin function can provide a first-swing transient stability assessment capability. The success of this method depends upon:

- Identification of the controlling UEP for this disturbance
- Accurate computation of the fault transient energy contributing to system separation

The importance of the correction for the fault transient energy that does not contribute to instability is clearly evident: if the correction procedure is not used, the critical clearing time would be grossly in error (as much as 24% error in the critical clearing times).

CHAPTER 6. STABILITY ASSESSMENT USING THE TRANSIENT ENERGY MARGIN

Assessing Stability of the System

The significance of the transient energy margin lies in its ability to represent a "margin of safety" before instability occurs. A positive margin implies that a more severe disturbance can be withstood; further, the margin's magnitude measures how much more energy can be absorbed (i.e., in order to drive the margin to zero). Therefore, the transient energy margin evaluates the unused potential energy absorbing capacity of the system that is available after the disturbance energy has been absorbed. This value is computed using the relevant UEP θ^u which is the local minimum nearest the escape point encountered on the critical trajectory (see Chapter 2). Thus, the transient energy margin attempts to directly evaluate the capacity of the current operating system to withstand a specific disturbance. It reports the uncommitted or reserve energy absorbing capacity that is assured to exist; it assumes a trajectory directly through the local minimum-energy escape point (i.e., the UEP) that is relevant to the critical trajectory. In this way it assesses directly the energy terrain that the critically disturbed trajectory will traverse, and measures the robustness of the existing system configuration and the current operating condition when subjected to a given disturbance.

The Transient Margin as a Tool

The transient energy margin is envisioned as a tool to be used in the direct assessment of transient security. To be a useful tool for on-line assessment, the transient energy margin must function to compare many possible disturbances and to provide a meaningful measure of the robustness of the system for a given operating point. A significant question which had to be resolved in this research was whether the UEP used to estimate critical energy is accurate enough to produce a relative ranking of the disturbance, that is whether the predicted ranking will provide meaningful comparison between different faults and different clearing schemes. Producing relative ranking is more difficult than merely calculating critical clearing. This task tests the uniformity of the predictions and the validity of comparing unrelated disturbances using the transient energy margin.

A Basis for On-Line Stability Assessment

A viable procedure for on-line transient stability assessment seems to be emerging from this research. Given a system operating at a steady state condition, on-line stability assessment requires the following steps:

1. Assemble the system model.
2. Formulate the required Y-bus matrices (i.e., pre-fault, during-fault, and post-fault).
3. Determine the speeds and angles of the generators

at the end of a particular disturbance (θ^{cl} and ω^{cl}).

4. Determine the critical machines and the relevant UEP for that disturbance and post-fault network.

5. Compute the transient energy margin, ΔV_c.

6. For other post-fault configurations (for the same disturbance), recompute the post-fault Y-bus, UEP, and margin.

7. For different disturbances, repeat steps 2-5.

8. Compile the energy margin results and report them in a meaningful way.

These steps outline a procedure for using the transient energy margin as a tool for on-line stability assessment. The computational effort appears to be well within the capabilities available in modern control centers. In this respect, each step deserves some detailed discussion.

Step 1: Assemble the System Model

This research used a classical model (i.e., constant voltage behind transient reactance, constant impedance loads.) This model is suitable for simulation of first-swing transients for a study area that is part of a larger power network. Proper equivalencing can be used to reduce the size of remote areas to produce a manageable number of machines. The Reduced Iowa System is a good example of such a model: the portion of the United States East of the Rocky Mountains was modeled with sufficient detail to provide meaningful security assessment. A 20-generator equivalent may be adequate for even a major power system. We note that the state of the art is such that on-line formulation of suitable equivalents is realizable, subject to some development work.

Step 2: Formulate the Required Y-Bus Matrices

Formation of the Y-bus matrices that are required (pre-fault, faulted, and post-fault Y-bus) is one of the major computational steps of this assessment scheme. The task seems reasonable, however, in terms of fast on-line application, especially for systems with 20 machines or less. Furthermore, once the pre-fault Y-bus has been formed, it can easily be modified to obtain the faulted and post-fault Y-bus. One such technique, using the well-known Householder formulation was used in some parts of this project (42).

Step 3: Determine θ^{cl}, ω^{cl}

Once the disturbed system's Y-bus matrix has been formulated, the process of simulating the disturbance is a relatively small task. Transient simulation programs are readily available.

Step 4: Determine θ^{u} and the Critical Machines

Correctly identifying the critical machines and the controlling UEP, as we have explained in Chapter 5, is a crucial step. If the disturbance clearly splits a small number of generators from the system, this task may be straightforward. However, it is not a simple task when the disturbance is at a point in the network at which the generators are clustered in a small area, and are electrically close to the disturbance (for example, the Ft. Calhoun disturbance in the 17-generator system). While conceptually this choice among the UEPs leaves an element of uncertainty as to the accuracy of the results, from a practical standpoint it can be readily overcome. For a given system, the critical machines associated with a particular disturbance can be determined in advance, using studies similar to that presented in Chapter 5.

Step 5: Compute the Margin

From the post-fault Y-bus, θ^{cl}, ω^{cl}, θ^{u} and identification of the critical machines, the transient energy margin ΔV_c is computed. This gives the margin for the particular disturbance under investigation (e.g., a 3-phase fault at a particular bus cleared in a specific manner). The computational effort involved in computing the margin is small.

Step 6: Recompute the Margin for Other Post-fault Networks

For the same disturbance, there are usually several possible post-fault configurations that might be realized, e.g., other lines that might be cleared in removing the fault. The margin ΔV_c can be computed for these various post-fault network configurations as a variation of the previous step; the new UEP and ΔV_c are computed using the new post-fault Y-bus. Since the clearing conditions are the same, only the post-fault Y-bus is different. The computational effort is reduced, especially when a program for modifying (rather than recomputing) the previous Y-bus is used.

Step 7: Repeat Steps 2-5 for other Disturbances

Steps 2 through 5 are repeated for different types of disturbances (3-phase and 1-phase faults, reclosing sequences, stuck breaker sequences, etc.), and for different locations. Therefore, different types of disturbances at the same locations, and disturbances at other locations in the network, are investigated. The number of choices might be minimized by an on-line decision process that chooses only the worst cases applicable for the current operating conditions.

Step 8: Results Compiled and Reported

The results of the complete study (steps 1 through 7) must be compiled and reported in a way that provide meaningful information about the status of the system security. The report must identify the weaknesses in the system in a way that suggests the source of the problem and a possible solution.

Normalizing the Transient Energy Margin

Step 8 in the above procedure is very important. Having computed the values of the transient energy margin ΔV_c for various disturbances, what inferences can be made? How can security be assessed, using the values of the transient energy margin for the various disturbances? This introduces an

obvious question: will the margin of ΔV_c = 6.0 pu always indicate a more robust system (farther from instability) than that of a situation in which the margin is ΔV_c = 5.0 pu? Intuitively, the answer is: no. Although the transient energy margin is indicative of the unused transient energy absorbing capacity after a particular fault has been fully absorbed as potential energy, its magnitude is of significance only as it compares with the transient energy injected into the system by the fault. For this reason, we proceed by normalizing the transient energy margin before the margin values are compared.

At clearing, for stability to be maintained, the component of transient energy that must be converted into potential energy (including the dissipative component), is the corrected transient kinetic energy (i.e., the kinetic energy at clearing corrected for that component not contributing to instability). The true margin of safety, therefore, is measured by comparing the margin ΔV_c to the corrected kinetic energy. In other words, a more meaningful measure of the robustness of the system is the ratio of the margin energy to the corrected kinetic energy, a ratio which provides a normalized energy margin ΔV_n:

$$\Delta V_n = \Delta V_c / \Delta KE_{corr} \qquad (6\text{-}1)$$

A different form of the same normalized energy margin is the

percent margin:

$$\%\Delta V = [\Delta V_c/(\Delta V_c + \Delta KE_{corr})]\ 100\% \tag{6-2}$$

These two definitions are based on the same normalizing concept, and one can be derived directly from the other:

$$\%\Delta V = [\Delta V_n/(1 + \Delta V_n)]\ 100\% \tag{6-3}$$

The normalized form given in equation 6-1 gives the margin energy per unit of disturbance energy, i.e., it is a measure of how many more such kinetic energy disturbances could be withstood. A margin of $\Delta V_n = 2.5$ means that "2 1/2 more such kinetic energy disturbances" could be safely absorbed. A zero margin implies critical stability.

The percent margin, given in equation 6-2, compares the unused margin to the potential energy available at clearing. This assesses the reserve potential energy capacity remaining unused after the fault has been absorbed. This form might appeal to operators, since it offers a more realistic physical meaning. The value is always less than 100; a margin of $\%\Delta V$ = 45% would mean that the fault left 45% of the kinetic energy absorbing capacity unused. Again, a zero margin would imply critical stability.

The choice between the two normalizing definitions is

strictly a matter of preference.

Transient Energy Margin Profile of the 17-Machine System

As explained in Chapter 3, the 17-generator test system is a reduced equivalent of the network of the State of Iowa. The study system, which is represented in sufficient detail for transient analysis, is the western area of the network, including the area known in this dissertation as the Missouri River transmission corridor. Seven generating plants are located along this corridor. The initial operating condition is the same as that used throughout this dissertation: the 1980 network, with 80% loads, and a prior outage of the Raun-Hinton line (Line 372-332). Details of these operating conditions are given in reference (42).

The normalized energy margin was computed for 37 cases: 13 3-phase faults and 24 single-line-to-ground faults with stuck breakers assumed. The results represent a transient energy margin profile of the 17-generator system. This information would be potentially useful for transient stability assessment of that system.

Types of Disturbances

The 17-generator Reduced Iowa System was investigated for disturbances at four busses on the Missouri River transmission

corridor:

- bus 372 (near Raun)
- bus 436 (near Council Bluffs)
- bus 773 (near Ft. Calhoun)
- bus 6 (near Cooper)

Two types of faults were considered at each location:

- A three-phase fault, applied to the high voltage (345 kV) transformer terminal, cleared at Ø.15 s (9 cycles) by clearing one line. (While the actual breaker clearing time is Ø.Ø8 s or 6 cycles, the 9-cycle fault duration was chosen to match cases which were already available and which would be too costly to repeat.) No reclosing sequences were considered.

- A single-line-to-ground fault, with a breaker failure, eventually cleared by backup protection. The sequence assumed was:

  -- One-line-to-ground fault applied, with clearing attempted at .Ø8 s (6 cycles); the breaker close to the fault is assumed to have failed to open, so only the distant end of the line is opened.

  -- Back-up protection isolates the fault at Ø.24 s. With the activation of backup protection, secondary lines might also be cleared.

Post-fault Networks

For each of the four fault locations and both of the fault sequences described above, the schematic diagrams for the breaker are inspected to determine all realizable post-fault network configurations that can result. The schematic diagrams are shown in Figure 6-1, for Raun, and Figure 6-2, for the other fault locations. The result of the combination of possible fault locations, types, and post-fault networks is 37 fault cases: 13 three-phase faults, and 24

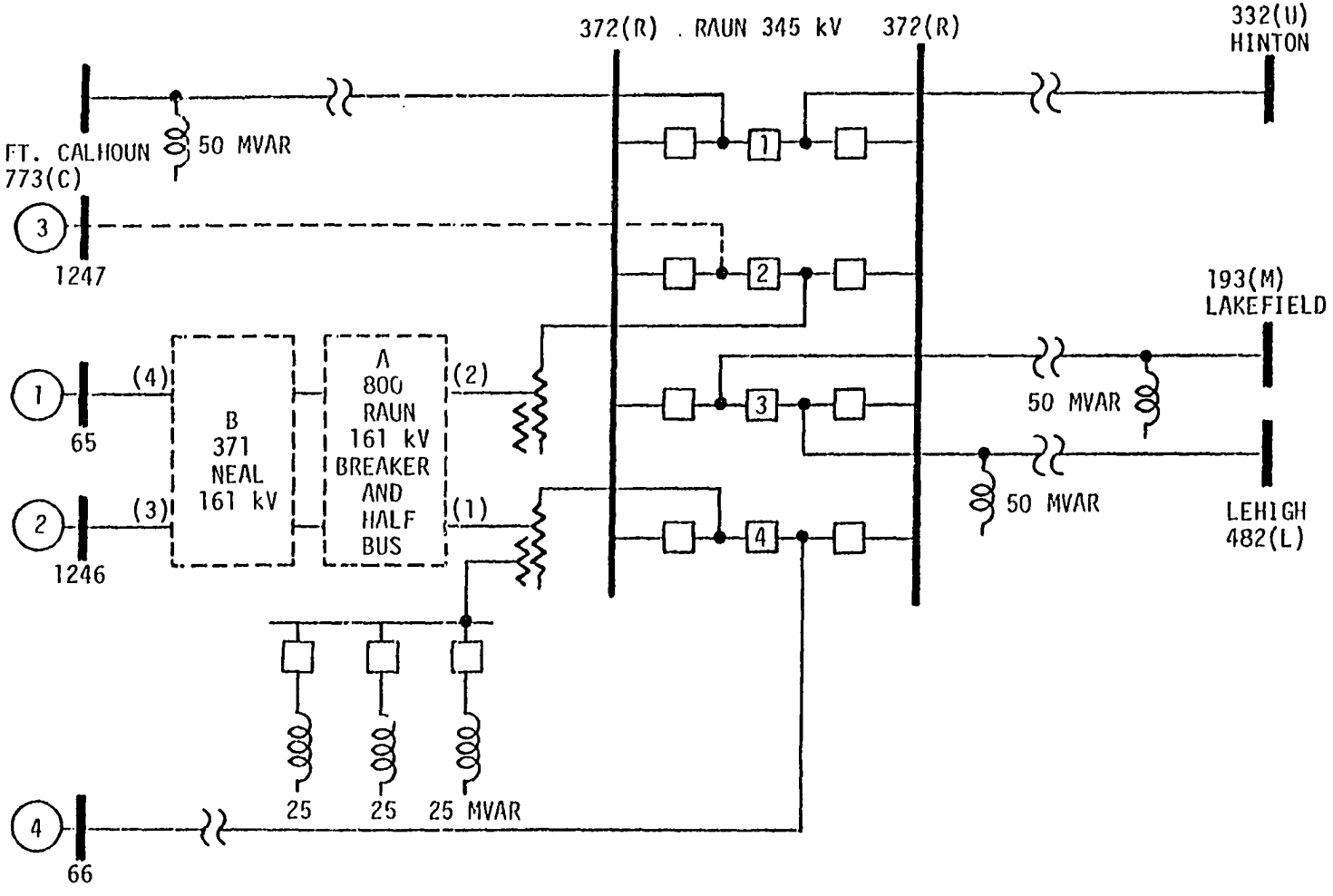

Figure 6-1. Raun 345 kV station.

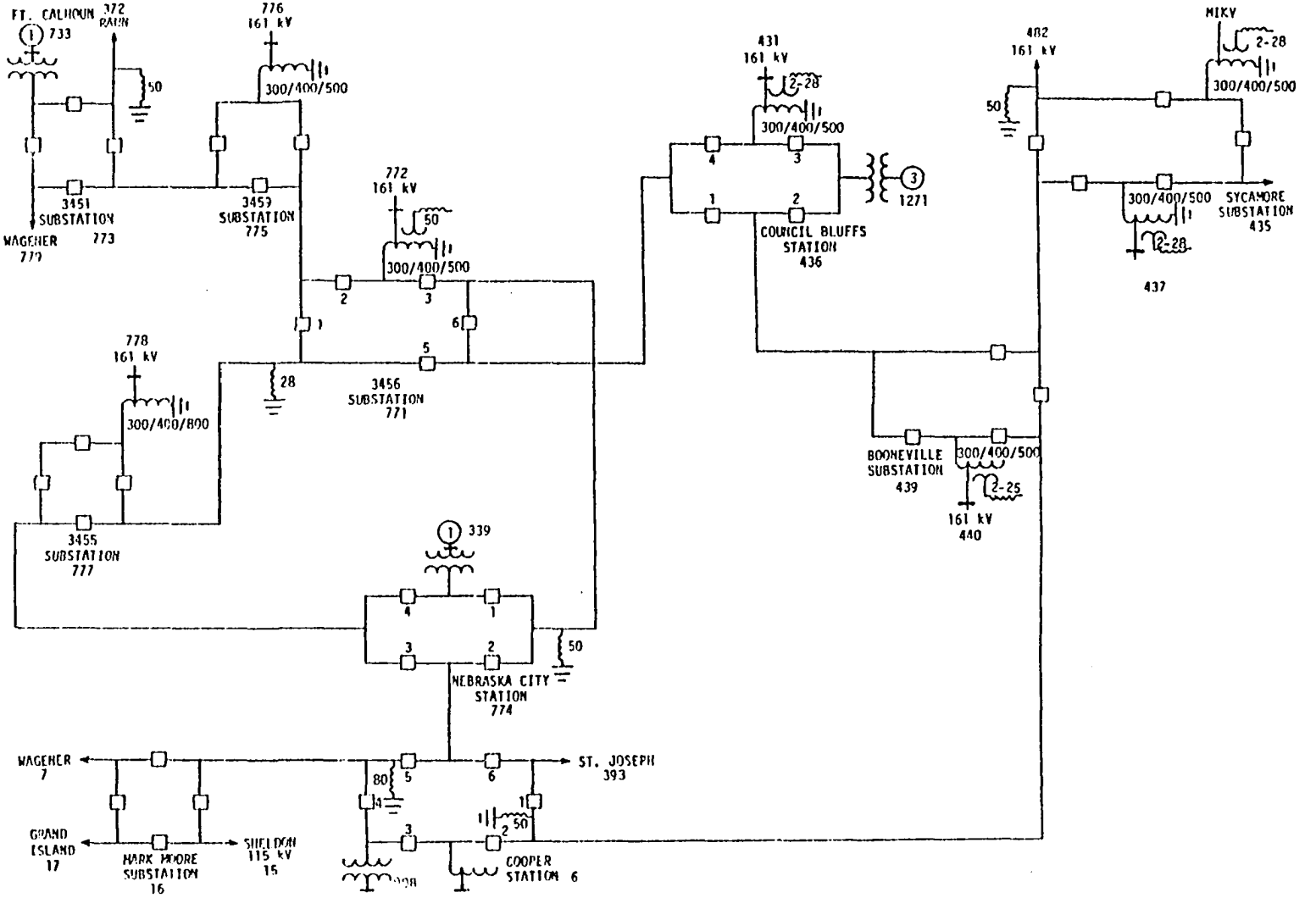

Figure 6-2. Substation breaker diagram

single-phase faults. The different post-fault networks are given below:

Three-phase Faults For the Raun fault, with prior outage of the 372-332 (raun-Hinton) line, the following post-fault networks are possible:

- Line 372-193 (Lakefield) cleared.
- Line 372-773 (Ft. Calhoun) cleared.
- Line 372-482 (Lehigh) cleared.
- One of the transformers 372-800 (Raun) opened.

For the Council Bluffs fault, the following post-fault networks are possible:

- Line 436-439 (Booneville) cleared.
- Line 431-771 (Substation 3456) cleared.

For the Ft. Calhoun fault, the following post-fault networks are possible:

- Line 773-372 (Raun) cleared.
- Line 773-779 (Wagner) cleared.
- Line 773-775 (Substation 3459) cleared.

For the Cooper fault, the following post-fault networks are possible:

- Line 6-774 (Nebraska City) cleared.
- Line 6-439 (Booneville) cleared.
- Line 6-16 (Moore) cleared.

- Line 6-393 (St. Joseph) cleared.

Single-line-to-ground Faults For the Raun fault, the following switching sequences are possible:

- Fault on line 372-193
  - --Line 372-193 cleared.
  - --Lines 372-193 and 372-482 cleared.
- Fault on line 372-773
  - --Line 372-773 cleared.
- Fault on line 372-482
  - --Line 372-482 cleared.
  - --Line 372-482 and 372-193 cleared.
- Fault on transformer 372-800
  - --One line 372-800 cleared.

For the Council Bluffs fault, the following switching sequences are possible:

- Fault on line 436-439
  - --Line 436-439 cleared.
  - --Line 436-439 and 436-771 cleared.
- Fault on line 436-771
  - --Line 436-771 cleared.
  - --Line 436-771 and 436-439 cleared.

For the Ft. Calhoun fault, the following switching sequences are possible:

- Fault on line 773-372

--Line 773-372 cleared.

--Line 773-372 and 773-775 cleared.

- Fault on line 773-779

--Line 773-779 cleared.

--Lines 773-779 and 773-775 cleared.

- Fault on line 773-775

--Line 773-775 cleared.

--Lines 773-775 and 773-372 cleared.

--Lines 773-775 and 773-779 cleared.

For the Cooper fault, the following switching sequences are possible:

- Fault on line 6-774

--Line 6-774 cleared.

--Lines 6-774 and 6-393 cleared.

--Lines 6-774 amd 6-16 cleared.

- Fault on line 6-439

--Line 6-439 cleared.

--Lines 6-439 and 6-393 cleared.

- Fault on line 6-16

--Line 6-16 cleared.

--Lines 6-16 and 6-774 cleared.

Limitations of the Study

A full transient security assessment study would not be limited to faults at only four locations. A full study would

represent a large number of possible fault locations, fault types, and network configurations. Prior outages, other than the Raun-Hinton outage assumed in this study, would further multiply this number. Since our objective is to demonstrate the value of ΔV_c for use in on-line security assessment, the 37 cases in this study represent only a limited number of the possible configurations. The strategy that would ultimately be used to apply the energy margin in a security assessment scheme would undoubtedly include a "smart" contingency selection procedure designed to limit the number of cases considered.

A Sample Calculation

In order to clarify the security assessment procedure used in this chapter, a sample of calculations is given for a three-phase and single-line-to-ground fault. The fault location is at Raun (near generator No. 6), cleared by opening line 372-193. As stated previously, the three-phase fault is cleared at Ø.15 s, while the single-line-to-ground fault assumes the far end of the transmission line 372-193 is cleared at Ø.Ø8 s, with the backup protection clearing the fault at Ø.24 s. In this case, the backup protection does not clear any secondary lines.

Table 6-1 shows the speeds and angles at clearing for the two faults, as well as the relevant UEP θ^u. In this case,

only one UEP is obtained, since the post-fault network is identical for the three-phase and single-phase faults. Had a second line been cleared by the backup protection, a second UEP would have been computed, reflecting the change in the post-fault network configuration.

The data used in calculating the transient energy margin, and its corresponding kinetic energy correction, are shown in Table 6-2. The table displays data for the kinetic energy correction computed using the energy of the equivalent two-machine system. Inspecting the data, we note the following:

- The kinetic energy correction represents an 18% adjustment to the energy margin in the three-phase fault, and a 4% adjustment in the margin for the single-phase fault. This kinetic energy correction is positive (as it must always be), and serves to increase the margin ΔV_c. (Other than the kinetic energy correction, no additional corrections were made to ΔV.)

- The value of ΔV for the single-line-to-ground fault is greater than that of the three-phase fault. This is to be expected; when backup protection does not clear additional lines, the single-phase fault is a less severe disturbance than the three-phase fault.

- The margin energy of the single-phase fault is nearly twice that of the three-phase fault; additionally, the kinetic energy of the three-phase fault is more than triple the kinetic energy of the single-phase fault. Consequently, the normalized margin ΔV_n indicates the single-phase fault to be six times more robust than the three-phase fault.

- Another way to state this comparison is using the percent margin

Table 6-1. Conditions at clearing and the corresponding UEP, fault at bus 372, line 372-193 cleared

No.	θ^{s1} (degrees) Arbitrary Reference	θ^{s1} (degrees) COI Reference	θ^{s2} (degrees) COI Reference	θ^{u} (degrees) (for this transient) COI Reference
1	-27.92	-6.26	-4.92	-1.41
2	-1.37	20.28	22.26	46.63
3	-16.28	5.38	5.60	9.68
4	-26.09	-4.42	-8.34	-23.95
5	-6.24	15.41	18.87	163.55
6	-4.56	17.10	21.57	144.87
7	-23.02	-1.35	-1.53	-15.96
8	-26.95	-5.29	-4.76	-7.98
9	-12.41	9.25	8.91	-6.62
10	-11.12	10.53	12.85	47.77
11	-24.30	-2.64	-1.17	10.28
12	-10.10	11.55	13.90	49.58
13	-28.10	-6.44	-6.61	-25.80
14	-26.76	-5.10	-5.08	-23.62
15	-21.09	0.56	-2.12	-17.61
16	-6.70	14.95	17.78	63.55
17	-4.35	17.30	19.43	50.06

Table 6-2. Calculation of the Transient Energy Margin, fault at bus 372 (Raun), line 372-193 cleared

	ω_{cr}	M_{cr}	ω_{sys}	M_{sys}	KE	ΔKE_{corr}	ΔV	ΔV_c	ΔV_n	$\%\Delta V$
3-phase fault	7.0650	0.2614	-.3597	4.8744	6.84	1.1311	6.377	7.508	1.10	52%
1-phase fault	3.6383	0.2614	-.1952	4.8744	1.82	0.462	12.075	12.537	6.88	87%

$\%\Delta V = 87\%$ vs $\%\Delta V = 52\%$
which indicates that 87% of the energy absorbing capacity at clearing remained unused for the single-line-to-ground fault, while only 52% remains for the three-phase fault.

Assessment Using the Transient Energy Margin

Thirty-seven fault cases were run on the Reduced Iowa System, as discussed earlier in this chapter. Thirteen cases proved to be uninteresting, because--as with the sample calculation above--the single-line-to-ground faults, with no additional line cleared, showed transient energy margins ΔV_c consistently higher than the corresponding three-phase fault or the single-phase fault with secondary lines cleared. Therefore, we will not examine these disturbances any further. The results of the calculations for the remaining 13 three-phase faults and 11 single-phase-to-ground faults are tabulated in Table 6-3. The energy margin, together with the two normalized energy margins (ΔV_n and $\%\Delta V$), are indicated for each case. The three-phase disturbances had energy margins ΔV_c ranging between 4.756 pu and 27.685 pu. The one-phase-to-ground fault ranged between 0.963 pu and 27.694 pu. The normalized margin ΔV_n ranged from a low of 0.691 pu to a high of 21.272 for the three-phase case, and between a low of 0.962 and a high of 146.374 for the one-phase fault cases. The $\%\Delta V$ margin ranged from 41% to 96% in the three-phase case, and from 49% to 99% in the single-line fault cases.

Table 6-3. Normalized Transient Energy Margin, 17-machine system

Fault Location (Bus and Line Faulted)	ΔV_c (pu)	Corrected KE (pu)	ΔV_n (pu)	%ΔV (%)
	Three-phase Fault			
Raun Fault				
372-193	7.432	6.878	1.080	52
372-773	4.756	6.878	0.691	41
372-482	9.159[a]	6.878	1.332	57
Transformer 372-800	12.147	6.878	1.766	64
Council Bluffs Fault				
436-439	12.831	3.831	3.283	77
436-771	6.208	3.831	1.620	62
Ft. Calhoun Fault				
773-372	22.513	1.302	17.291	95
773-779	27.512	1.302	21.131	95
773-775	27.685	1.302	21.272	96
Cooper Fault				
6-774	5.200	3.158	1.647	62
6-439	6.502	3.158	2.059	67
6-16	6.278	3.158	1.988	67
6-393	6.596	3.158	2.089	68

[a] See discussion of table 5-4.

SLG Fault

Additional Line Out	ΔV_c (pu)	Corrected KE (pu)	ΔV_n (pu)	%ΔV (%)
372-482	7.879	1.824	4.319	81
-	-	-	-	-
372-193	7.523	1.791	4.200	81
-	-	-	-	-
436-771	4.350	0.998	4.354	81
436-439	3.408	1.658	2.057	67
773-775	21.980	0.643	34.205	97
773-775	27.097	0.498	54.379	98
773-372	22.660	0.189	119.767	99
773-779	27.694	0.189	146.374	99
6-16	5.561	1.002	5.530	85
6-393	0.963	1.002	0.962	49
6-393	3.217	0.969	3.321	77
6-774	5.457	0.975	5.596	85

Ranking of the Disturbances

Table 6-4 shows the ranking of the three-phase faults, tabulated in decreasing order; the most severe disturbances, with the lowest margin, are shown first. The transient energy margin ΔV_c and the normalized values (ΔV_n and $\%\Delta V$) are shown for all 13 three-phase Faults. Critical clearing times for some of these faults were obtained to test the validity of the ranking. This information is also given in Table 6-4. In Table 6-4, we observe the following:

- The data show the critical clearing time for each disturbance. It is clear that the relative ranking offered by this technique provided very good results; the critical clearing time increases consistently with the increased ranking. This is particularly significant when it is realized that some of the critical clearing times differ in terms of thousandths of a second.

- There is a discrepancy at the Raun transformer (372-800, ranked fourth in Table 6-4): the data in Table 6-4 does not match that shown in Table 6-3. The reason for this discrepancy is that Table 6-3 assumes a critical group (and the UEP) that includes machines 5 and 6. Direct simulation, used to validate the UEP and determine the critical clearing time, showed the critical machine to actually be generator No. 6 alone. Using the new θ_u, corresponding to machine No. 6 alone, the following values are obtained:

$$\Delta V = 9.87 \text{ pu}$$

$$\Delta V_n = 1.53$$

$$\%\Delta V = 60\ \%$$

These values are used to formulate the ranking and are shown in Table 6-4.

Table 6-4. Ranking of the three-phase faults shown in Table 6-3

Rank	ΔV_n	%ΔV	ΔV	Fault Location	clearing times	
					Stable	Unstable
1	0.691	41	4.756	Raun, line 372-773	0.117	0.180
2	1.080	52	7.432	Raun, line 372-193	0.1923	0.1924
3	1.332	57	9.159	Raun, line 372,482	0.192	0.196
4	1.530	60	9.870	Raun, transformer 372-800	0.196	0.200
5	1.620	62	6.208	Council Bluffs, line 436-771	0.200	0.204
6	1.647	62	5.200	Cooper, line 6-774	0.204	0.212
7	1.988	67	6.278	Cooper, line 6-16	0.212	0.216
8	2.059	67	6.502	Cooper, line 6-439	0.216	0.220
9	2.089	68	6.596	Cooper, line 6-393	---	---
10	3.293	77	12.579	Council Bluffs, line 436-439	---	---
11	17.298	95	22.513	Ft. Calhoun, line 773-372	---	---
12	21.139	95	27.512	Ft. Calhoun, line 773-779	0.345	0.356
13	21.272	96	27.685	Ft. Calhoun, line 773-775	---	---

- Ranking According to the transient energy margin predicted that the fault at Raun (clearing line 372-482) with a transient margin of 9.159 pu is more severe than other faults with considerably smaller values of ΔV_c. For example, the Council Bluffs fault (clearing line 436-771) has an energy margin of 6.208 pu, but is predicted by the normalizing process to be more severe. The information about critical clearing times indicates that this, indeed, is correct.

- The normalized margin appears to be capable of separating closely clustered cases into a proper ranking, even when the disturbances are similar in nature (e.g., on the same bus) and differ only according to which lines are cleared. For example, the cases ranked as 7 and 8 in Table 6-4 have normalized margins that differ by only a small amount; nonetheless, the ranking seems correct, as validated by the critical clearing times.

- The ability of the normalized margin to separate closely clustered cases seems to hold, even when the cases are not at the same location, and when the energy margins differ substantially (i.e., as in the cases ranked 4 and 5).

- An important question is whether the critical clearing times provide a true means of comparing unrelated faults that differ in location and type. It remains unclear what is involved in the comparison of the severity of a fault at one location with one at another location. Clearly, however, the top of the list represents the weak links in the system; the most severe response is at Raun (with a margin of 41%), where over half of the energy absorbing capacity which remained after clearing was consumed by the fault kinetic energy.

- Table 6-4 not only gives the operator knowledge that trouble is possible, but, by identifying the source of the problem, implies solutions for the operator's consideration. For example, it is clear from the above assessment that the three-phase disturbance at Raun and the stuck breaker fault at Cooper are the two conditions that come closest to threatening the system. Off-loading these generators will increase the margins.

The 11 single-line-to-ground faults, cleared with backup

protection after a breaker failure, are now ranked according to the same criterion. This information is displayed in Table 6-5. No information is given in Table 6-5 about the time solution. The computer program packages described in Chapter 5 do not have the capability of simulating single-phase faults. For this reason, the exhaustive studies needed to confirm the critical group encountered in each single-line-to-ground fault were not feasible. Consequently, the ranking given in Table 6-5 is based on the assumption that the modes of instability and the identification of the critical group are the same as those encountered for the three-phase faults.

The Alert State

An important issue still must be resolved: how do we assess the stability of the system with this information? One very elementary approach is: merely choose a limit to the normalized margin, and alert the operator if this limit is violated.

A key question in this process is: what is the value of the normalized transient energy margin which constitutes an alertable situation? There is no clear answer to this question. One possibility, that is purely arbitrary, is to use a scheme that alerts the operator if the normalized margin ΔV_n becomes less than 1.0 (this corresponds to a percent

Table 6-5. Ranking of single-phase faults, 17-generator system

Rank	ΔV_n	ΔV_c	Disturbance	
			Faulted Bus	Lines Removed
1	0.962	0.963	Cooper	6-774, 6-393
2	2.057	3.408	Council Bluffs	436-771, 436-439
3	3.321	3.217	Cooper	6-439, 6-393
4	4.200	7.523	Raun	372-482, 372-193
5	4.319	7.879	Raun	372-193, 372-482
6	4.354	4.350	Council Bluffs	436-439, 436-771
7	5.550	5.561	Cooper	6-774, 6-16
8	34.205	21.980	Ft. Calhoun	773-372, 773-775
9	54.379	27.097	Ft. Calhoun	773-779, 773-775
10	119.767	22.660	Ft. Calhoun	773-775, 773-372
11	146.374	27.694	Ft. Calhoun	773-775, 773-779

transient margin $\%\Delta V$ of 50%). Fouad et al. (48) suggested the following criteria:

Situation	ΔV_n	Suggested Action
Warning	1.0-2.0	None
Alert	0.5-1.0	Diagnostic
Severe Alert	0.0-0.5	Diagnostic Suggest remedial action
Potential Emergency	<0	Same

It is emphasized by Fouad, however, that this classification is arbitrary and judgemental. The ultimate choice of the alert criteria should be made at the local level and be based on the system operating policy.

CHAPTER 7. SECURITY ASSESSMENT USING A MODIFIED TRANSIENT ENERGY MARGIN

The key to accurately assessing transient stability by the procedure presented in Chapter 6 is the correct determination of a) the critical potential energy value, V_{cr}, and of b) the kinetic energy component which does not contribute to instability. The value of V_{cr} has been carefully studied, and Chapter 4 has shown that, for all practical purposes, the UEP energy, V_u, may be taken as the critical potential energy, V_{cr}. Chapter 5 utilized a kinetic energy correction based on system trajectories at the instant of clearing. Chapter 6 used this technique to produce a highly accurate ranking of various disturbances. Nevertheless, an in-depth look at the nature of the kinetic energy not contributing to instability is still necessary, and that is the purpose of this chapter.

The additional work covered by this chapter showed the kinetic energy not contributing to instability to be a very sensitive parameter; its value changes drastically with small changes in the system. This may be a major obstacle in that it brings into question the reliability of the previous assessment procedure for practical on-line decision-making. Consequently, an alternate technique is proposed in this chapter. In this new technique, the value of the kinetic

energy is not sensitive, and is, therefore, reliable for on-line decision-making. Thus, Chapter 7 addresses the question of reliable application of the energy margin and points the direction for additional research on this subject.

Kinetic Energy not Contributing to Instability

The kinetic energy not contributing to instability is merely the kinetic energy possessed by the system at the point of escape on the critical trajectory. It is the kinetic energy at the so-called stationary instant: when the center-of-inertia of the unstable group is at zero velocity with respect to the center-of-inertia of the stable group, and when the synchronizing force between these two groups has dropped to zero.

The motion of the machines at this instant is motion around the two stationary inertial centers and does not contribute to the separation of the two groups. Thus, the kinetic energy of this motion, in effect, absorbs (or consumes) a portion of the transient energy injected into the system by the fault. This portion of the transient energy is a contribution to stability. Therefore, to accurately assess stability we must compute the capacity of the system to absorb fault energy as both potential energy and kinetic energy and remain stable.

The Role of Kinetic Energy in Absorbing Fault Energy

In order to understand the role of both potential and kinetic energy in absorbing fault energy, it is helpful to inspect the process by which the fault energy drives the system unstable. At question is:

1. Where does the fault kinetic energy go (as potential and kinetic energy) in driving the system unstable?
2. What exactly is the smallest amount of kinetic energy that can drive the system unstable?
3. What exactly is the portion of this kinetic energy that is not contributing to instability?

In answering these questions, it is first necessary to establish exactly how fault energy drives the system unstable. To do this it is necessary to firmly establish the critical potential-energy-capacity of a system and the manner in which this capacity is exceeded by the fault-injected energy.

Only the case of a simple 1-machine instability is considered. Consideration of more complex cases, with ill-defined modes of separation, is proposed as a topic for further study.

Potential Energy Computed via Numerical Integration

The critical energy (V_{cr}) is identified by direct numerical integration of the values of potential energy stored by individual machines, using digital computer simulation of

critical trajectories. This critical potential energy is then compared to the fault-injected energy to determine the exact amount required to drive the system unstable.

Numerical integration of the values of potential energy is relatively easy to accomplish. Figure No. 7-1 illustrates the potential energy of interest, using a one-machine, infinite-bus system. The power-angle curve of this system is re-drawn, with time as its abscissa rather than angle. The horizontal line, P_i, is the mechanical power reduced by the constant dissipation. The curved line, P_e, is the electrical power transmitted through the transmission lines. The difference between P_e and P_i at each instant is called mismatch power. The area under P_e and above P_i (Area A) defines the potential-energy-absorbing capacity of the generator. This is the limit to the generator's ability to absorb potential energy by virtue of its angular position. This area can be found by numerical integration during the computer simulation of the faulted system trajectory between the two equilibrium points t_1 and t_2:

$$P.E. = \int_{t_1}^{t_2} [P_i - P_e] \quad dt \tag{7-1}$$

For machine i of an n-machine system, P_i (the mechanical power reduced by constant dissipation) is:

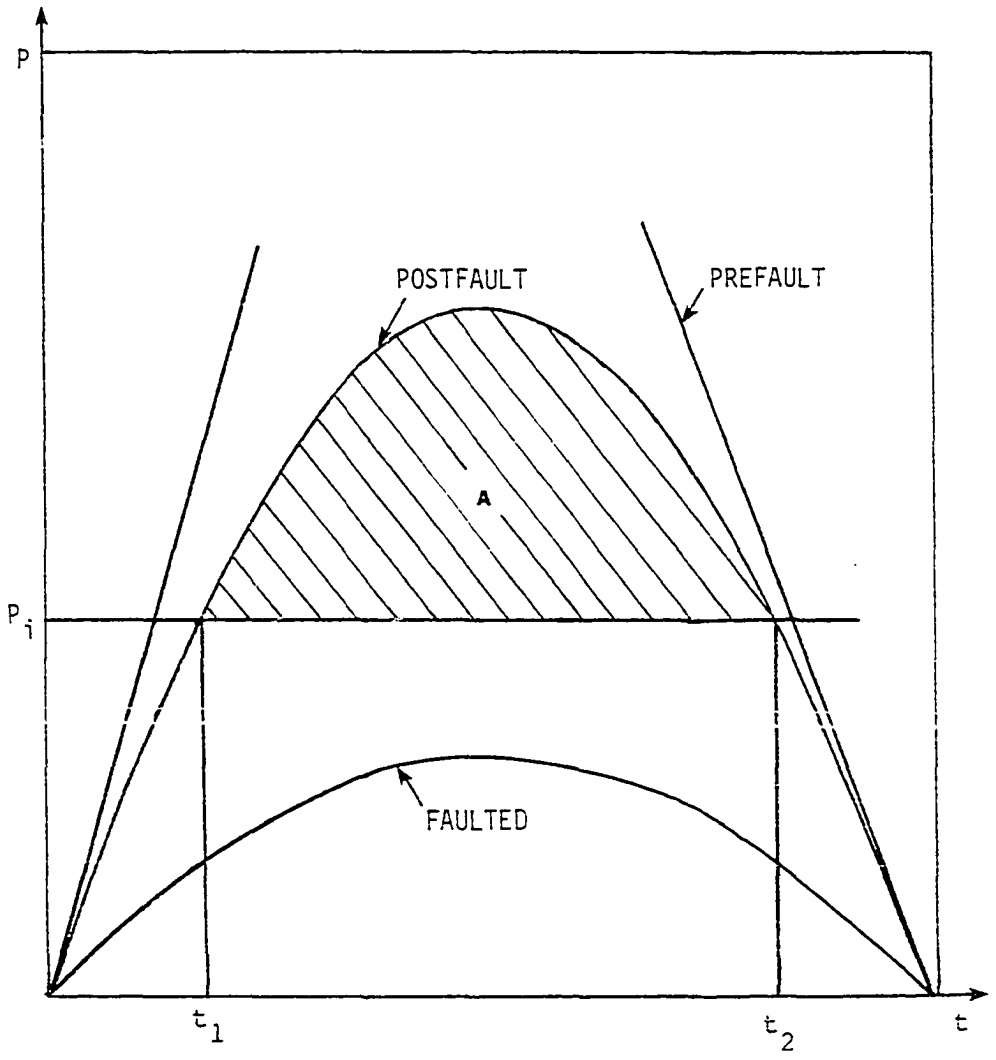

Figure 7-1. Power-time curve (P_e) for one-machine-infinite-bus system (transfer conductances neglected). Area A between t_1 and t_2, defines the potential-energy-absorbing-capacity of the generator

$$P_i = P_{mi} - E_i^2 G_{ii} \tag{7-2}$$

The P_e (electrical power transmitted through the transmission system) is:

$$P_{ei} = \sum_{\substack{i=1 \\ i \neq j}}^{n} [E_i E_j B_{ij} \sin\theta_{ij} + E_i E_j \cos\theta_{ij}] \tag{7-3}$$

For machine i of an n-machine system, the integration of power (to give potential energy) between the two equilibrium points t_1 and t_2 (see figure 7-1) becomes:

$$P.E._i = \int_{t_1}^{t_2} [P_i - P_{ei} - (M_i/M_t) P_{coi}] \, dt \tag{7-4}$$

The numerical integration of this function uses the expression

$$P.E._i = \sum [P_i(t_k) - P_{ei}(t_k) - (M_i/M_t) P_{coi}(t_k)] \, \Delta t \tag{7-5}$$

where t_k is the time at each step in the computer simulation between the two zero mismatch points (t_1 and t_2) encountered on the fault trajectory. The numerical integration is easily accomplished within a transient stability program. Care must be taken, however, in computing mismatch: the mismatch power must be computed using the post-fault admittance values for the entire period between t_1 and t_2.

Analysis of Energy for the Ft. Calhoun Instability

This study investigated a three-phase fault applied to Bus No. 773 (near Ft. Calhoun) on the 17-generator reduced Iowa System. Two cases were run. In one case, the fault was cleared at .3528 seconds and the system remained stable. In the second case, the fault was cleared at .3564 seconds and machine No. 16 (Ft. Calhoun) became unstable. In both cases, the fault was cleared by removing the 345 kV line between Ft. Calhoun and sub 3454 (Bus No. 779). These two cases are, respectively, the critically stable and critically unstable cases, and thus bracket the actual critical trajectory.

Analysis of Potential Energy

The two Fort Calhoun cases were simulated, and the potential energy absorbed by the generator was computed, using the numerical integration technique described above. Figure 7-2 depicts these two cases: (a) and (b) show selected machine trajectories, and (c) and (d) show the corresponding power-time curves for generator No. 16. The results of the numerical integration for generator No. 16 are also indicated on this figure. Figure 7-2(e) shows selected power-time curves for the other 16 generators for the unstable case.

Establishing the Critical Instant The disturbance sends generator No. 16 toward instability. In the critical

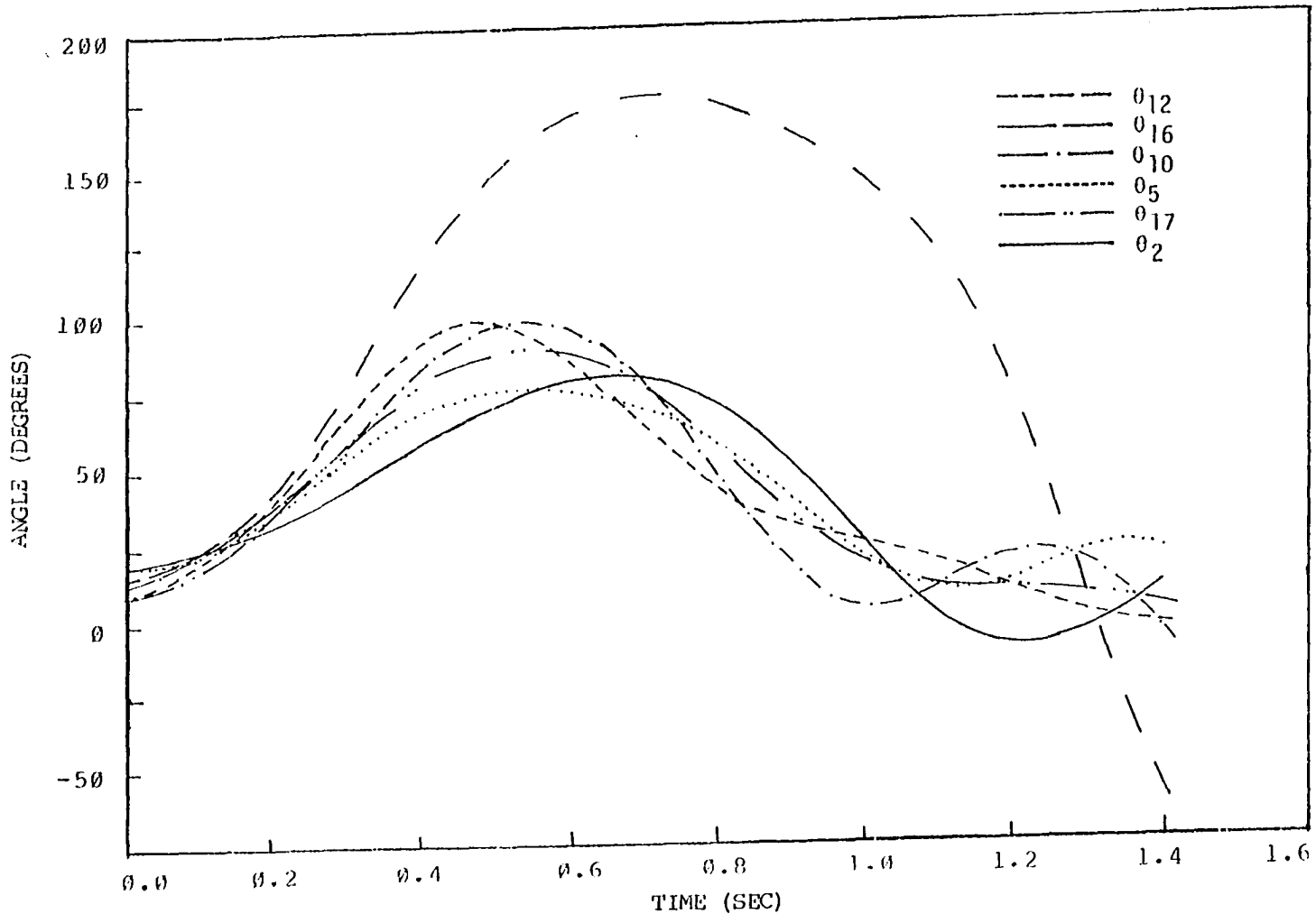

Figure 7-2(a). Selected trajectories for a Ft. Calhoun fault cleared at 0.3528s (stable)

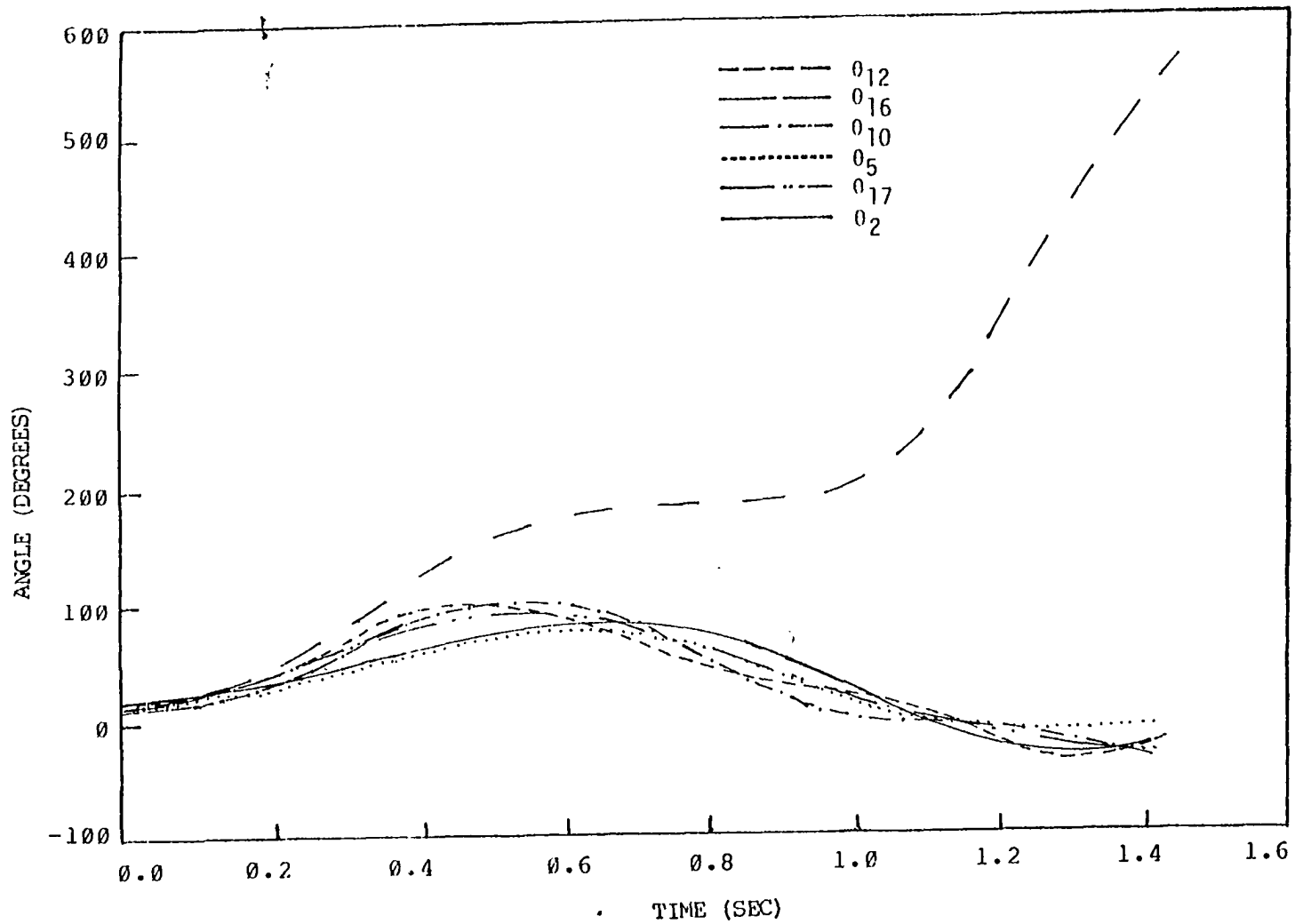

Figure 7-2(b). Selected trajectories for a Ft. Calhoun fault cleared at 0.3564s

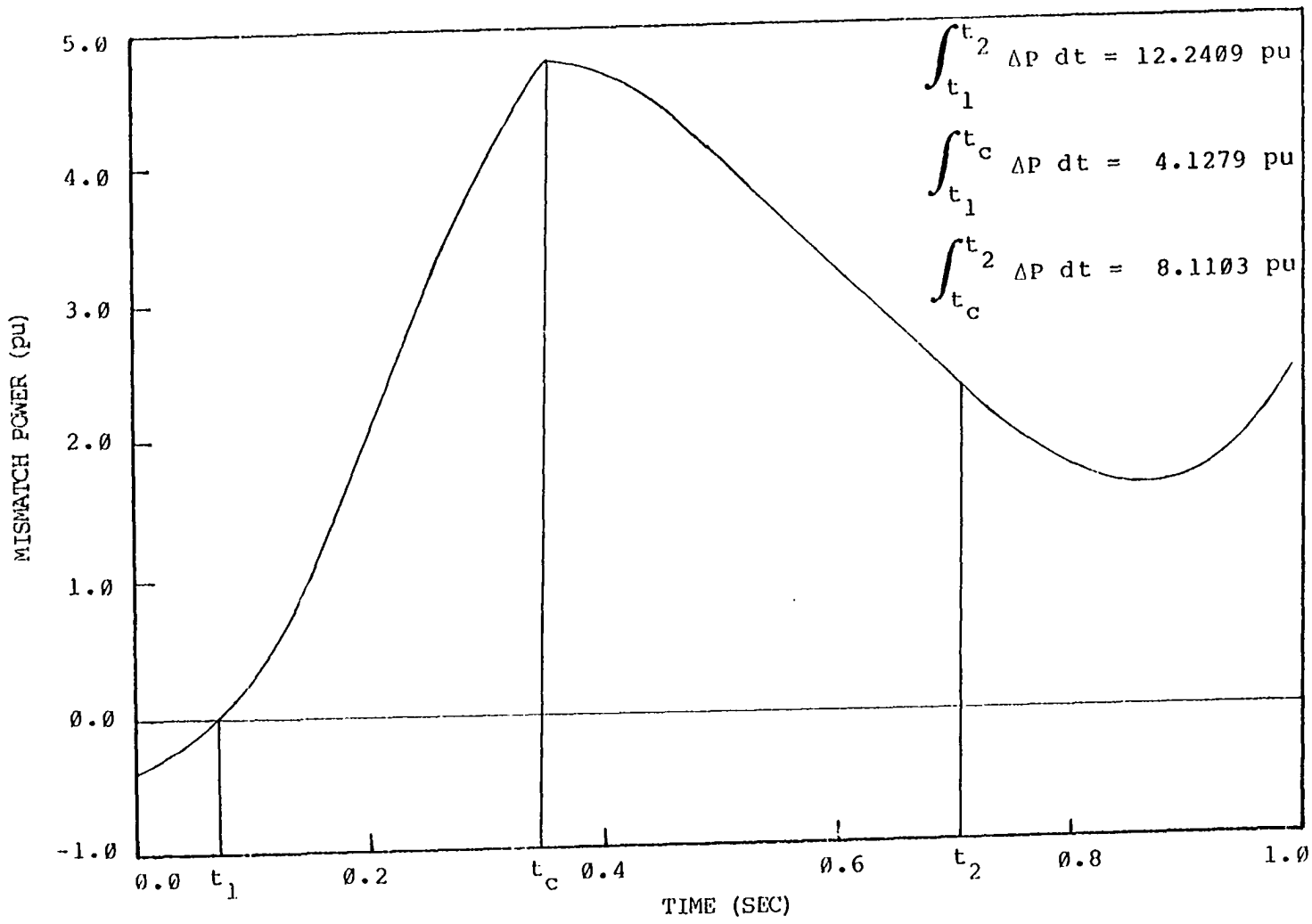

Figure 7-2(c). Mismatch power for the Ft. Calhoun generator, fault at Ft. Calhoun cleared at .3528s (stable)

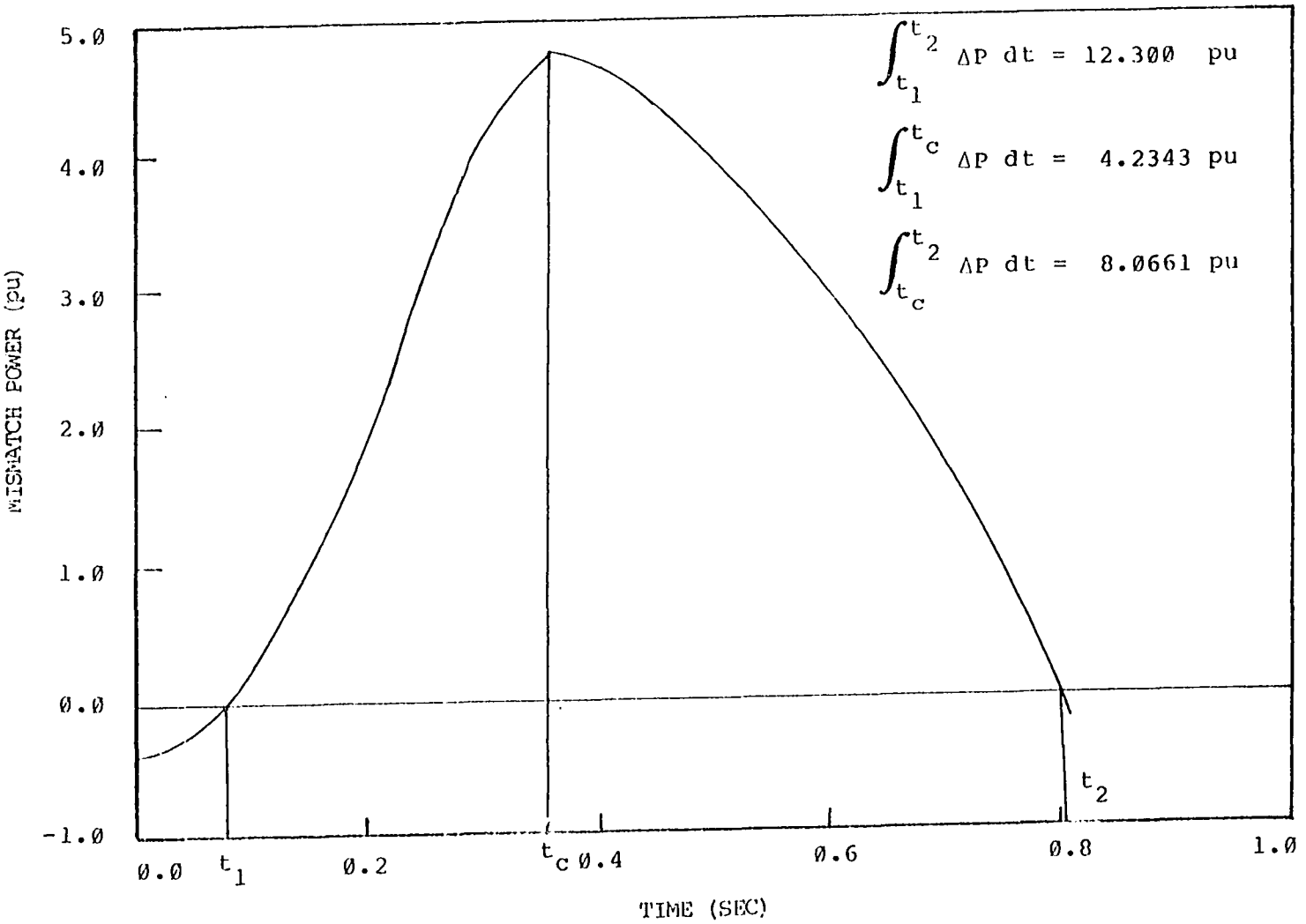

Figure 7-2(d). Mismatch power for the Ft. Calhoun generator, fault at Ft. Calhoun cleared at 0.3564s (unstable)

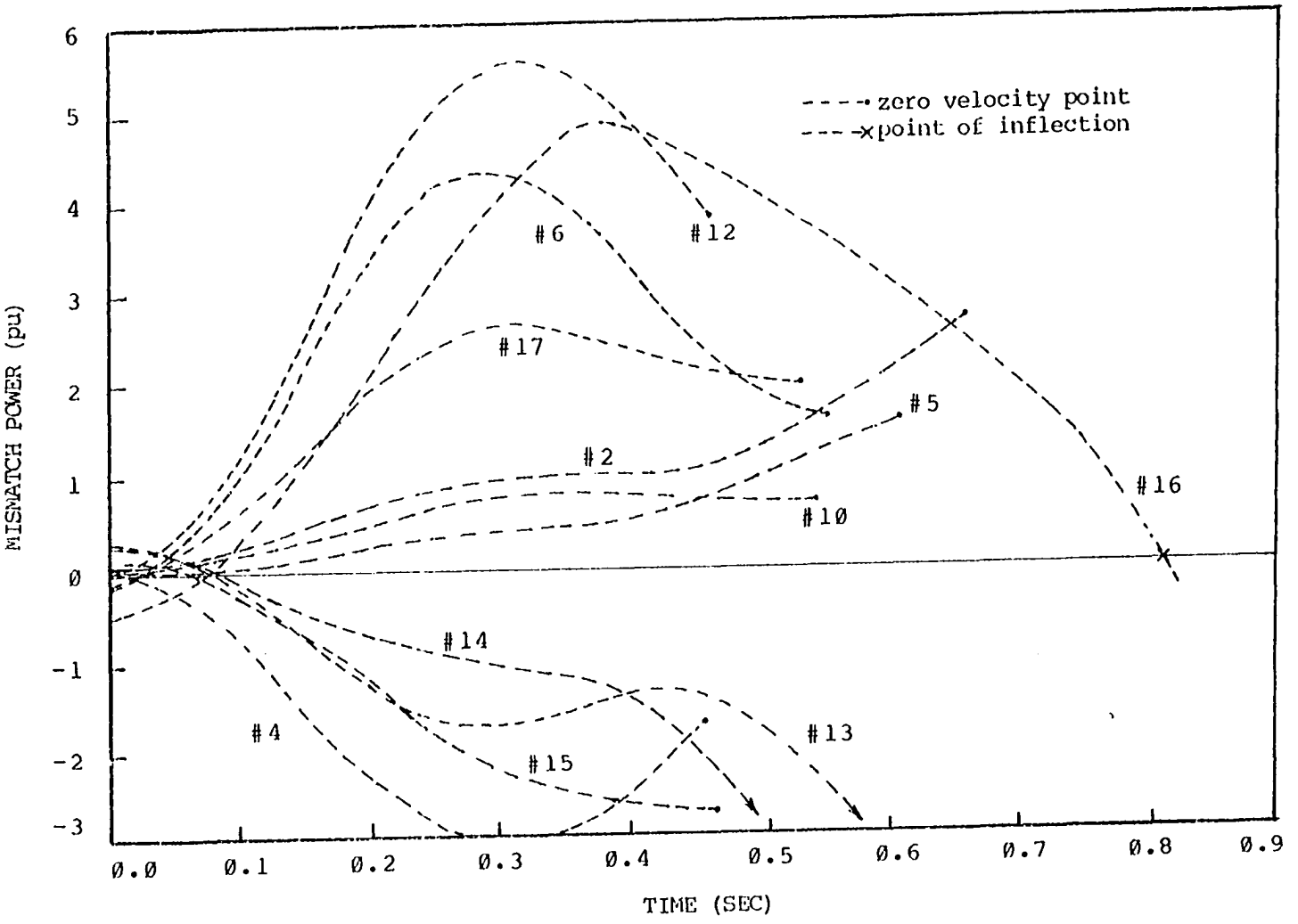

Figure 7-2(e). Mismatch power for selected generators, fault at Ft. Calhoun cleared at .3564s (unstable)

but stable trajectory, generator No. 16 reaches the peak of its swing, with respect to all other generators, at t = .704. This is the stationary instant when generator No. 16 is at zero velocity with respect to the inertial center of the 16 other generators. We indicate this condition as

$$\bar{\omega}_{16} = \emptyset$$

where the bar indicates velocity with respect to the inertial center of the 16 other machines. (This is in contrast to the nomenclature, ω_{16}, which indicates velocity with respect to the 17-generator inertial center.)

In the critical but unstable trajectory, there is no peak-of-the-swing for No. 16, but instead the critical instant is seen as a reversal in the acceleration of No. 16 with respect to the inertial center of the other 16 generators. The result is a point-of-inflection as the acceleration becomes momentarily zero. We indicate this condition as

$$\dot{\bar{\omega}}_{16} = \emptyset$$

In the critical but unstable case, this point-of-inflection occurs at t = .804s.

P.E. at the Critical Instant: Unstable Generator The numerical integration for generator No. 16 determines the area under the power-time curve. This depicts the potential energy stored by generator No. 16. Since the two cases represent the critically stable and the critically unstable cases, the

resulting potential energy brackets the exact critical energy of generator No. 16. For the stable case, the potential energy stored by No. 16 at the instant of zero velocity, ($\bar{\omega}_{16}$=Ø), is 12.2409 pu (see Figure 7-2(c)). For the unstable case, the potential energy stored at the instant of the point-of-inflection ($\dot{\bar{\omega}}_{16}$=Ø) is 12.300 pu (see Figure 7-2(d)). We conclude that machine No. 16 has a maximum potential energy capacity (critical energy) of

$$12.2409 < V_{cr(16)} < 12.300 \quad \text{pu}$$

The exact value of V_{cr} lies within this range and is the potential energy stored at the point on the critical trajectory satisfying the condition:

$$\bar{\omega}_{16} = \dot{\text{Ø}}$$
$$\dot{\bar{\omega}}_{16} = \text{Ø}$$

This condition specifies the stationary point on the critical trajectory, and is the crucial point-of-no-return for the disturbance.

P.E. at the Critical Instant: Other Generators For the fault cleared at .3564s, the total potential energy stored by all 16 stable generators at the critical instant is

$$\text{P.E.} = 11.634 \text{ pu}$$

The potential energy stored by all 17 generators is the sum of

the potential energy of generator No. 16 (P.E. = 12.300 pu) and the 16 other generators (P.E. = 11.634 pu), or

P.E. = 23.934 pu

For the critical trajectory, not one other generator reached the point where $\dot{\omega}=0$ (i.e., the second zero mismatch point corresponding to t_2 in Figure 7-1). Thus, though the numerical integration can compute the potential energy absorbed, it cannot compute the maximum capacity of those machines. Clearly the 16 stable generators do absorb a significant amount of transient energy. However, the stable generators do not exceed their critical energy values. We are focusing only on the potential energy stored in generator No. 16 because it exceeded its potential energy capacity. No other generator reached its capacity; no other generator went unstable.

P.E. at Clearing The critically stable case is cleared at t = 0.3528 s. As seen in Figure No. 7-2(c), generator No. 16 has absorbed 4.1279 pu of its capacity at this instant, leaving 8.1130 units of potential energy capacity remaining. (The 16 other generators have absorbed 12.010 units of potential energy at clearing, giving a total potential energy absorbed by all 17 generators at clearing of P.E. = 16.138 pu.)

The critically unstable case was cleared at t = 0.3564 s.

Figure 7-2(d) indicates that generator No. 16 absorbed 4.2343 pu of potential energy, leaving 8.0661 pu of potential energy capacity remaining. (The 16 other generators have absorbed 12.280 units of potential energy giving a 17-generator total of P.E. = 16.514 pu.) We conclude that, for generator No. 16, the potential energy capacity remaining at clearing is

$$8.0661 < \text{P.E.} < 8.1130 \text{ pu}$$

as indicated in Figure 7-2(c) and (d).

Analysis of Kinetic Energy

Finding a value for the critical potential energy is only half of the energy accounting problem. The other half is evaluating the kinetic energy.

For the stable case the total system kinetic energy at clearing is given (by simulation) as

$$KE = 11.824 \text{ pu}$$

while the kinetic energy at clearing for the unstable case is given as

$$KE = 11.958 \text{ pu}$$

We conclude that the critical total system kinetic energy is

$$11.824 < KE < 11.958 \text{ pu}$$

We are interested in determining generator No. 16s share of this fault-injected kinetic energy at the critical instant on the critical trajectory. The critical instant is the point on the critical trajectory that exactly satisfies the

condition

$$\bar{\omega}_{16} = \emptyset$$
$$\dot{\bar{\omega}}_{16} = \emptyset \qquad (7\text{-}6)$$

The kinetic energy at this instant is the kinetic energy not contributing to instability. The value of kinetic energy at this instant is not known because the critical trajectory is not known. However, the critical trajectory is closely bracketed by the stable and unstable cases. The situation at the critical instant is estimated by interpolation between these stable cases. (Table 7-1 summarizes the data for the two cases.)

The Stable Case The critically cleared but stable case has a kinetic energy of 3.16 pu (as determined by simulation) when $\bar{\omega}_{16}=\emptyset$, $\dot{\bar{\omega}}_{16}=\emptyset$. The 3.16 units of energy is from motion of generators around the stationary center of inertia of the stable group and does not contribute to the unstable motion of No. 16. This 3.16 units of kinetic energy, therefore, is the portion of the 11.824 units of fault-injected kinetic energy that does not contribute to the separation of No. 16. The 3.16 pu is not absorbed as potential energy. Instead, we find that, at the stationary instant, the system has absorbed

$$11.824 - 3.16 = 8.66 \text{ pu}$$

of the kinetic energy that was injected at clearing. (This number is entered in Table 7-1.) We note (with considerable interest) that Figure 7-2(c) shows the energy absorbed by generator No. 16 only to be 8.113 pu (found by numerical integration). Thus, it appears that at this

Table 7-1. Interpolation between the stable case (cleared at Ø.3528s) and the unstable case (cleared at Ø.3564s) to estimate the critical P.E. of generator No. 16

	critically stable	critically unstable	interpolated estimate
total KE at clearing	11.824	11.958	11.884
KE when $\bar{\omega}_{16}=0$ or $\dot{\bar{\omega}}_{16}=0$	3.16	4.57	3.80
portion of KE contributing to instability	8.66	7.39	8.09
PE of #16 remaining at clearing	8.113	8.06	8.09
PE of all other generators	Ø.55	-Ø.67	0.0
condition realized	$\bar{\omega}_{16} = 0$ $\dot{\bar{\omega}}_{16} < 0$	$\bar{\omega}_{16} > 0$ $\dot{\bar{\omega}}_{16} = 0$	$\bar{\omega}_{16} = 0$ $\dot{\bar{\omega}}_{16} = 0$

instant, virtually all of the fault-injected kinetic energy is absorbed by generator No. 16: only Ø.55 pu is absorbed by all other generators combined.

The Unstable Case The critically cleared but unstable case is analyzed in a similar fashion. The total kinetic energy at clearing is 11.958 pu. When $\bar{\omega}_{16}=Ø$ the kinetic energy is 4.57 pu. We compute that the system has absorbed

$$11.958 - 4.57 = 7.39 \quad \text{pu}$$

units of kinetic energy. Numerical integration indicates that generator No. 16 absorbed 8.Ø6 units (see Figure 7-2(d)), meaning that all of the other generators must store -Ø.67 units of energy (i.e., they contribute Ø.67 units of energy). Again, No. 16 holds almost all of the kinetic energy that had been injected at clearing. The energy of all other machines, as a group, is virtually the same as at clearing (differing by only Ø.67 units of energy).

Interpolating Between the Stable and Unstable Cases

Since the stable and unstable cases bracket the critical instant, we conclude that the kinetic energy absorbed by generator No. 16 at the critical instant is

$$8.113 < \text{K.E.} < 8.Ø6 \quad \text{pu}$$

and the kinetic energy absorbed by all other machines is

$$-Ø.67 < \text{KE} < Ø.55 \quad \text{pu} \tag{7-6}$$

Table 7-1 summarizes the above calculations and, additionally, shows the results of interpolating.

To fix the critical instant, we must interpolate between the two cases: one where $\bar{\omega}_{16}=Ø$ is realized and the other

where $\dot{\bar{\omega}}_{16}=\emptyset$ is realized. Since the bracket of kinetic energy in equation 7-6 is so close to zero, it is tempting to assume the interpolated value ($\bar{\omega}_{16}=\emptyset$, $\dot{\bar{\omega}}_{16}=\emptyset$) is exactly zero. This assumption means that zero energy is absorbed by the stable machines and that all of the kinetic energy absorbed as potential energy is absorbed by machine No. 16. Though the exactness of this assumption may be subject to doubt, the maximum amount of error possible would be only -Ø.67 units. This assumption is reflected in Table 7-1, which fixes the kinetic energy not contributing to No. 16s motion at 3.8Ø pu, and the critical energy absorbing capacity at 8.Ø9 pu. This assumption confirms that the kinetic energy not contributing to the instability of No. 16 is the kinetic energy that exists at the critical instant on the critical trajectory.

Summary and Conclusions Numerical integration of the critically stable and critically unstable Ft. Calhoun trajectories has yielded some interesting information. First a critical or stationary instant was identified for the stable and unstable trajectories. These instants were then investigated and the corresponding potential energies noted for each generator. By interpolating between these energy values, it was possible to identify the potential energy of each generator at the critical escape point on the critical

trajectory. This energy was then compared to the critical kinetic energy injected by the disturbance. We conclude that:

1. Generator No. 16 becomes unstable when the fault injects more energy into No. 16 than No. 16 can hold. For the Ft. Calhoun fault, the energy required for Ft. Calhoun to become unstable is

$$V_{cr} = 11.884 \text{ pu}$$

2. Not all of the kinetic energy at clearing is absorbed as potential energy at the critical instant; the kinetic energy at the critical instant of the critical trajectory (the instant satisfying the conditions $\bar{\omega}_{16}=0, \dot{\bar{\omega}}_{16}=0$) is the kinetic energy not contributing to the instability of No. 16. For the Ft. Calhoun fault, this kinetic energy is

$$KE = 3.80 \text{ pu}$$

3. At the critical instant, virtually all of the kinetic energy that is absorbed as potential energy by the system after clearing is absorbed by No. 16 to produce instability; the total potential energy value of all other generators is virtually unchanged from the value at clearing.

Assessing Stability

An accurate assessment can now be made for the Ft. Calhoun fault. We know that, at the instant of fault clearing, the energy required to drive No. 16 unstable is:

$$P.E. = 8.09 \text{ pu (from Table 7-1)}$$

We also know that, at the critical instant of the critical trajectory, a total kinetic energy of

$$KE = 3.80 \text{ pu (from Table 7-1)}$$

will not contribute to instability. The kinetic energy at

clearing, less this kinetic energy not contributing to instability, must be compared to the escape energy in order to assess stability. For the two cases, an assessment of stability is shown in Table 7-2. The accuracy of the assessment reflects the accuracy of the potential energy value (found by numerical integration) and the accuracy of the kinetic energy value at the critical instant (found by simulation).

The Nature of the Kinetic Energy Not Contributing to Instability

For the simple case studied here, i.e., the case of one critical machine swinging with respect to the rest of the system, the kinetic energy not contributing to instability is the kinetic energy existing at the critical instant on the critical trajectory. It is important to take a closer look at this kinetic energy. Figure 7-3 shows a plot of the kinetic energy as a function of time for both the critically stable and critically unstable cases. The kinetic energy at the stationary point ($\bar{\omega}_{16}=0$) is indicated on the curves. The interpolated value of kinetic energy, estimated for the critical instant when $\bar{\omega}_{16}=0$, $\dot{\bar{\omega}}_{16}=0$, is also shown (KE = 3.80 pu) as point "A".

It is now possible to study the nature of the kinetic energy that is not contributing to instability. The kinetic

Table 7-2. Assessment of stability at Ft. Calhoun for fault cleared at .3528s (stable) and .3564s (unstable)

Stable Case:		
K.E. @ clearing	11.824	pu
K.E. @ $\tilde{\omega}=0$, $\dot{\tilde{\omega}}=0$	3.80	pu
Transient energy into #16	8.02	pu
Energy absorbing capacity of #16	8.09	pu
Conclusion: 8.02 < 8.09, therefore stable		
Unstable Case:		
K.E. @ clearing	11.958	pu
K.E. @ $\tilde{\omega}=0$, $\dot{\tilde{\omega}}=0$	3.80	pu
Transient energy into No. 16	8.16	pu
Energy absorbing capacity of #16	8.09	pu
Conclusion: 8.16 > 8.09, therefore unstable		

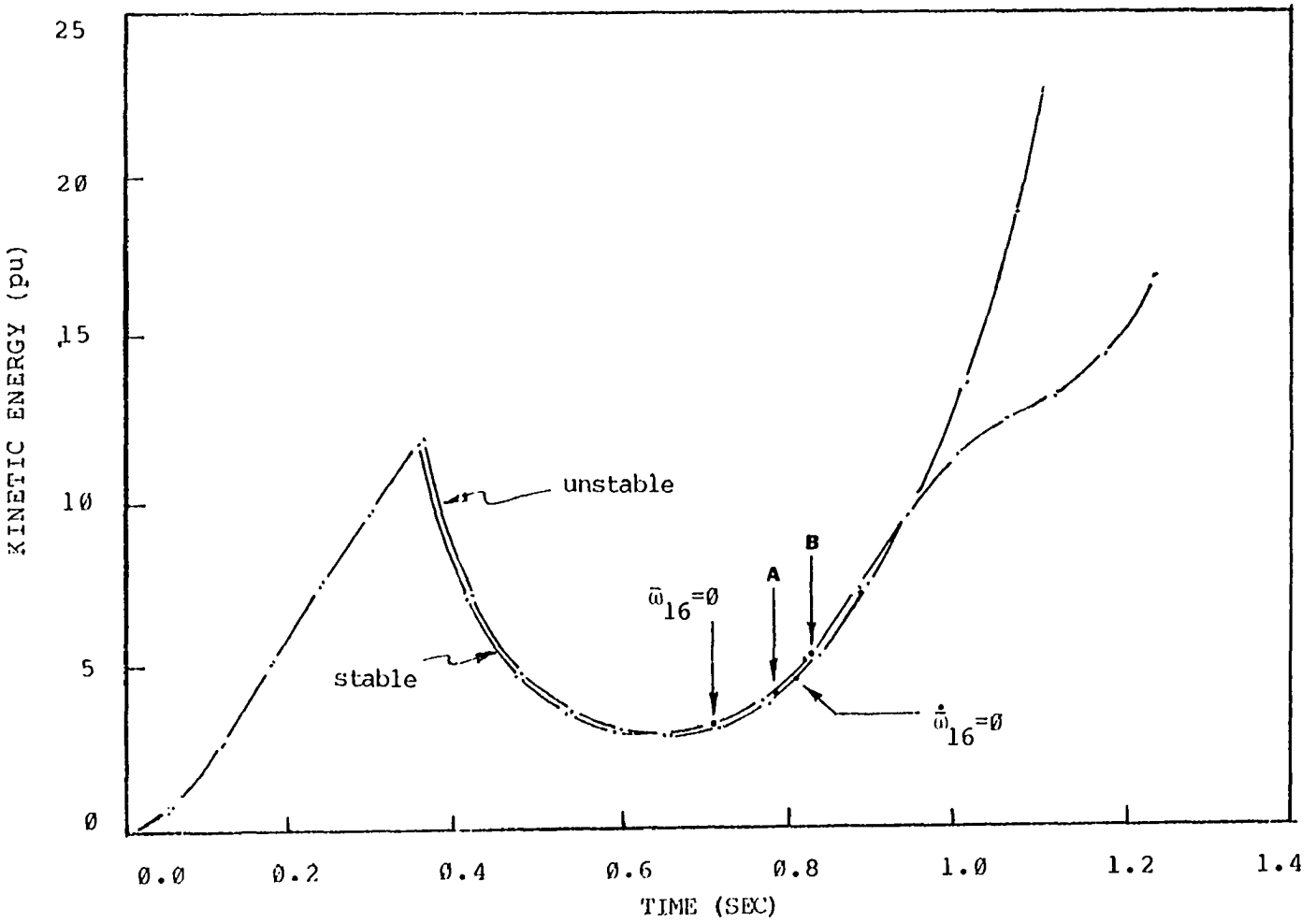

Figure 7-3. K.E. vs time for the Ft. Calhoun faults cleared at .3528s (stable) and .3564s (unstable)

energy at the critical instant ($\bar{\omega}=0$, $\dot{\bar{\alpha}}=0$) is the kinetic energy not contributing to instability.

Because the value of this kinetic energy is quite sensitive to the time at which the critical instant is reached, the actual magnitude of this kinetic energy is difficult to predict. This sensitivity can be deduced by inspecting Figure 7-3, where a small change in the time at which the critical instant is reached results in a large change in that kinetic energy which does not contribute to instability. In the above case, for example, we concluded that the critical instant (at the point marked "A") was at the instant when the kinetic energy which did not contribute to instability was 3.80 pu. If the zero velocity instant occurs only .06 seconds later (at the point marked "B"), the kinetic energy not contributing to instability increases by 38% (from 3.80 pu to 5.23 pu).

To make matters worse, this kind of change in the time of the critical instant, from point "A" to point "B", is exactly the kind of change that is likely to occur. That this change is likely can be seen by inspecting Table 7-1. The first row shows the kinetic energy injected by the disturbance. The stable and unstable values differ by only 0.13 pu of kinetic energy. This <u>small</u> additional injection of fault kinetic energy shifts the peak-of-the-swing by 0.10 second (see Column 6); the consequence is a <u>large</u> change in

the kinetic energy at the peak (row 3). Only Ø.13 pu of additional fault kinetic energy resulted in a 1.27 pu change in kinetic energy contributing to instability.

Thus, it appears that small changes may be expected to alter significantly the time of the peak on the critical trajectory; this can significantly change the kinetic energy and the stability of the response of an individual case.

Implications to Direct Methods of Stability Assessment

It appears that small system changes that are able to make small changes in the time of the critical instant are able to alter significantly the system's stability characteristics. In general, therefore, any single stability case can be expected to be sensitive to small changes in the parameters assumed at the start. Wide variations in predicted stability may result from small changes in the fault, the model, or the initial conditions.

This high degree of sensitivity introduces a problem: valid operating decisions should not be based on a system response that is highly sensitive to small changes in the system. Wide variations in control actions would be required in order to respond to relatively minor changes in the system. Furthermore, this condition might lead to a false measure of security, since a small change may make a safe system insecure.

A Modified Transient Energy Margin

The presence of a component of energy with a high degree of variability is not an insurmountable problem. It is possible to obtain a security assessment, using a modified transient energy margin, that is not subject to wide variations with small system changes. This modified margin assesses only the invariant portion of the kinetic energy in question by using a lower bound on the kinetic energy not contributing to instability. This lower bound is the amount of kinetic energy that is assured to exist. Any kinetic energy above this amount is subject to change and is therefore not used in the assessment.

Therefore, a modified kinetic energy correction technique is employed: this technique uses the minimum kinetic energy value on the critical trajectory as the kinetic energy component not contributing to instability. This minimum kinetic energy value is the lower bound on the kinetic energy component not contributing to instability. In Figure 7-3, the lower bound is the minimum kinetic energy value of

$$KE_m = 2.907 \quad pu$$

occurring at t = 0.647 s. (The nomenclature KE_m is used for the minimum kinetic energy along the trajectory.)

The Concept of an Energy Minimum

Using a local energy minimum value, rather than the exact energy value, is consistent with other techniques used in direct assessment of stability. The energy of the relevant UEP, for example, is a local minimum escape energy value that is used instead of the exact value of V_{cr}. Assessing robustness with KE_m and V_u, which are both local energy minimums, is equivalent to assessing the worst possible trajectory that is close to the actual critical trajectory. The technique is intended to give a reliable evaluation of robustness. Assessing energy, either in terms of position (V_u) or velocity (KE_m), will not be sensitive to the time of the actual critical instant. The assessment will use only the components of kinetic energy and potential energy that are assured to exist at the critical instant. This assessment methodology in effect defines robustness in terms of the assured energy capacity only; this is independent of

- the timing of the critical instant
- the proximity of the trajectory and the relevant UEP at this critical instant.

Accuracy of Critical Clearing Time

A consequence of such an assessment technique is that we can no longer expect precise predictions of the critical clearing times; that is, the technique cannot rank the

transient response precisely in terms of critical clearing times as was accomplished by the technique described in Chapter 6. This is because the minimum kinetic energy value will differ from the actual kinetic energy component not contributing to instability; this difference will vary from case to case.

The technique of using local minimums, rather than actual energy values, in essence evaluates a local worst-case condition in order to assure a valid basis for decision-making. This approach loses the precise stability predictions and gains a measure of locally-assured robustness. The important distinction to be made here is between a technique which accurately assesses stability and a technique which accurately assesses robustness.

Example: The Ft. Calhoun Fault

The Ft. Calhoun fault study described in considerable detail in this chapter exemplifies the proposed technique. The critical trajectory realizes a kinetic energy not contributing to instability of

$$KE = 3.80 \text{ pu}$$

(see Table 7-2). Using the minimum KE from Figure 7-3, the minimum kinetic energy is

$$KE_m = 2.90 \text{ pu}$$

(where the subscript m is used to indicate the minimum kinetic

energy on the critical trajectory.) The proposed method of assessing the robustness of the system would repeat the assessment of Table 7-2, substituting the value of KE_m = 2.90 pu for the value of KE = 3.80 pu. Table 7-3 shows this assessment for the critically stable case. The result is a mis-assessment of stability; the critically stable case is assessed as being unstable by an energy margin of -0.83 pu. Using the KE_m of 2.90 pu to predict critical clearing yields a prediction of:

$$t_{cr} = 0.3514 \text{ s}$$

This compares to a correct critical clearing time (see Table 7-1) of:

$$0.3528 < t_{cr} < 0.3564 \text{ s}$$

Table 7-3. Assessment of the stable Ft. Calhoun fault using the minimum KE on the critical trajectory (KE_m)

K.E. at clearing	11.824	pu
KE_m	2.90	pu
Transient energy into #16	8.92	pu
Energy absorbing capacity	8.09	pu

Conclusion: 8.92 > 8.09, therefore stability is NOT assured

MARGIN: 8.09 - 8.92 = -0.83 at No. 16

Thus, the -0.83 pu "error" in predicting stability does not drastically alter the prediction of t_{cr}. Also, it appears that the critical clearing time of

$$0.3528 < t_{cr} < 0.3564 \quad s$$

is subject to some amount of variation, depending upon when the stationary instant actually occurs. Thus, some amount of the robustness implied by a critical clearing time of

$$0.3528 < t_{cr} < 0.3564 \quad s$$

may vanish if small changes in system parameters alter the timing of the critical instant. Using KE_m = 2.90 pu for the assessment eliminates this concern and evaluates the fault by means of a criterion that defines robustness in terms of a local worst-case fault-energy-absorbing capacity.

Re-assessment of the Three-Phase Faults

We now apply the proposed assessment methodology to the 13 three-phase faults (in the Reduced Iowa System) that were presented in Chapter 6.

The Assessment Procedure

The assessment procedure is exactly the same as presented in Chapter 6, except for the estimate of the kinetic energy correction, ΔKE_{corr}. For this value, we use the minimum kinetic energy of the critical trajectory, KE_m.

The assessment procedure is, then:

1. Compute the energy margin (i.e. the energy function evaluated between clearing and the relevant UEP:

$$\Delta V = V\Big|_{\theta^{cl}}^{\theta^{u}}$$

2. Increase the energy margin by the kinetic energy correction, KE_m:

$$\Delta V_c' = V\Big|_{\theta^{cl}}^{\theta^{u}} + KE_m$$

(The prime notation denotes that KE_m is used instead of ΔKE_{corr}.)

3. Reduce the kinetic energy at clearing by KE_m:

$$KE_c' = KE_{cl} - KE_m$$

4. Normalize the energy margin $\Delta V_c'$ by dividing by the KE_c' to obtain the normalized transient energy margin, $\Delta V_n'$:

$$\Delta V_n' = \Delta V_c' / KE_c'$$

The alternate normalizing technique will give the percent margin, $\%\Delta V'$:

$$\%\Delta V' = \Delta V_c'/(\Delta V_c' + KE_c')\ 100\%$$

The Assessment

Table 7-4 shows the results of this security assessment procedure as applied to the 13 three-phase faults of Chapter 6. Table 7-5 ranks these 13 cases in order of decreasing robustness.

Comparison can be made between Table 7-5 and Table 6-4 in Chapter 6. The ranking shown in Table 7-5 does not match exactly that shown in Table 6-4. However, inspection of the critical clearing times in Table 7-5 shows the ranking to be

Table 7-4. Normalized transient energy margin (using ΔKE_m) for the 17-generator system; three-phase faults cleared at 0.15s

Fault Location (Bus and Line Faulted)	KE_m	$\Delta V_c'$ (pu)	Corrected Fault KE	$\Delta V_n'$
Raun fault				
372-193	1.77	8.081	6.229	1.297
372-773	1.63	5.265	6.368	0.827
372-482	2.22	10.258	5.790	1.772
Transformer 372-800	1.61	9.914	6.388	1.552
Council Bluffs fault				
436-439	2.99	13.104	3.306	3.964
436-771	1.49	5.233	4.806	1.089
Ft. Calhoun fault				
773-372	4.63	29.500	*	*
773-779	2.88	27.745	1.115	24.883
773-775	3.94	29.129	0.06	483.3
Cooper fault				
6-774	2.11	4.230	4.130	1.024
6-439	4.32	6.712	2.949	2.276
6-16	2.89	6.057	3.379	1.793
6-393	4.99	8.476	1.279	6.628

* KE_m is larger than the fault KE in this case

Table 7-5. Ranking of the three-phase faults shown in Table 7-4

Rank	ΔVn'	%ΔV'	ΔV'	Fault Location	clearing times Stable	clearing times Unstable
1	Ø.827	45.3	5.265	Raun, line 372-773	Ø.117	Ø.180
2	1.Ø24	5Ø.6	4.23Ø	Cooper, line 6-774	Ø.2Ø4	Ø.212
3	1.Ø89	52.1	5.233	Council Bluffs, line 436-439	Ø.2ØØ	Ø.2Ø4
4	1.297	56.5	8.Ø81	Raun, line 372-193	Ø.1923	Ø.1924
5	1.552	6Ø.8	9.914	Raun, transformer 372-8ØØ	Ø.196	Ø.2ØØ
6	1.772	63.9	1Ø.258	Raun, line 372-482	Ø.192	Ø.196
7	1.793	64.2	6.Ø57	Cooper, line 6-16	Ø.212	Ø.216
8	2.276	69.5	6.712	Cooper, line 6-439	Ø.216	Ø.22Ø
9	3.964	8Ø.Ø	13.964	Council Bluffs, line 436-439	Ø.225	Ø.25Ø
1Ø	6.628	86.9	8.416	Cooper, line 6-393	Ø.22Ø	Ø.225
11	24.773	96.1	27.745	Ft. Calhoun, line 773-779	Ø.345	Ø.356
12	483.3Ø	99.8	29.129	Ft. Calhoun, line 773-775	Ø.325	Ø.34Ø
13	*	*	29.5ØØ	Ft. Calhoun, line 773-372	Ø.34Ø	Ø.345

* KE is larger than the fault KE in this case

more or less the same. Though the clearing times are not in precise sequence, the list starts with low critical clearing times and increases to larger values as we move down the list. No case is more than about Ø.Ø2 S out of position, though the critical clearing values range from Ø.117 s to Ø.356 s. We conclude that the effect of using a local minimum kinetic energy correction may have a minimal effect on the overall ranking of the system; it will, however, make the ranking not sensitive as to the time the critical instant actually occurs.

Comparison can also be made between Table 7-4 and Table 6-3. Looking at column 1 it can be seen that some $\Delta V_c'$ values are above the corresponding ΔV_c values, and some are below. Since $\Delta V_c'$ is supposed to contain a conservative estimate on kinetic energy, one might first think that $\Delta V_c'$ should always be less than ΔV_c. This, in fact, does not need to be the case. The reason is found in the difference between the two kinetic energy correction techniques. In Chapter 6, the ΔKE_{corr} values were obtained for the <u>non-critical trajectory</u>, e.g., for the trajectory cleared at Ø.15 seconds. The method used in Chapter 7, however, obtains KE_m for the <u>critical trajectory</u>, e.g., for the Ft. Calhoun fault cleared at Ø.3564 seconds. The ΔKE_{corr} of the non-critical trajectory is not necessarily larger than the lower bound on the kinetic energy of the critical trajectory. Thus, the values of ΔKE_{corr} may above or below the values of KE_m, and the value of $\Delta V_c'$ may

likewise be below or above ΔV_c.

It is interesting to note that the security assessment of Table 7-5 (made in terms of nearby worst-case conditions) does not identify a weakness in any one location. The stability assessment of Table 6-4, on the other hand, clearly identified RAUN as the weak link in the system.

The lack of a clearly defined point of weakness might seem reasonable. The original design process attempted to carefully isolate the worst-case problems and design the system to survive specific impacts with no part of the system being overdesigned relative to the other. We might conjecture that, if worst-case conditions are assessed (using a direct method), this design strategy should appear. That no single point of weakness is apparent may merely show that the system is well-designed for the worst trajectories possible in the current configuration. (In the assessment implied in Table 7-5, Ft. Calhoun would appear to be over-designed for this particular fault and configuration.)

Summary and Discussion

The previous chapter, Chapter 6, computed a kinetic energy correction (ΔKE_{corr}) using the speed of the critical group at the clearing instant. The method led to an accurate ranking of various faults in terms of the critical clearing times. In Chapter 7, a careful investigation of where the

energy resides after a disturbance has suggested a slightly different technique. Instead of ΔKE_{corr}, we used the minimum kinetic energy value actually realized by the critical trajectory (KE_m).

Though the analysis in this chapter is somewhat detailed, the reader should not lose sight of the simplicity of what Chapter 7 proposes. The only change between Chapter 6 and Chapter 7 is in computing the kinetic energy correction: in Chapter 6 the kinetic energy corrections ΔKE_{corr} is used as the kinetic energy not contributing to instability; in Chapter 7 a lower bound is used as the kinetic energy not contributing to instability.

To obtain the ranking shown in Table 7-5, we merely used a conservative lower bound in place of a sensitive parameter. Using a conservative limiting value rather than an uncertain ΔKE_{corr} is intended to give an assessment that is suited for decision making.

The method uses a simple logic: at the point of escape, the critical trajectory has both a potential energy value (V_{cr}) and a kinetic energy value (kinetic energy not contributing to instability); the energy of the UEP actually realized by the critical trajectory is taken as a safe upper bound on the value of the potential energy at escape, and the kinetic energy minimum actually realized by the critical trajectory is taken as a safe upper bound on the value of the

kinetic energy at escape. That is, the energy of the UEP is taken as a safe estimate of V_{cr}, and minimum kinetic energy on the critical trajectory is taken as a safe estimate of the kinetic energy that does not contribute to instability. An assessment made on this basis avoids the high sensitivity of the kinetic energy not contributing to instability to the actual time the critical instant occurs, and does not require knowledge of the angles at the actual point of escape.

The focus on assessing assured robustness, rather than on merely predicting stability is one of the more subtle results of Chapter 7. The distinction is an important one. To assess stability requires precise knowledge of exact responses. As such the assessment ignores the conditions that are merely "close-by". To assess security, on the other hand, the precise response is not desired. Instead, we must evaluate the posture of the system in terms of the worst possible response that is "close-by". To be considered secure the system must be sound in spite of the minor changes in the system; it must provide decisions that accommodate the minor ebb and flow of the system.

This chapter has chosen to assess the local minimum energy conditions as a measure of security. It is reasoned that the local worst-case trajectory will realize these local minimum energy conditions. These energy minimal thus evaluate the local worst-case trajectory that is close to the actual

trajectory that will be encountered. A system is considered secure only if the local energy minima are safely within acceptable limits.

The assessment of energy minima is the fundamental concept behind security assessment using transient energy margin analysis. The technique is well-suited to the task. However, more work has to be done and, in this respect, the technique proposed in this chapter is not an end in itself; rather, it is a point-of-beginning. The intent is to open a direction for continued study, not to claim its accomplishment; to focus on the concept of a decision-making assessment of robustness, rather than on a means of merely assessing stability.

CHAPTER 8. CONCLUSIONS

This dissertation used the normalized transient energy margin to establish a ranking of possible disturbances for a given operating condition. The ranking was confirmed in terms of critical clearing times to demonstrate an accurate measure of the relative stability of the system. The ranking is relative to the severity of the possible disturbances, measured in terms of critical clearing times.

The dissertation suggests that a meaningful assessment of security requires more than just assessing stability; the assessment must exclude the energy components that are highly sensitive to change and thus unreliable for use in decision-making. Using local minimum energy values in lieu of of sensitive energy components, a security assessment methodology is proposed amd applied to a real-world test system.

The resulting margin ranking gives a listing of the evident weak links that exist in the system at a given moment. It seems reasonable that an alert should be issued when the weakest of these links corresponds to the margin ΔV_c that is below some specified limit. The operator will most likely be familiar already with the problem to which he is being alerted. Now, he will know what his margin of safety is. He will be in a postion to assess the severity of the alert, and

to determine whether corrective action is necessary.

The function of the transient security assessment process would be:

- To alert the operator when circumstances arise that might need his attention.
- To identify the margin-of-safety.
- To report the weak links that threaten the system, thus suggesting corrective measures.

The on-line security assessment process assures the operator that he is fully informed about the status of the system. The operator can ascertain how well his current operating strategy meets the dynamic system performance criteria in effect at the moment. An alert not only gives the operator knowledge that trouble is possible, but, by identifying the source of the problem, implies remedial action that will alter the situation. With information provided by this transient security assessment, the operator could control his system and safely operate close to the "edge" of transient stability.

Accomplishments of This Research

Development of the proposed methodology for automated transient security assessment required several advances in the state-of-the-art for direct methods of stability analysis. These advances were:

- Defining the transient energy margin.

- Identifying the gross motion of a group of machines (as indicated by their center of inertia) as the motion which controls stability. This led to developing two additional concepts:

  -- the controlling UEP is that UEP approached (by the critical group) during the critical trajectory.

  -- a substantial part of the fault energy does not contribute to instability (namely the kinetic energy associated with intermachine motion, about the inertial centers, at the instant when $\bar{\omega}=0$ and $\dot{\bar{\omega}}=0$).

- Verifying that the energy of the controlling UEP may be used, for all practical purposes, as being equal to V_{cr}.

- Calculating the kinetic energy not contributing to instability by computing the kinetic energy associated with intermachine motion, around the inertial centers, at the clearing instant.

- Demonstrating that accurate first swing transient security can be assessed if:

  -- the fault energy is computed at clearing, including a correction for KE not contributing to instability, and

-- the critical energy is computed as the energy associated with the controlling UEP.

o Developing an assessment methodology using the normalized transient energy margin to produce a relative ranking of the disturbances. This methodology yields:

-- a means of detecting that an unstable transient response is possible;

-- a means of quantitatively measuring the robustness of the system (i.e., the margin-of-safety);

-- a means of identifying the evident weak links that exist at a given operating condition, implying the need for corrective measures.

o Confirming by demonstration that direct methods can give an analysis that is sufficiently accurate, in terms of comparative or relative ranking, to allow system operational decision-making based on the analysis results.

o Demonstrating, by using a practical, real-world test system, the potential of the proposed methodology for accomplishing transient security assessment.

o Proposing a security assessment technique using the

minimum kinetic energy on the critical trajectory; this technique avoids an assessment that is highly sensitive to when the peak of the swing occurs during the critical trajectory. The approach does require additional computation; it may be necessary to reproduce the critical trajectory in order to determine the minimum kinetic energy on the critical trajectory.

In accomplishing these advancements, the research followed the strategy of assigning physical meaning to the abstract mathematical concepts implied in the energy function analysis. Assigning physical meaning to the unstable equilibrium points and to the system kinetic energy led to the proper use of the energy that they represented.

Future Work

A great deal of work needs to be done in the area of automated transient stability analysis. There is a large difference between proposing a tool for assessing transient stability, and accomplishing practical, computer automated, transient security analysis. It is the opinion of this researcher that future investigations into direct methods of transient security assessment must accomplish three principal goals:

- Develop a thorough understanding of the physical phenomenon of transient instability.

- Resolve special topic issues remaining in the energy assessment methodology, including assurances of conservative results.

- Establish a decision criterion that is generally accepted (at the industrial level) as valid for operational decision-making.

Research Topics

Several research topics seem appropriate as means of accomplishing these goals. They are introduced here as topics for continued research.

- Physical distribution of energy

  It appears that we still do not know exactly what drives generators unstable. The research reported in this dissertation studied how the system fault energy (potential and kinetic) is distributed in time. An important issue still to be resolved is how this fault energy (potential and kinetic) is distributed geographically. In Chapter 7, the energy in each machine was computed during a fault

simulation using numerical integration. Only one machine instabilities were studied, where the mode of instabillity was clearly defined. The techniques of Chapter 7 should be applied to the multimachine case and cases where the mode of instability is not clear. The potential energy associated with each machine can be computed, giving a geographical distribution showing where the transient energy physically resides. A study of this distribution should help identify what, exactly, drives the machines unstable, and what system energy does or does not contribute to that instability. The introductory work in this area (Chapter 7) seems quite promising; what appears to be emerging is an understanding, on a machine by machine basis, of how fault injected energy drives individual machines or groups of machines unstable. The work of Chapter 7 must be continued.

- Energy invariant equivalent

Chapter 7 suggested that all of the fault kinetic energy contributing to instability was imbedded in the unstable machines at the critical instant, with virtually no fault kinetic energy residing in all

other machines combined. From this it appears that energy storage elements (lines, transformers, etc.) that are remote from the fault location might, as a whole, contribute little to the stability of critically stable machines. If this were true, there may be a reduced need for detailed models, particularly for remote parts of the system. Energy equivalent models might be devised to simplify the security assessment process. Details of parts of the system that are not near the faulted generator might not be required and might be equivalenced. It may be possible to obtain a sufficient model using only knowledge of major lines or lines near generators where faults are assumed. This information may be available without extensive telemetering. Thus, a study of where the fault kinetic energy resides at the stationary instant may lead to identification of a significant amount of system data that are not essential in assessing security.

- The controlling UEP

Determining the controlling UEP is a crucial step in the direct assessment methodology. This

dissertation considered the controlling UEP to be the one physically realized (in terms of the critical group) by the critically cleared trajectory. It appears from this research that identification of the controlling UEP can be pre-determined through careful study. It would be particularly useful, however, if the critical group and corresponding UEP could be identified as part of the direct assessment methodology. This is clearly an area for additional research.

- New normalizing criteria

For each controlling UEP there is an energy margin which, according to the direct assessment methodology, is normalized to obtain a meaningful ranking of the disturbances. One normalizing scheme (dividing the kinetic energy at clearing) was presented in this dissertation. However, more work is needed in this area. New normalizing schemes should be considered, aimed at resolving the energy margin into physically meaningful parameters over which the operator has direct or indirect control. Reporting of the transient energy margin as physically meaningful parameters

would be very useful in practical application. Probably the most useful parameters would be:

- -- ΔP (load or generation changes allowed)
- -- ΔV (voltage changes allowed)
- -- ΔY (admittance changes allowed)

o Effects of exciters, power system stabilizers, etc.

This dissertation utilized a classical model. At first the use of this model might seem quite limiting. On the other hand, the simplicity of the classical model is particularly appealing in assessing transient stability, which typically requires great mathematical complexity. A significant question is whether the simple classical model captures the essence of stability with sufficient accuracy to be a realistic basis for decision making. This issue questions whether it is better to use a thoroughly understood, simple model rather than the accurate but elaborate system models. It may be possible, for example, to conservatively estimate the effects of exciters, power system stabilizers, DC transmission lines, etc., on the transient energy absorbing capacity of the system. On the other hand, the inclusion of

more elaborate models may be necessary for practical assessment of security. Only further research can resolve the issue.

- Two-machine equivalent

The concept that the gross motion of two principal groups determines stability suggests that a disturbance might be viewed as two equivalent machines in motion. It would be interesting to pursue the question of developing a two-machine equivalent system based on the critical grouping. The question raised is whether conservative or safe assumptions can be used in resolving the n-machine system into a two-machine system that preserves the essential properties of the gross motion of the original system, i.e., transient stability.

- Assurance of conservativeness

The assurance of conservative results, that use of the UEP traditionally offers, has been lost with the use of the controlling UEP and the kinetic energy correction. A significant question is: Can the assurance of conservative results be

re-introduced? The issue here is whether the use of the physically realized UEP and the physically realized minimum kinetic energy can be resolved into a least-upper-bound on system energy that is mathematically assured. Assurance of the conservative nature of the results will promote general acceptance of the validity of assessment methodology for decision-making.

- Validation of the methodology

Any method of assessing transient security must ultimately be tested in a field application. The transient security analysis methodology outlined in this dissertation could benefit from limited field testing in which the techniques can be put into a control center on an experimental basis. The methodology could establish a track record while in limited use. The system could be refined and evaluated in a carefully monitored, practical environment, even if the process is not fully automated or optimized.

ACKNOWLEDGEMENTS

The author wishes to express his sincere appreciation to his major professor, Dr. Aziz Fouad, for his encouragement and invaluable guidance during this research. Special thanks are also extended to Dr. Harry Hale, Dr. R. Grover Brown, Dr. Gerald Smith, Dr. M. A. Pai, and Dr. Ken Kruempel for their participation as members of the author's graduate committee.

The author is also indebted to the Electric Power Research Institute, the sponsors of the Power Affiliates Program, and Computed Power Systems, Inc., for their financial assistance.

Finally, the author wishes to thank his wife, Colina, for her confidence and encouragement throughout his graduate program.

APPENDIX: THE COMPUTER PROGRAMS

Description of Computer Programs

Five computer programs were utilized in the research reported in this dissertation:

PETS

TESA

TSWING

UEPMARGIN

YMOD

The first two programs (PETS and TESA) are batch programs obtained from outside sources; and the last three (TSWING, UEPMARGIN, AND YMOD) are interactive programs developed for the research project of which this dissertation is a part. Only TSWING and UEPMARGIN were developed by the author.

The Batch Programs

Two computer program packages were obtained from outside sources at the start of this research project:

1. The Philadelphia Electric Transient Stability program (PETS), and its companion loadflow program, was available from the Power System Computer Service at Iowa State University. This package was used to simulate disturbances by time solution of the network.

2. Transient Energy Stability Analysis, (TESA), was provided by Systems Control, Inc. The TESA progams estimate the unstable equlibrium angles, the critical energy, and the energy at the time of the fault clearing. Though this program was not specifically used to generate the data in this dissertation, several subroutines were used in the programs TSWING and UEPMARGIN.

These two programs operate in the batch mode on an ITEL-AS6 computer at the Iowa State University Computer Center.

The Interactive Programs

In addition to the two batch-mode programs obtained from outside sources, three interactive-mode programs were developed in the course of this research. The first two, "TSWING" and UEPMARGIN", were written by the author. They borrow several subroutines from the TESA package. The third program, YMOD, was developed by colleagues as an efficient method of generating the modified Y-Bus matrices required in this work. All three programs are written for interactive-mode operation on the VAX-780 computer system at Iowa State University.

TSWING

The program TSWING simulates the disturbance by time simulation. At each time step it computes and plots various parameters. It includes the following basic features:

- Computes and plots rotor angles with respect to the system inertial center.

- Computes and plots the rms deviation between the

rotor angles and a specified set of UEP angles.

- Computes and plots kinetic energy, position energy, magnetic energy, dissipation energy, potential energy, and total energy.

- Injects additional disturbances, in the form of additional generation or load, in any distribution and at any instant.

- Generates the reduced Y-Bus matrix used in program UEPMARGIN.

The basic network reduction and swing simulation are accomplished by subroutines borrowed from TESA. Data requirements for executing TSWING are documented in the comment cards at the beginning of the TSWING program. The TSWING program provides a means of inspecting energy shifts and the resulting trajectories for a wide range of disturbances.

UEPMARGIN

The program UEPMARGIN computes the energy function between any two system states, a and b, i.e., calculates $\dot{V}$. When "a" is the system states (angles and velocities) at the

instant of clearing, and "b" is the system states at the UEP, then the result is the energy margin. The program also allows for a change in the generator powers; the program recomputes the UEP and computes the corresponding energy margin.

The basic features of UEPMARGIN are:

- Computes the SEP and UEP angles for a given system condition and for an initial estimate of the SEP and UEP. This utilizes a Davidon-Fletcher-Powel subroutine from TESA.

- Computes the energy function between any two points ("a" and "b") in the state space, the speeds and angles of which are known:

$$\text{Energy} = V\Big|_{\theta^a}^{\theta^b}$$

- With "a" representing the speeds and angles at clearing, and "b" representing the UEP angle, computes the energy margin.

- Computes the kinetic energy correction (ΔKE_{corr}) and adjusts the energy margin accordingly.

- Computes the energy, broken down in line-by-line

and node-by-node fashion. This provides a complete dissecting of when the energy resides in the system.

- Computes the new values of the UEP for any adjustment in generator powers; computes a new energy margin for this new UEP. This routine can be repeated any number of times, with the powers input via the interactive keyboard.

The data requirements for executing UEPMARGIN are documented in the comment cards at the beginning of the UEPMARGIN program.

YMOD

The "YMOD" progaram performs reduction of the full Y-Bus matrix to the reduced Y-bus corresponding to the internal nodes. For a given disturbance, but for a variety of post disturbance networks, considerable savings in computational effort can be achieved if the Y-Bus of the postfault network can be modified directly instead of reconstructing the Y-Bus "from scratch". An efficient method for this has been developed by Mamandur (cited in 42) for use in this project. The method was originally applied to simulate network disturbances and is used here merely to achieve a more

efficient computation. The method stores all the necessary steps in the process of reduction, namely, in the form of triangular matrix factors of the Y-Bus matrix. Then it uses these triangular matrix factors to efficiently compute the changes to the reduced Y-Bus matrix due to various network disturbances such as tripping or closing of lines.

The program uses an efficient technique to find the changes to the reduced Y-Bus matrix. However, the program is not in its most efficient form, in the sense that it does not exploit sparsity to the fullest extent both for storing and operations.

The YMOD program can eventually replace the Network Reduction Subroutine now used to generate the reduced Y-Bus matrices for both TSWING and UEPMARGIN and be useful in assessment of network changes.

The data requirements for executing YMOD are documented in the comment cards at the beginning of the YMOD program. In general, the line, transformer and bus data requirements match that of the program TSWING.

State of the Programs

Two of the computer programs developed in this project, TSWING and UEPMARGIN, are primarily research tools, i.e., in their present form they are useful only to a researcher who is familiar with them and is comfortable with the VAX interactive

computer system. The third program, YMOD, is a more general purpose matrix reduction program and would be suitable for application in other areas of research.

All three programs are well-tested, versatile, and powerful. Numerous cross-checks were made on the results obtained by these programs. In short, they can reliably dissect the trajectory of a multimachine power system in terms of where the energy resides in the system and investigate in detail the motion of groups of machines. Unstable equilibrium points can be obtained and transient energy margins can be computed with the appropriate corrections made.

The packages are currently dimensioned for a 170-bus, 39-machine system. They require approximately 400 K of core to execute the most core-intensive steps (on an ITEL AS-6 computer). The 170-bus, 39-machine limit can easily be re-dimensioned upward. For example, the 170-bus, 39-machine program is itself a re-dimensioned version of a 120-bus program.

The main disadvantages to these programs are; 1) they are not well-documented, and 2) they are written for use on the interactive facilities at Iowa State University. They represent a mixed collection of routines that are well-tested, but do not represent a production grade research package.

The programs YMOD and TSWING were written for use in an interactive mode with the researcher directing the program

execution from the on-line terminal. Input data files are mixed in an assortment of formats and locations designed to neet the particular need of the researcher, depending on the job performed (and not necessarily in a logical and easily understood format). Output files are created by one program as input to other routines. File management is not automated and is rather cumbersome. In short, inputs and outputs are device dependent and execution options are complicated.

Program YMOD, in contrast to MARGIN and TSWING, was developed in a single development step to accomplish a well-focused result. Thus, it is systematically written and is neither device dependent nor strictly an interactive tool.

The Davidon-Fletcher-Powel Subroutine

The program UEPMARGIN contains a minimization routine known as the Davidon-Fletcher-Powel (DFP) routine (49,50). The DFP minimization technique is a non-linear programming method that uses the gradient of the objective function to achieve fast convergence characteristics. Though the technique is considered to be a second order gradient method, only the first derivative of the objective function is required.

The DFP technique has been used since 1966 and is widely available as part of the standard IMSL library package at many

computer centers. In general, the algorithm accomplishes the following:

1. Chooses a search direction (i.e., search ray) using the gradient of the function at the point $\underline{x}_i$.
2. Performs a linear minimization of the function along the search ray to obtain
$$\min [f(\underline{x}_i + \underline{x}_i]$$
3. The gradient at $\underline{x}_i$ and $\underline{x}_i + \underline{x}_i$ is used to estimate a second order gradient for the function at $\underline{x}_i$.
4. The first and second gradients of the function are used to choose a new search ray to apply at the point $\underline{x}_{i+1}$.
5. Return to step 2.

Steps 2 through 5 are repeated until the absolute distance of $\underline{x}$ is less than some predetermined value.

REFERENCES

1. F. I. Denney, et al. (Current Operational Problems Working Group--Power Systems Engineering Committee.) "System Security practices." IEEE paper No. A 79107-4 presented at PES Winter Meeting, New York, 1979.

2. M. Cuenod, et al. "Report by the System Planning and Operation Committee." CIGRE (1972): 32-12.

3. O. Saito, et al. "Security Monitoring Systems Including Fast Transient Stability Studies." IEEE Trans. PAS-94, (1975): 1789-1805.

4. B. Minakawa, et al. "Practical Assessment and Strategy for Improvement of Dynamic Performance of Power Systems." CIGRE 11 (1976): 32-03.

5. T. Miki. "Application of Dynamic Reliability Evaluation Method to Model Systems." Electric Engineering in Japan 97, No. 2 (1977): 64-81.

6. A. Shalaby, et al. "On-line Computer Monitoring of Complex Power System Stability Limits." Eleventh PICA Conference Proceedings, IEEE Publication No. 79, CH 1381-3-PWR (1979): 64-72.

7. T. Dyliacco. "Control of Power Systems via the Multi-level Concept." Case Western Reserve University Systems Research Center Report No. SRO-68-19, June 1968.

8. L. H. Fink and K. Carlsen. "Operating Under Stress and Strain." IEEE Spectrum 15 (March 1978): 48-53.

9. P. F. Albrecht. "Discussion of 'Reliability Criteria for System Dynamic Performance.'" IEEE Trans. PAS-96 (1977): 1816.

10. P. F. Albrecht. "Overview of Power System Reliability." EPRI Workshop, EPRI Report No. WS-77-60, October 1978.

11. C. Concordia. "Assessment of System Performance and Reliability." A paper presented at the Symposium on Reliability Criteria for System Dynamic Performance, IEEE-PES Summer Meeting, Portland, Oregon, July 1976.

12. R. Lugtu. "Security Constrained Dispatch." IEEE Trans. PAS-98 (1978): 270-274.

13. K. Najaf-Zadeh and S. W. Anderson. "Sensitivity Analysis in Optimal Simultaneous Power Interchange." IEEE-PES Paper F78267-7, presented at the Winter Meeting, New York, January 1978.

14. K. Suzuki, et al. "An Interactive Dispatching System for Power Network Operation Considering Power System Security." IEEE Paper No. A79470-6, presented at the IEEE-PES Summer Meeting, Vancouver, B.C., July 1979.

15. F. G. Vervloet and A. Brameller. "A. C. Security Assessment." Proceedings of IEE 122 (June 1975): 897-902.

16. L. L. Garver, et al. "Load Supply Capability of Generation-Transmission Networks." IEEE Trans. PAS-98 (1979): 957-962.

17. B. Scott and E. Hobson. "Power System Security Control Calculations using Linear Programming, Parts I and II." IEEE Trans. PAS-97 (1978):1713-1731.

18. S. M. Chan and F. C. Schweppe. "A Generation Reallocation and Load Shedding Algorithm." IEEE Trans. PAS-98 (1978): 26-34.

19. J. G. Blaschak, et al. "A Generation Dispatch Strategy for Power Systems Operating under Alert Status." IEEE-PAS Paper No. A79474-8, presented at Summer Meeting, Vancouver, B.C., July 1979.

20. J. Jarjis and F. D. Galiana. "Quantitative Analysis of Steady State Stability in Power Networks." IEEE-PAS Paper No. F79753-5, presented at Summer Meeting, Vancouver, B.C., July 1979.

21. V. A. Venikov, et al., "Estimation of Operational Limits for Electric Power Systems." Vol. 2. Proceedings of the Power System Computer Conference, Darmstadt, Germany, 1978.

22. S. Ohkubo, S. Takeda, and K. Umeura. "Steady State Stability of Interconnected Power System Taking into Account the Loading Conditions." Electrical Engineering in Japan 98, No. 5 (1978): 68-74.

23. R. D. Tiechgaeber, F. W. Harris and G. L. Johnson. "New Stability Measure for Multi-machine Power Systems." IEEE Trans. PAS-89: (1970) 233-239.

24. A. Rahimi, K. N. Stanton and D. M. Salmon. "Dynamic Aggregation and Calculation of Transient Stability Indices." IEEE Trans. PAS-91 (1972): 118-122.

25. P. R. S. Kuruganty and R. Billington. "Probalistic Assessment of Transient Stability." Electric Power Energy Systems 2, No. 2 (April 1980): 115-119.

26. M. Ribbens-Pavella, A. Calaver, and J. Gheury. "Transient Stability Index for On-line Evaluation." IEEE Paper No. A 80 013-3, Winter Meeting, New York, February, 1980.

27. U. Di Caprio. "An Approach to the On-line Evaluation of Stability Margins in Multi-area Systems." Power Systems Computer Conference Proceedings, 1972.

28. U. Di Caprio and M. Ribbens-Pavella. "Stability Margins in the Large for Multi-areas Power Systems." Seminar on Stability of Large-Scale Power Systems Proceedings, University of Liege, Belgium, 1972.

29. A. A. Fouad. "Long Range View of Stability Studies." Proceedings of the 1976 Engineering Foundation Conference on Power Systems Planning and Operation: Future Problems and Research Needs. EPRI Report No. EPRI EL-377-SR (1976): 6-42 to 6-55.

30. V. I. Zotov, et al. "Vector Quality Criterion of Fault Transient Processes in Complex Power Systems." A 1972 English Translation of a Soviet Paper (source unknown).

31. A. A. Fouad. "Stability Theory - Criteria for Transient Stability." Proceedings of the English Foundation Conference on Systems Engineering for Power, Henniker, New Hampshire, Publication No. CONF-750867 (1975): 421-450.

32. P. C. Magnusson. "The Transient-Energy Method of Calculating Stability." AIEE Trans. 66 (1947): 747-55.

33. P. D. Aylett. "The Energy-Integral Criterion of Transient Stability Limits of Power Systems." IEE (London) 105(C) (July 1958): 527-536.

34. T. Athay, R. Podmore and S. Virmani. "A Practical Method for Direct Analysis of Transient Stability." IEEE Trans. PAS-98, No. 2 (1979): 573-584.

35. T. Athay, V. R. Sherket, R. Podmore, S. Virmani and C. Puech. "Transient Energy Stability Analysis." Systems Engineering for Power: Emergency Operating State Control - Section IV, U. S. Department of Energy Publication No. CONF-790904-PL.

36. F. S. Prabhakara and A. H. El-Abiad, "A Simplified Determination of Transient Stability Regions for Liapunov Methods." IEEE Trans. PAS-94 (1975): 672-689.

37. M. Ribbens-Pavella, B. Lemal and W. Pirard. "On-Line Operation of Liapunov Criterion for Transient Stability Studies." Proc. of 1977 IFAC Symposium, Melbourne, Australia, pp. 292-96.

38. A. A. Fouad and R. L. Lugtu. "Transient Stability Analysis of Power systems Using Liapunov's Second Method." IEEE Paper No. C 72 145-6, Winter Meeting, New York, February 1972.

39. C. J. Tavora and O. J. M. Smith. "Characterization of Equilibrium and Stability in Power Systems." IEEE Trans. PAS-91 (1972): 1127-1130.

40. N. Kakimoto, Y. Ohsawa and M. Hayashi. "Transient Stability Analysis of Electric Power System via Lure Type Lyapunov Function. Part I. New Critical Value for Transient Stability." Trans. IEE of Japan 98, No. 5/6 (May/June 1978): 62-71.

41. N. Kakimoto, Y. Ohsawa and M. Hayashi. "Transient Stability Analysis of Electric Power Systems via Lure Type Lyapunov Function. Part II. Modification of Lure Type Lyapunov Function with Effect of Transfer Conductances." Trans. IEE of Japan 98, No. 5/6 (May/June 1978): 72-79.

42. A. A. Fouad, et al. "Transient Stability Margin as a Tool for Dynamic Security Assessment." Final Report of Project 1355-3, Electric Power Research Institute, Palo Alto, Ca. #EPRI EL-1755, 1980.

43. P. M. Anderson and A. A. Fouad. Power System Control and Stability. Ames, Iowa: Iowa State University Press, 1977.

44. A. A. Fouad and S. E. Stanton. "Transient Stablility of a Multi-machine Power System. Part I. Investigation of System Trajectories." IEEE Trans. PAS-100 (1981): 3408-3416.

45. A. A. Fouad and S. E. Stanton. "Transient Stability of a Multi-machine Power System. Part II. Critical Transient Energy." IEEE Trans. PAS-100 (1981): 3417-3424.

46. K. Uemura, J. Matsuki, I. Yamasa and T. Tsuji. "Approximation of an Energy Function in Transient Stability Analysis of Power Systems." Electrical Engineering in Japan 92, No. 6 (1972): 96-100.

47. E. W. Kimbark. Power System Stability. Vol 1. New York: John Wiley and Sons, Inc., 1965.

48. A. A. Fouad, S. E. Stanton, K. R. C. Mamandur and K. C. Kruempel. "Contingency Analysis Using the Transient Energy Margin Technique." IEEE-PAS Paper No. 81 SM397-9, presented at Summer Meeting, 1981.

49. R. Fletcher and M. J. D. Powel. "A Rapidly Convergent Descent Method for Minimization." Computer Journal 6 (1963): 163-168.

50. W. C. Davidon. "Variable Metric Method for Minimization." Argonne National Laboratory Report ANL-5990, Revised February, 1966.